TEMPLATE-DIRECTED PHOTOCHEMICAL [2+2] CYCLOADDITION REACTIONS OF NAPHTHALENE ACRYLIC ACID DERIVATIVES AND AN INVESTIGATION OF SINGLE-CRYSTAL-TO-SINGLE-CRYSTAL TRANSFORMATION

THESIS SUBMITTED TO
THE GRADUATE SCHOOL OF ENGINEERING AND SCIENCE
OF BILKENT UNIVERSITY
IN PARTIAL FULFILLMENT OF THE REQUIREMENTS FOR
THE DEGREE OF
MASTER OF SCIENCE
IN CHEMISTRY

By

Merve Temel

August 2024

TEMPLATE-DIRECTED PHOTOCHEMICAL [2+2] CYCLOADDITION REACTIONS OF NAPHTHALENE ACRYLIC ACID DERIVATIVES AND AN INVESTIGATION OF SINGLE-CRYSTAL-TO-SINGLE-CRYSTAL TRANSFORMATION

By Merve Temel

August 2024

We certify that we have read this thesis and that in our opinion it is fully adequate, in scope and in quality, as a thesis for the degree of Master of Science.

Yunus Emre TÜRKMEN (Advisor)

Halil İbrahim OKUR

Akın AKDAĞ

Approved for the Graduate School of Engineering and Science:

Orhan ARIKAN
Director of the Graduate School

ABSTRACT

TEMPLATE-DIRECTED PHOTOCHEMICAL [2+2] CYCLOADDITION REACTIONS OF NAPHTHALENE ACRYLIC ACID DERIVATIVES AND AN INVESTIGATION OF SINGLE-CRYSTAL-TO-SINGLE-CRYSTAL TRANSFORMATION

Merve Temel

M.S.c in Chemistry

Advisor: Yunus Emre Türkmen

August 2024

The first part of the thesis investigated the methodology study on the use of 1,8-dihydroxynaphthalene as a covalent template in the photochemical [2+2] cycloaddition reactions of naphthalene acrylic acid derivatives. This study showed that both in solution and solid state reactions, from the unsymmetrical template-bound diesters, the [2+2] cycloadducts can be formed. Importantly, the removal of the template molecule provided the products with high diastereoselectivities, whereas reactions in solution phase provided higher yields compared to solid state reactions.

In the second part of the thesis, the same strategy was applied to the template-bound symmetrical diester. Photochemical [2+2] cycloaddition reactions were investigated in three different phases: (*i*) in powder form, (*ii*) as a single crystal, (*iii*) in solution, under 365 nm UV light. In addition to that, the effect of daylight on the cyclization of symmetrical diester was examined. For the single crystal, single-crystal-to-single-crystal (SCSC) transformation

was studied. In all cases, the [2+2] cycloadduct was synthesized and isolated in good yields and with high diastereoselectivity.

Keywords: cyclobutane, 1,8-dihydroxynaphthalene, naphthalene acrylic acid, single-crystal-to-single-crystal transformation, template-bound photochemical [2+2] cyclization.

ÖZET

KALIP MOLEKÜLÜ ARACILIĞI İLE NAFTALİN AKRİLİK ASİT ÜZERİNE FOTOKİMYASAL [2+2] SİKLOKATILMA REAKSİYON ÜRÜNLERİNİN ELDESİ VE TEK KRİSTALDEN TEK KRİSTALE GERÇEKLEŞEN REAKSİYON ÇALIŞMASI

Merve Temel

Kimya, Yüksek Lisans

Tez Danışmanı: Yunus Emre Türkmen

Ağustos 2024

Bu tezin ilk bölümünde kalıp molekülü olarak 1,8-dihidroksinaftalin kullanılmıştır. Kalıp molekülü ile simetrik olmayan siklobütan ürünleri fotokimyasal [2+2] siklokatılma reaksiyonu sonucunda elde edilmiştir. Hem çözelti içerisinde hem de katı halde ışınlanan kalıba bağlı naftalin akrilik asit türev molekülleri ile gerçekleşen tepkimeler sonucunda ürünler yüksek bir diastereo-seçicilikle elde edilirken çözelti fazındaki reaksiyonların katı haldekilere nazaran daha yüksek verim verdiği gözlenmiştir.

İkinci bölümde kalıp moleküle bağlı simetrik naftalin akrilik asit üzerine [2+2] siklokatılma reaksiyonu incelenmiştir. Bu reaksiyonlarda başlangıç maddesi 365 nm dalgaboyuna sahip morötesi ışığa maruz bırakılan üç faklı halde yürütülmüştür: (*i*) toz halinde, (*ii*) tek kristaller halinde, (*iii*) çözelti içerisinde. Bunun yanı sıra çözelti içerisindeki başlangıç molekülü gün ışığına maruz bırakılmış ve etkisi araştırılmıştır. Tek kristal

reaksiyonu için tek kristalden tek kristale dönüşüm üzerine çalışılmıştır. Bütün bu reaksiyonlarda [2+2] siklokatılma ürünü yüksek verim ve diastero-seçicilikle elde edilmiştir.

Anahtar Kelimeler: [2+2] fotokimyasal siklokatılma reaksiyonları, 1,8-dihidroksinaftalin, naptalin akrilik asit, siklobutan, tek kristalden tek kristale dönüşüm.

ACKNOWLEDGEMENT

Firstly, I want to express my gratitude to my advisor Dr. Yunus Emre Türkmen. I am truly grateful for your constant support since the first day of my study in your laboratory. Without your brilliant insights and guidance, I could not experience such a valuable journey that contributed to my professional growth. I appreciate your trust in me. I have learned a lot from you; I hope I was able to contribute positively. I am also grateful to my examining committee, Prof. Akın Akdağ, and Dr. Halil İbrahim Okur. Their guidance in finalizing my study is extremely supportive. During the study, Prof. Onur Şahin contributed with his knowledge of crystallography; it was also invaluable.

My sincere and heartfelt thanks are to my family. I am extremely honored to be part of your family. To my mother, Elif Temel, and my father, Mehmet Temel: I am grateful for how you raised my lovely sister, Melis, and me. Without your effort, sacrifice, support, and belief, I could not imagine this success. My sister Melis Temel Özkılıç was always by my side. I cannot put into words my feelings and gratitude to you. Thank you for your existence. Since my childhood, I have wished for a brother. I am grateful to Mahmut Özkılıç, who fulfilled this dream of mine. Lastly, I would like to thank my greatest cousin, Ali Bertan Soysüren; he always listened to me. I appreciate for every single moment that I spent with all of you.

I am also grateful to my precious friends. My special thanks to the former and current members of Türkmen Research Group: Eylül Çalıkyılmaz, Bilge Banu Yağcı, Dilgam

Ahmadli, Badar Munir, Suay Bilgin, Gizem Yılmaz, Umut Mert Karacoğlu, Damla Gül, Kaan Berkay Ceyhan, Palvan Jumayev and İsmail Yaşar Kökçüler. Every day in the laboratory was full of fun, and informative thanks to you. I learned a lot from you, thank you for everything. I also thank my friend, Elif Sena Temirci, for being there and supporting me since high school. I met Rana Uzunlar a little bit late, but I hope you will always be there. Your support was insane. And, Elif Sıla Akbulut, you are the proof that the distance doesn't matter, I am grateful for your friendship.

LIST OF ABBREVIATIONS

1,8-DHN	1,8-dihydroxynaphthalene
Å	Ångström
ATR	Attenuated Total Reflection
DCC	*N*,*N*′-Dicyclohexylcarbodiimide
DCM	Dichloromethane
DCU	Dicyclohexylurea
DMAP	4-Dimethylaminopyridine
DMF	Dimethylformamide
FTIR	Fourier-Transform Infrared
HRMS	High-Resolution Mass Spectrometry
M.P.	Melting Point
nm	Nanometer
NMR	Nuclear Magnetic Resonance
R*f*	Retention Factor
SC	Single Crystal
SCSC	Single-Crystal-to- Single-Crystal
THF	Tetrahydrofuran
TMS	Tetramethylsilane
TLC	Thin Layer Chromatography
UV	Ultraviolet
UV-Vis	Ultra-violet Visible
XRD	X-ray diffraction

TABLE OF CONTENTS

LIST OF FIGURES

LIST OF SCHEMES

LIST OF TABLES

1. Template-Directed Photochemical [2+2] Cycloaddition Reactions of Naphthalene Acrylic Acid Derivatives

1.1 Introduction

1.1.1 Cyclobutane Ring in Natural Products

Natural products are secondary metabolites produced by living life forms, and they are often biologically active. Natural products and their derivatives, such as alkaloids and flavonoids, can be utilized as medicine, and as an example, they can be used during cancer treatment and chemotherapy.[1] Because of this crucial feature, natural products are one of the focus of organic and medicinal chemists.

(S)-Norcoclaurine **Cholestrerol**

Figure 1. Examples of natural products (S)-norcoclaurine, and cholesterol

Developing new drug molecules, natural products, and their analogs required analytical tools for isolation, characterization, etc. From the 1990s up to today, studies have given rise to the development of new technologies and strategies (e.g., genome mining).[2] Therefore, works on natural product synthesis contribute to organic chemistry, medicinal chemistry, and the pharmaceutical industry and burst the innovation of new technologies.

Figure 2 shows four examples of natural products, containing cyclobutane rings in their core structure. Sagerinic acid is a secondary metabolite resulting from the dimerization reactions of phenylpropanoid molecules, and it can be isolated from sage.[1,3] Traditionally, for decades, people have been consuming sage for digestion purposes.[4] Diseselin A and palhinoside D belong to the coumarin family and flavonoid class, respectively. Lastly, tengerensine is a member of isoquinoline alkaloids known for antifungal, antiviral, and antitumor characteristics.[5] Those four examples show the existence and importance of the cyclobutane core in natural products. Their biologically active features make the methodology development of synthesis cyclobutane rings valuable.

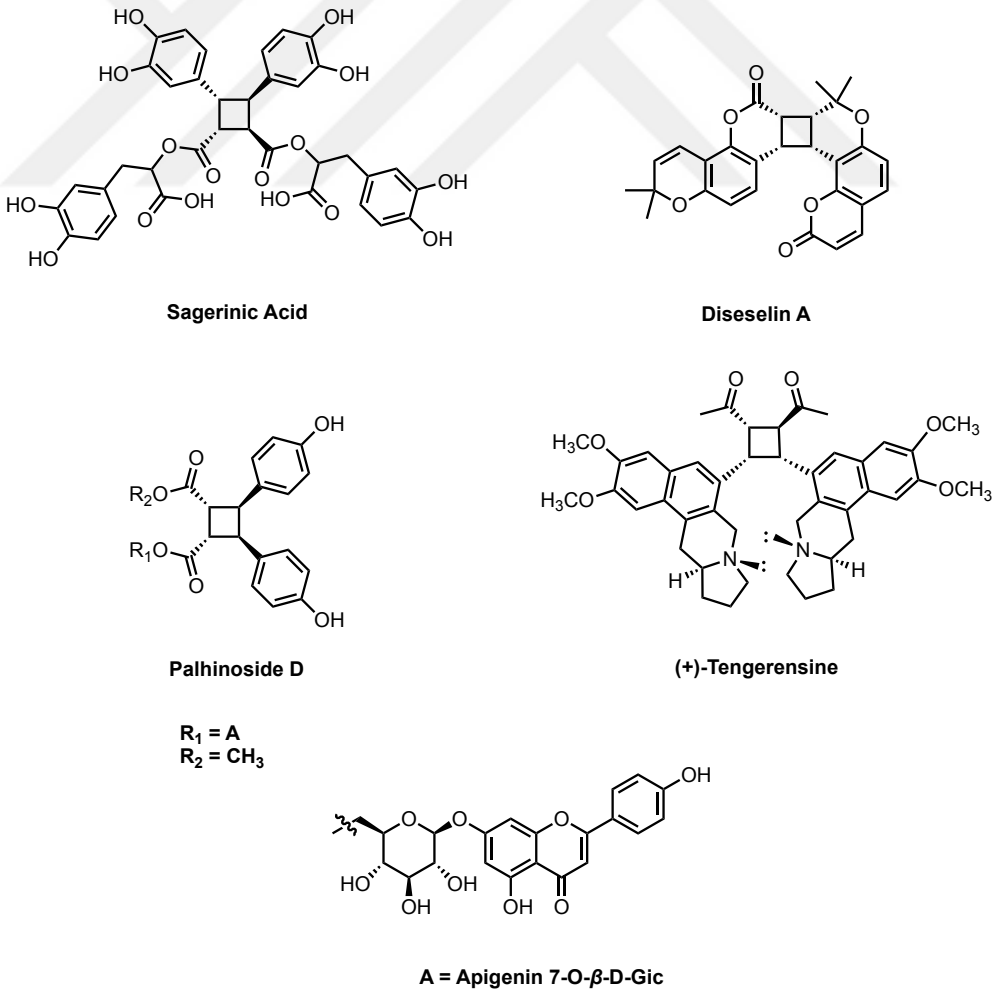

Figure 2. Examples of natural products with cyclobutane ring

1.1.2 Methods for the Synthesis of Cyclobutanes

Four-membered rings can be constructed via various routes with different conditions and reagents. [2+2] Cycloadditions (intramolecular or intermolecular) is one of the examples. In addition to that, Wolff rearrangement can also be employed in cyclobutane ring construction by benefitting from the formed ketene molecules in the next steps. The formed ketene molecules, due to the Wolff rearrangement, can undergo [2+2] cycloaddition reaction and construct a cyclobutane ring.[5,6]

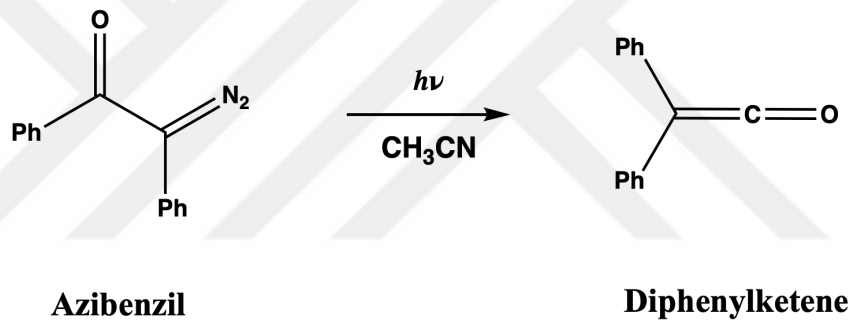

Azibenzil **Diphenylketene**

Scheme 1. Wolff rearrangement of azibenzil

The Wolff rearrangement ends up with the formation of ketene (Scheme 1).[6] As well known, ketenes are highly reactive molecules or intermediates, and this feature makes their isolation generally uneligible. However, they can undergo a reaction right after their formation in the reaction medium and yield a four-membered ring. Therefore, those reactive intermediates are important and efficient tools for cycloaddition reactions; they can give ß-lactam, a heterocyclic four-membered ring, as a result of the reaction (Scheme 2).[7]

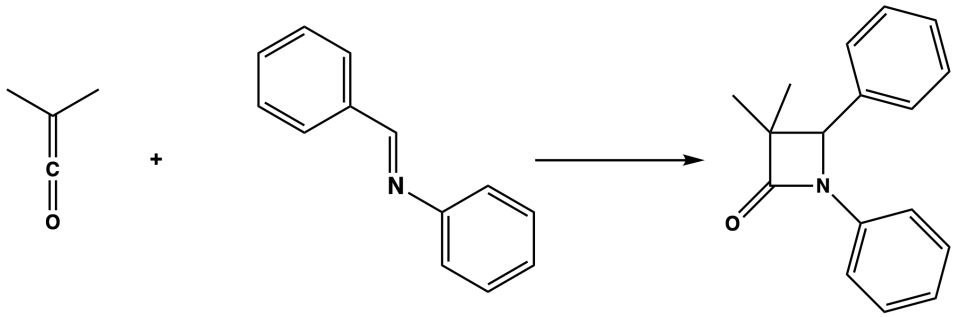

Dimethylketene **N-Phenyl Benzylideneamine** **3,3-dimethyl-1,4-diphenyl-azetidin-2-one**

Scheme 2. Staudinger synthesis; reaction of dimethylketene and *N*-phenyl benzylideneamine

In addition to ketenes, alkenes can be employed in cyclobutane synthesis. Through cycloaddition reactions, two olefin molecules or an olefin and enone molecules can form a four-membered ring structure; however, because light is essential for the reaction, this type of cycloaddition reaction is called [2+2] photocycloaddition reaction.[8] Without light, those reactions cannot occur due to the lack of constructive interference.

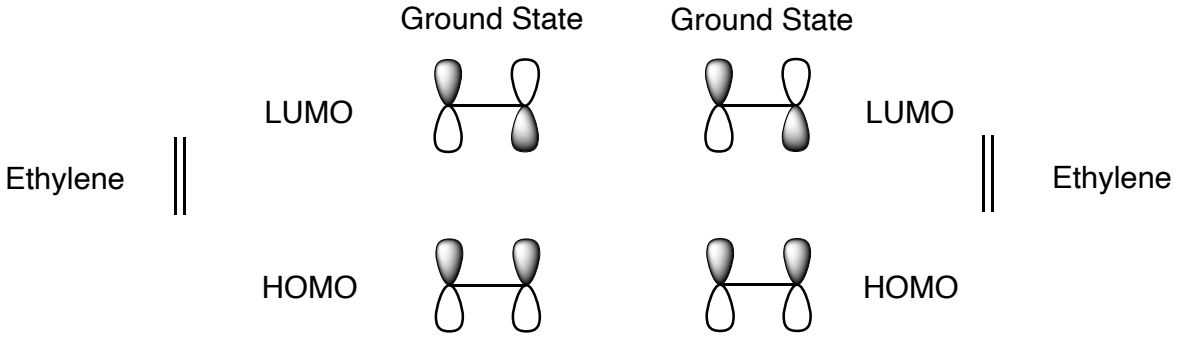

Figure 3. Ground state HOMO and LUMO of ethylene molecules

The ground state HOMO and LUMO of the two ethylene molecules are shown in Figure 3. Without light, the following phase in Figure 4 is inevitable because electrons in

both ethylene molecules will stay in their ground state. Due to the destructive overlap, this phase cannot give rise to σ-bond formation; thus, cyclobutane ring cannot be formed.

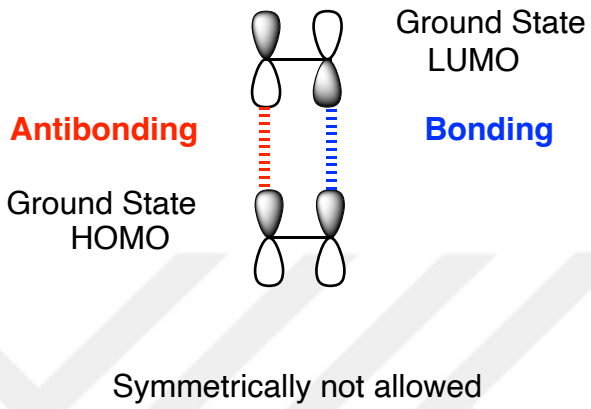

Figure 4. One of the ethylene molecule's ground state HOMO, and the other's ground state of LUMO

As stated, under this circumstance, suprafacial overlapping is not possible. Therefore, cyclization cannot take place. However, photons can excite electrons from HOMO to LUMO. This excitation causes the new highest occupied molecular orbital, as shown in Figure 5.

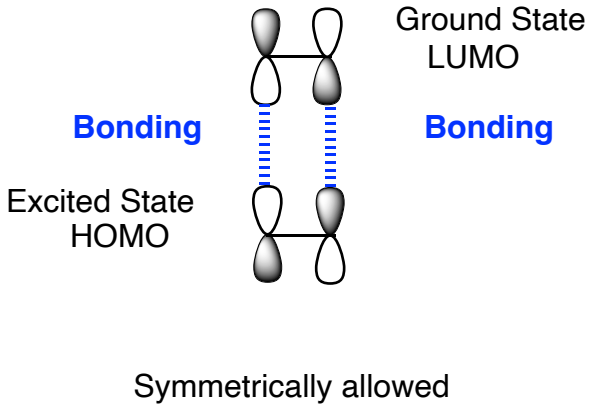

Figure 5. One of the ethylene molecule's excited state HOMO, and the other's ground state of LUMO

With the excitation of the electrons from HOMO to LUMO, suprafacial overlapping becomes possible between the ground-state ethylene molecule's LUMO and the new excited state HOMO of another ethylene molecule.[9] Interaction between those MOs creates two new sigma bonds and, therefore, cyclobutane structure thanks to the absorption of light.

As described, absorption of light is crucial for this reaction and it is clearly stated by Grotthuss-Draper law. To achieve a successful photochemical reaction, absorption of light is vital.[10] In addition to that, the wavelength of the absorbed light will determine the electronic level of the molecule that the electron is going to be promoted. Because, as mentioned in Kasha's rule, the energy of the light, can promote the electron to LUMO or LUMO+n etc. However, even if the electrons are at higher energy LUMO+n after the absorption of light, they will relax to LUMO.[11] Therefore, what is important for these reactions to occur is the absorption of light.

1.1.3 Template-Directed [2+2] Photodimerization

Described [2+2] photocycloaddition reactions can be run in solid state or solution. In solution without a template that partially restricts the movement of the molecule, there is a great possibility of *cis-trans* isomerization, as well as the formation of various diastereomers, and side products. For example, 1,2-diphenylethylene (stilbene) can give homodimer in the solid state, but the intramolecular reaction between the double bond of alkene and phenyl group gives phenyl-olefin dimerization product (Scheme 3).[12]

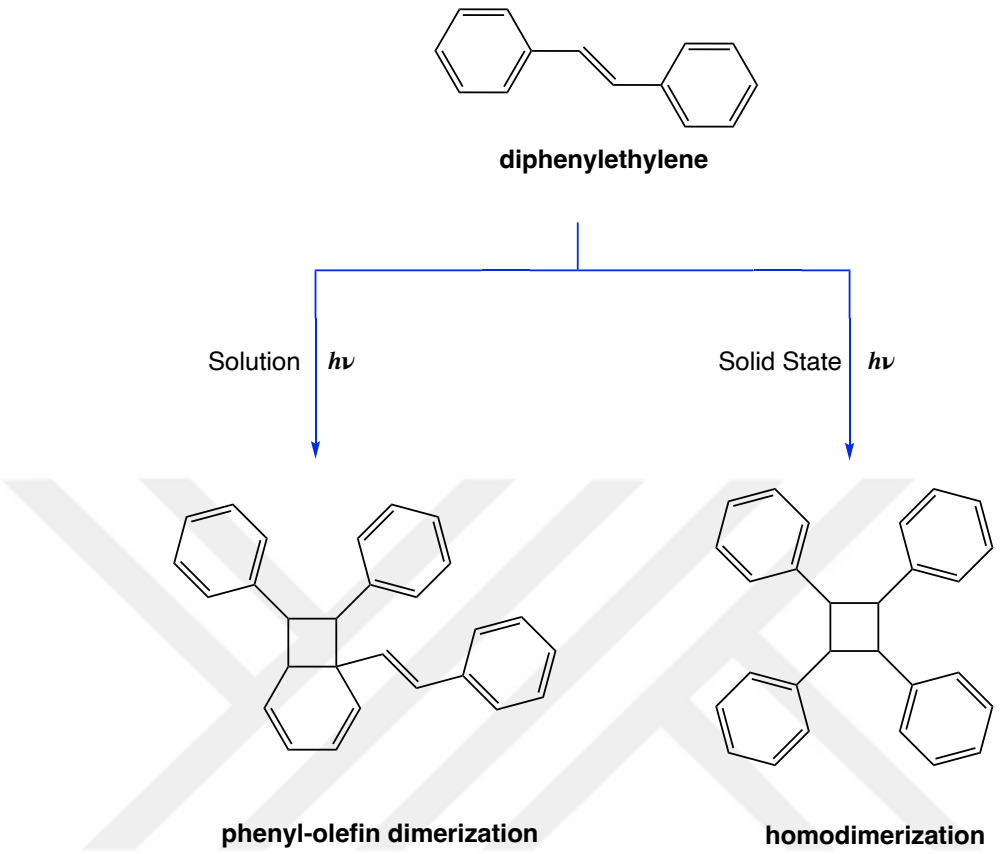

Scheme 3. Cyclization of diphenylethylene

However, in the example of template-directed photocyclization reaction in solution, Fleming and coworkers demonstrated that the styrenyl group can be attached to the alkene moiety as a template molecule and results in selective *cis*-cyclobutane product formation after the irradiation and template removal, respectively (Scheme 4).[13]

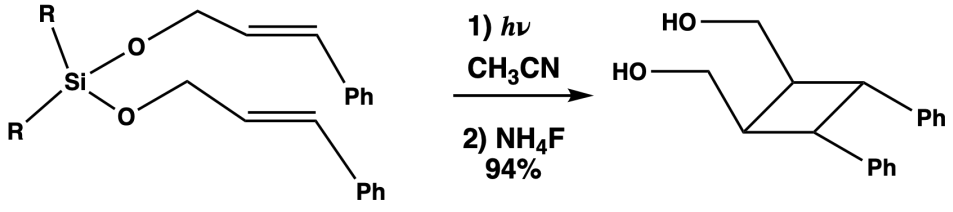

Scheme 4. Dicinnamyloxysilane photohomodimerization

Besides Fleming's work, König and co-workers demonstrated that three diols are also good templates for the homodimerization reaction of cinnamic acid in solution. However, it was only applicable for *trans*-cinnamic acid's photocyclization (Scheme 5).[14]

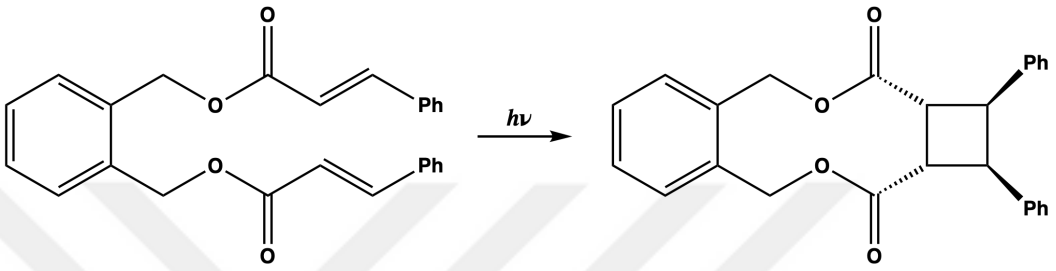

Scheme 5. Template-bound homodimerization of *trans*-cinnamic acid

For solid-state reactions, researchers have been studying practical methods to synthesize cyclobutane rings for decades. Those studies are based on the Schmidt criteria. If the criteria defined by Schmidt and co-workers are met, the formation of a sigma bond between two carbon atoms is observable. These criteria emphasize the existence of the two parallelly aligned double bonds, or alkenes, separated by the distance d. The distance, d, between the alkenes placed on top of each other must be smaller than 4.2 Å and greater than 3.5 Å (Scheme 6).[15]

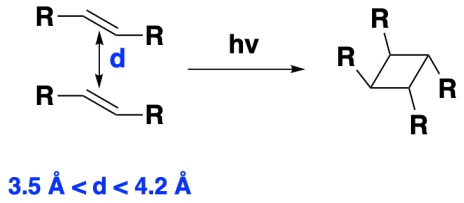

Scheme 6. Schmidt criteria and [2+2] photocycloaddition in solid state

Running such reactions in a solid state has several advantages. First, solvent use is minimized in the solid state, making the chemistry greener. Secondly, as mentioned above,

there is a higher possibility of *cis-trans* isomerization in solution. Also, the construction of single diastereomers is possible with the template molecule in solid-state irradiation. Due to all these reasons, strategies for template-directed photochemical cyclization have been developed (Scheme 7).[16]

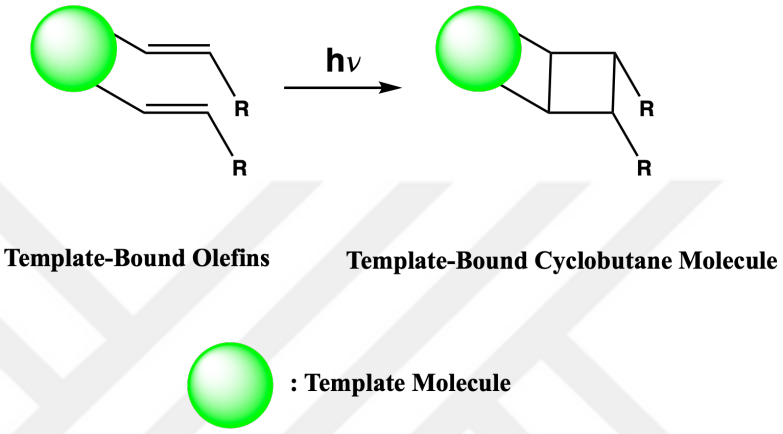

Scheme 7. Template-directed [2+2] photodimerization

Several features can be taken advantage of when selecting a suitable template. For instance, MacGillivray and co-workers' study uses the hydrogen bonding ability of template molecules, 1,3-dihydroxybenzene (resorcinol), and the reactant. In this way, they provided the appropriate distance between parallelly aligned double bonds. The reported distance for the given olefins is approximately 4.0 Å; therefore, they could construct a cyclobutane product after the irradiation of crystals (Scheme 8).[17]

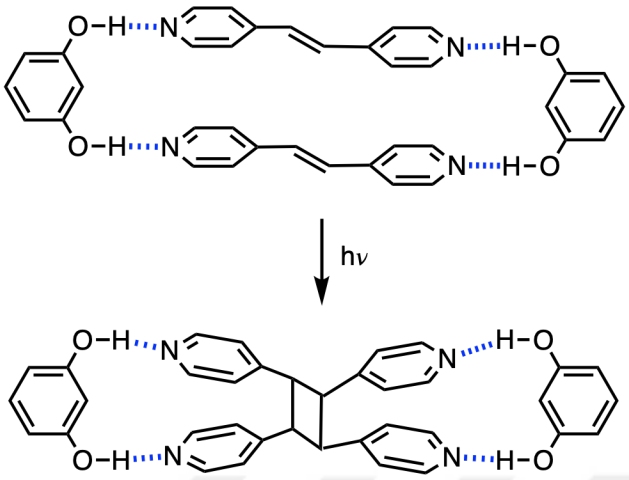

Scheme 8. Photochemical [2+2] cycloaddition reaction of *trans*-1,2-bis(4-pyridyl)ethylene

In addition to hydrogen bonding, template molecules can be covalently bound to the reactants, and after the construction of the ring, they can be removed. An example of a covalent template can be seen in Scheme 9. Wolf and co-workers investigated the bisaniline molecule's efficiency as a template in homodimerization reactions of two *trans*-cinnamic acid derivatives. They reported high yields for the irradiation of template-bound alkenes when Ar groups are Ph or 3,4-Me_2-Ph. Template removal is also possible with acid treatment: 30% HCl.[18]

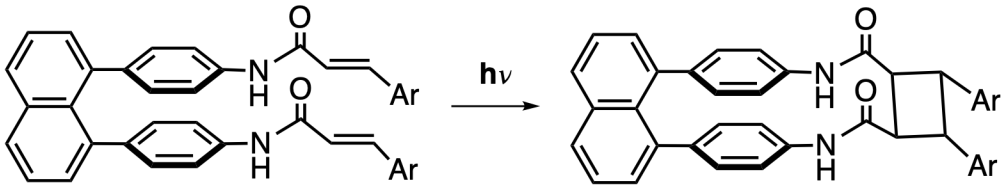

Scheme 9. Bisaniline-bound [2+2] photocyclization reaction

As another example, Hopf and co-workers' pioneering study with the covalent template (**1**), which was synthesized in 8 eight steps, can be examined. However, as is the limitation with other given templates, cycloaddition with 4,15-diamino[2.2]paracyclophane (**1**) is also restricted by the homodimerization of cinnamic acid.[19]

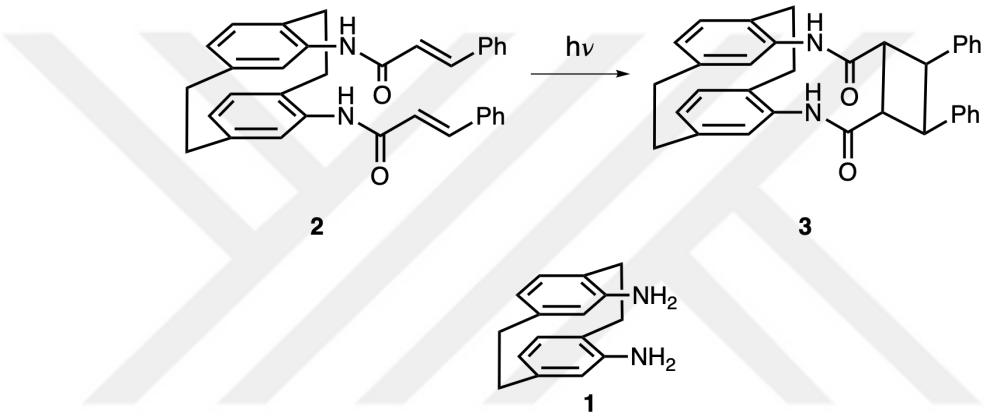

Scheme 10. The use of a paracyclophane-based template molecule in a [2+2] photocyclization reaction

1.1.4. 1,8-Dihydroxynaphthalene as Template Molecule

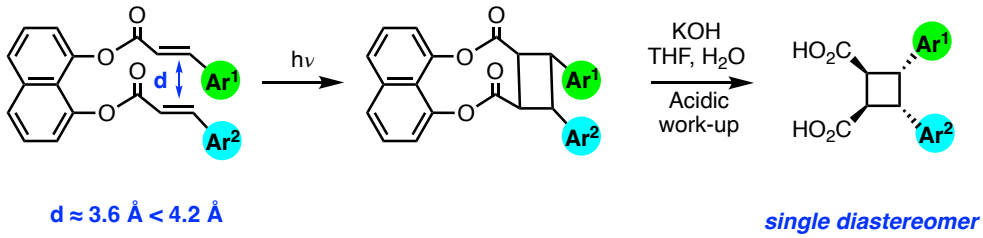

Scheme 11. 1,8-Dihydroxynaphthalene-bound photochemical [2+2] cycloaddition

Previously given examples and many others in the literature are effective for the homodimerization of the olefins. Especially for the [2+2] photocycloaddition reaction of cinnamic acid and vinylogous cinnamic acid derivatives, there was a gap in which 1,8-dihydroxynaphthalene fills perfectly. In 2021, for the first time, Türkmen and co-workers reported 1,8-DHN as a covalent template in the [2+2] photochemical cycloaddition reactions of cinnamic acids. This methodology is applicable for both homo- and heterodimerization reactions of cinnamic acid derivatives and investigated in broad substrate scope in 2023.[20,21] Further studies by Türkmen and co-workers in 2024 proved that this new methodology is also applicable to vinylogous cinnamic acids.[22] In addition to tha,t importantly, this path can construct cyclobutane products as single diastereomers in solid-state reactions with good to excellent yields.[20–22]

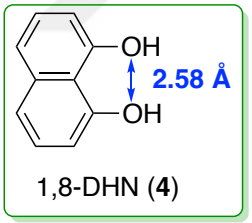

Figure 6. The structure of 1,8-dihydroxynaphthalene

1,8-DHN was promising for the Schmidt criteria due to the parallel alignment of the two hydroxyl groups with the distance d corresponding to 2.58 Å. In addition to that feature, in 2018 and 2020, Türkmen and co-workers demonstrated that 1,8-DHN has intramolecular hydrogen bonding and may allow sequential modification for further reactions besides the pKa differences.[23–25]

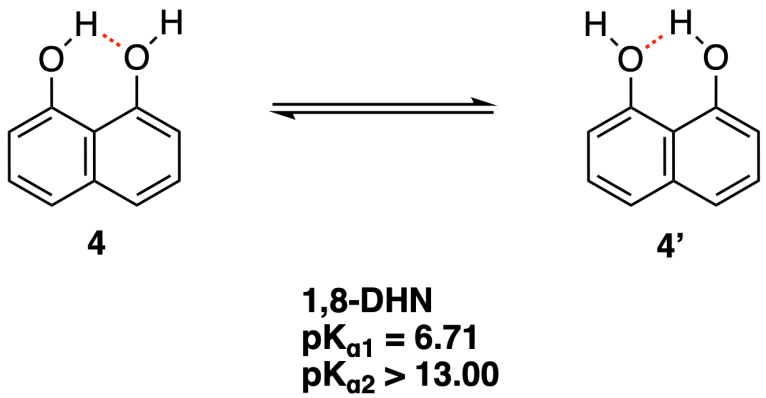

Scheme 12. Intramolecular hydrogen bonding of 1,8-dihydroxynaphthalene

In addition to the given features, 1,8-DHN is also commercially available. That opportunity shortens the synthetic route to yield cyclobutane structure because there is no need to synthesize the template.

1.1.5. Aim of the First Part of the Thesis

Considering the previous success of the 1,8-DHN-bound pathway for the photochemical [2+2] cycloaddition reaction of cinnamic acid and vinylogous cinnamic acid derivatives, we aimed to work on the template-directed cycloaddition reactions of naphthalene acrylic acids. It was important due to the unknown reactivity of naphthalene rings in the template-bound photochemical [2+2] cycloaddition reaction because of the high conjugation. When one compares the previous studies of Türkmen and co-workers, it is recognizable that heteroaryl and substituted phenyl-containing reactions were examined during these studies. Those previous template-bound reactions gave excellent results for aryl- and heteroaryl-containing cinnamic acid and vinylogous cinnamic acid derivatives with diastereocontrol.[21,22,26] However, there is no data for the template-bound reactions of naphthalene acrylic acid. Additionally, naphthalene acrylic acid's template-bound

cycloaddition reactions have the potential for further analog of natural product synthesis. With this purpose, a reaction pathway was designed in four main steps for symmetrical and unsymmetrical cyclobutane construction. (*i*) synthesis of naphthalene acrylic acid from 1-naphthol, (*ii*) synthesis of template-bound cinnamic acid derivatives, (*iii*) template-bound diester formation in solid state and solution, (*iv*) removal of the templates after the irradiation with 365 nm UV light (Scheme 11). All new compounds synthesized in this work have been fully characterized by ^{1}H NMR, ^{13}C NMR and ATR-IR spectroscopies, and HRMS.

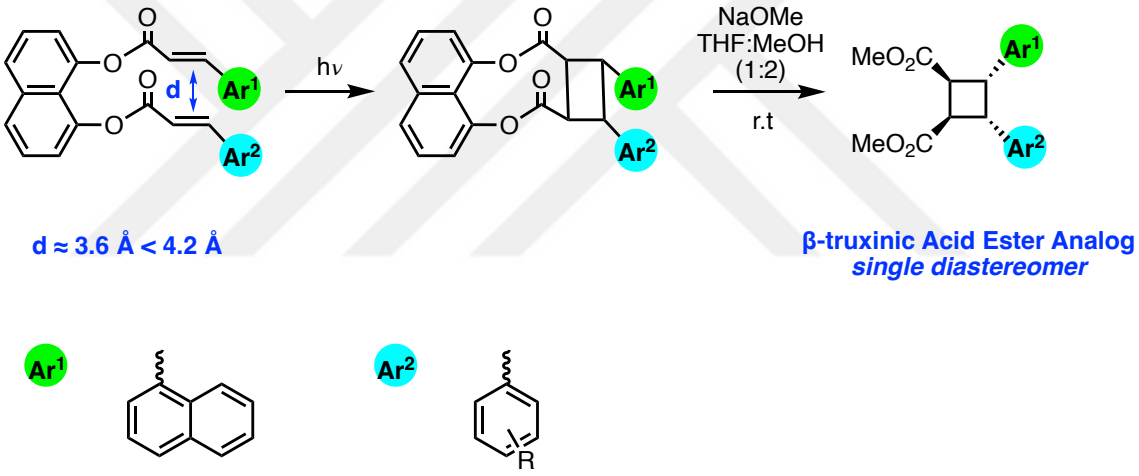

Scheme 13. Synthesis pathway of ß-truxinic acid ester analogs

1.2. Results And Discussion

1.2.1. Synthesis of 3-(1-Naphthyl)acrylic Acid

In order to synthesize unsymmetrical diesters of naphthalene acrylic acid, 1-naphthol was utilized (Scheme 14).

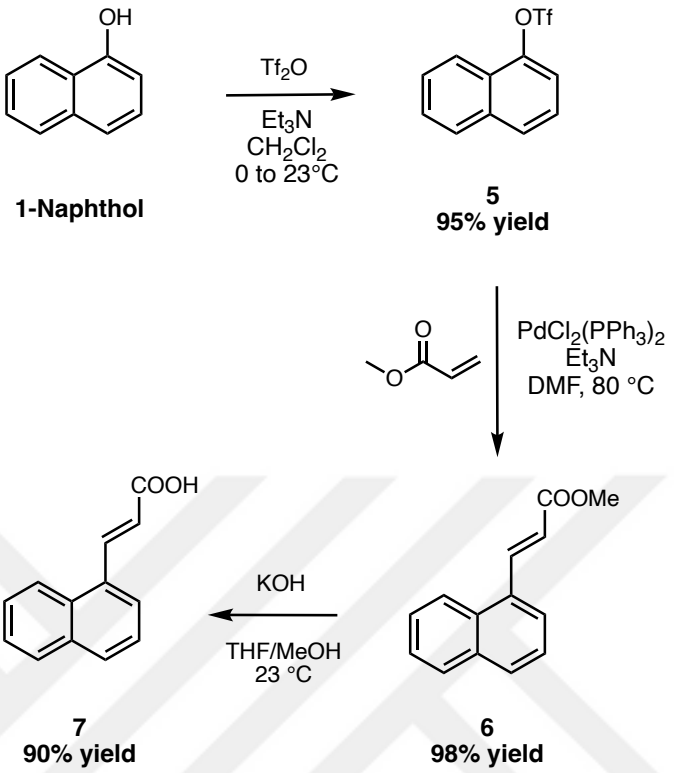

Scheme 14. Synthesis Pathway of 1-Naphthalene Acrylic Acid

As known, the Mizoroki-Heck coupling reaction can be used for C-C bond formation between an aryl and vinyl halide and alkene catalyzed by a Pd catalyst.[27] Therefore, (*E*)-methyl-3-(1-naphthyl)acrylate (**6**) was synthesized through Mizoroki-Heck coupling between aryl triflate **5** and methyl acrylate with *trans* selectivity in 98% yield. This cross-coupling reaction consists of four main steps: oxidative addition, migratory insertion, ß-hydride elimination, and reductive elimination. However, before directly using 1-naphthol in the C-C bond formation reaction, it had to be prepared for the oxidative addition step. Because when one checks the order of reactivity, it is mentioned that the -OTf group gives a better rate than -OH and -Cl in the Mizoroki-Heck cross-coupling reaction.[27]

After getting molecule **5** through a triflation reaction of 1-naphthol using triflic anhydride under basic conditions in 95% yield, Mizoroki-Heck coupling was applied to

compound **5** and methyl acrylate. Like various examples in literature [28,29], compound **6** was also synthesized successfully. Since carboxylic acid gives a better yield while synthesizing template-bound monoester from acyl chloride and is required for Steglich esterification, the synthesized molecule **6** was hydrolyzed to reach the target molecule **7**.[21,30] By simple hydrolysis with potassium hydroxide, 3-(1-naphthyl)acrylic acid was synthesized in 90% yield. The synthesized molecules **6** and **7** were characterized by ^{1}H NMR spectroscopy. However, unlike the compound **6**, 3-(1-naphthyl)acrylic acid had a solubility problem in $CDCl_3$. Therefore, deuterated dimethylsulfoxide was used for ^{1}H NMR. In addition, whether compound **7** was a polymorph of commercially available 3-(1-naphthyl)acrylic acid was determined by examining its melting point. As a result of this analysis, it was concluded that compound **7** has the same melting point (211.8-212.4 °C) as the commercially available 3-(1-naphthyl)acrylic acid (210 to 212 °C).[31]

During the synthesis of compounds **6** and **7**, it was understood from ^{1}H NMR studies that the configurations of the double bonds of compounds **6** and **7** are *trans*. In 1959, Karplus showed that the coupling constants of *trans* protons are larger than the *cis* ones.[32] For the vinyl *trans* protons, the coupling constant *J* is in the range of 11-18 Hz, while it is between 6-15 Hz for the vinyl *cis* protons.[33] Therefore, although the splitting patterns, number of peaks, and integrals are identical, one can identify the conformation of the synthesized compounds from the coupling constant.

For compound **6**, protons of alkene give two peaks at 8.55 (1H, d, J = 15.8 Hz) ppm and 6.54 (1H, d, J = 15.8 Hz) ppm in deuterated chloroform and prove it has *trans* configuration. For compound **7**, protons of alkene give two peaks at 8.43 (1H, d, J = 15.7

Hz) ppm and 6.64 (1H, d, J = 15.7 Hz) ppm in deuterated dimethylsulfoxide and prove it also has *trans* configuration.

1.2.2. Synthesis of Unsymmetrical Diesters

A previously reported procedure by Türkmen Research Group was followed to synthesize unsymmetrical diesters, with a minor change in reaction period and equivalence, to get a 1,8-DHN bound mono-ester.[21] Initially, for compound **11**, phenyl was selected as the aryl group to investigate the effect of high conjugation of naphthalene in template-bound photochemical [2+2] cycloaddition reaction (Scheme 15). From commercially available *trans*-cinnamic acid, acyl chloride **9** was prepared, and through esterification, monoester **10** was synthesized in 78% yield. Due to the full conversion of acyl chloride, column chromatography was not applied to it; however, this was not the case for monoester. There was a side product of diester (double addition of compound **9** to template) with the excess 1,8-DHN in the reaction medium. Therefore, further purification was carried out for the monoester **10**.

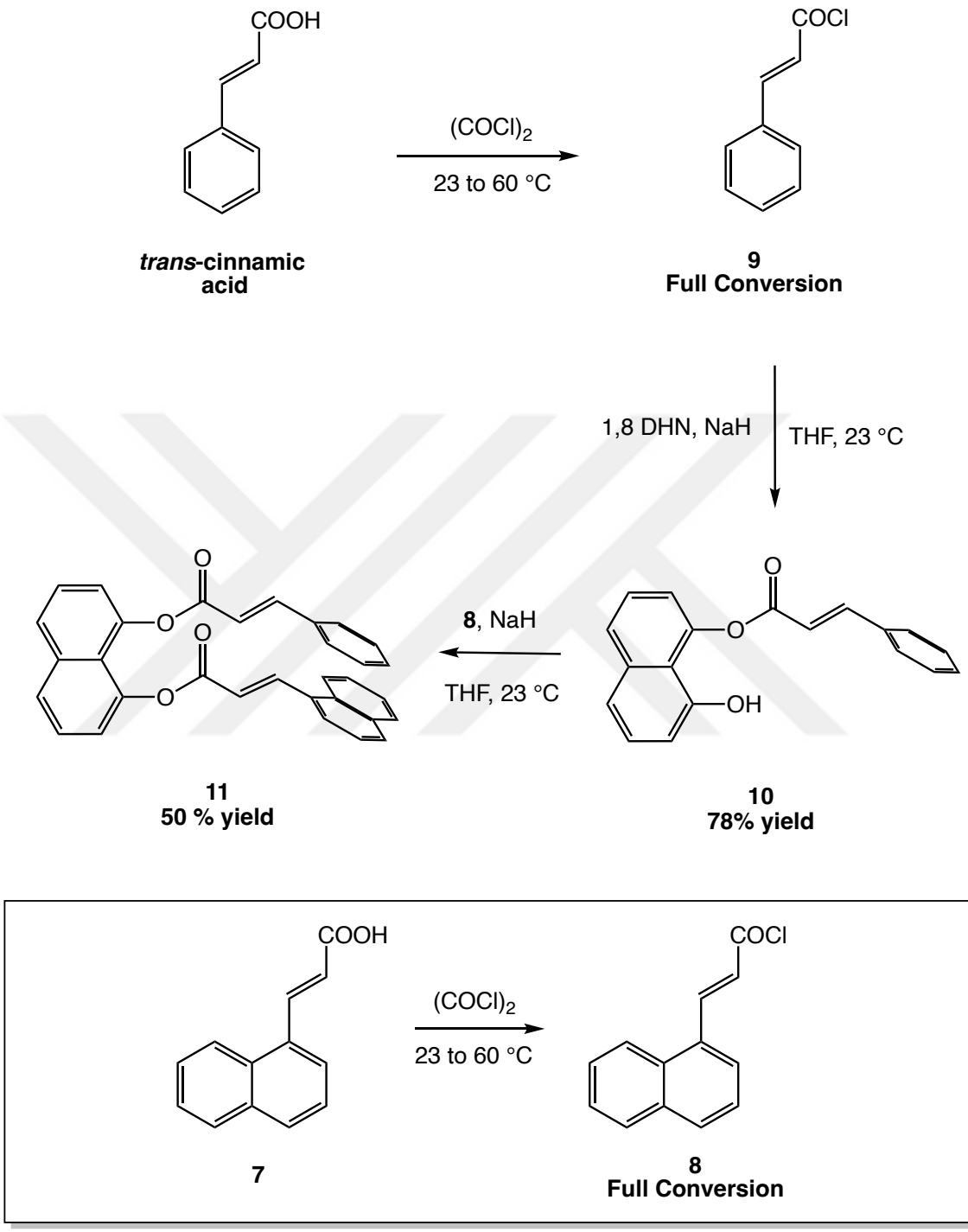

Scheme 15. Synthesis pathway of unsymmetrical diester **11**

Compound **7** was planned to be attached to the template after synthesizing the monoester **10**. The same procedure was followed to synthesize acyl chloride from compound

7, and full conversion was provided. After that the formation of yellow solid acyl chloride **8**, it bound to the monoester **10** through esterification. The reaction yield was 50% as a result of the overnight reaction at room temperature.

Due to the high conjugation, the synthesized diester **11** was stored after covering the scintillation vial with aluminum foil. As known, when conjugation increases in the molecule, the UV absorption wavelength (λ) also shifts to longer wavelengths.[34] Therefore, taking precautions to minimize the effect of the daylight was also important.

The same synthesis strategy was applied to the diester **16**. In this molecule, 4-methoxycinnamic acid was selected as the aryl group, which has higher electron density due to the electron-donating methoxy group and bulkier feature than phenyl (Scheme **16**). Acyl chloride compounds **14** and **8**, were synthesized with full conversion and underwent reactions with 1,8-DHN and monoester **15**, respectively. Overnight reaction of monoester **15** and acyl chloride **14** produced the foam-like yellow diester **16,** and it was purified with 51% yield. Due to the high conjugation, like diester **11**, the synthesized compound **16** was also stored after covering the scintillation vial with aluminum foil.

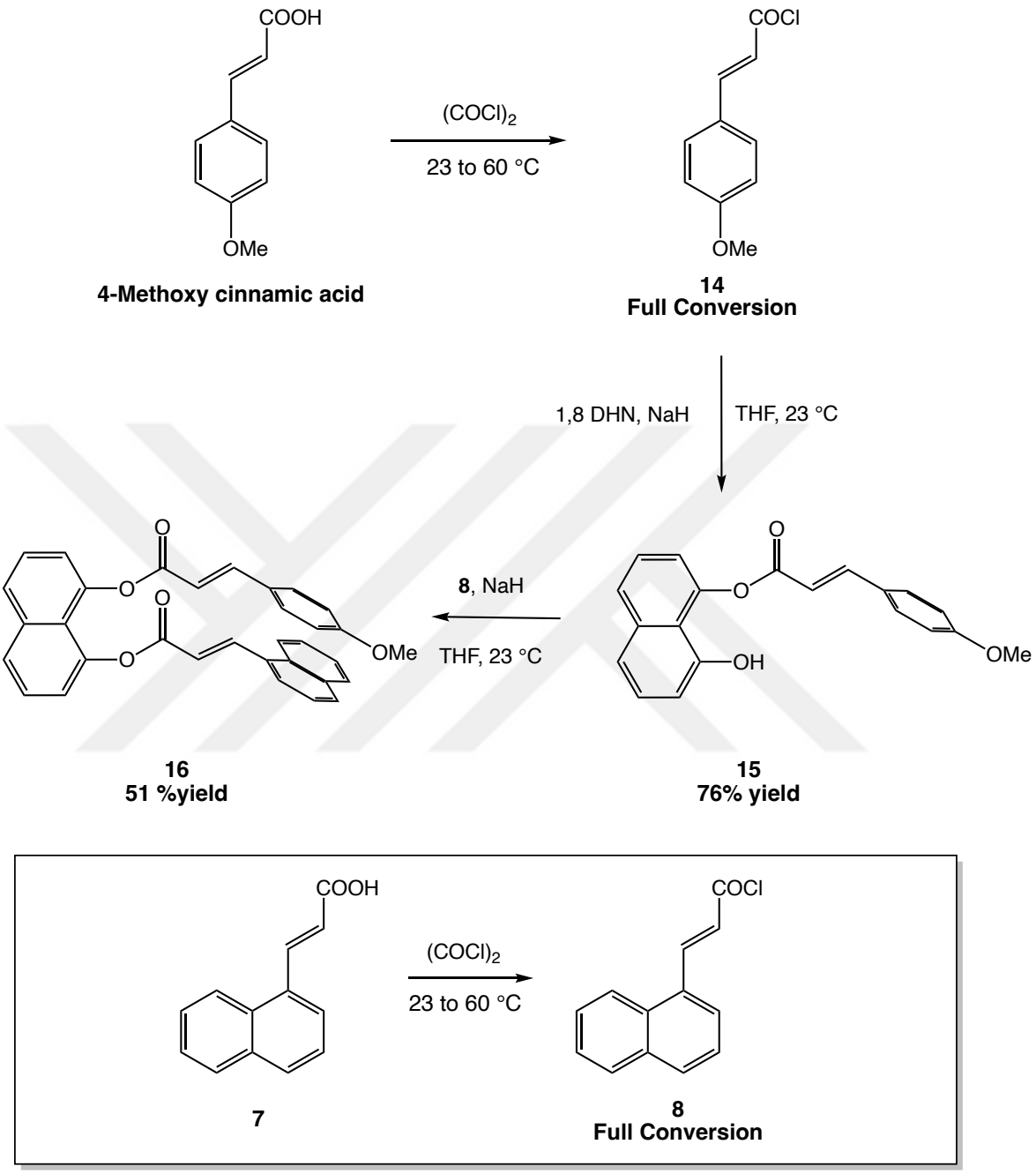

Scheme 16. Synthesis pathway of unsymmetrical diester **16**

1.2.3. Photochemical [2+2] Cycloaddition Reactions of Unsymmetrical Diesters in Solid State

As explained previously with examples from the literature, photochemical [2+2] cycloaddition reactions can occur in both liquid and solid states when the criteria are met. The synthesized diester molecules were reacted under 365 nm UV light in both solid and liquid states. For solid state reactions, quartz glass microscope slides that transmit light of 365 nm wavelength were used.[35] The experimental set-up consisted of a regular nail dryer equipped with four 9-Watt fluorescent bulbs (UVA, 365 nm), quartz microscope slides, and paper clips to fix the slides. The simplicity of the setup is also one of the advantages of the previously designed methodology.[26]

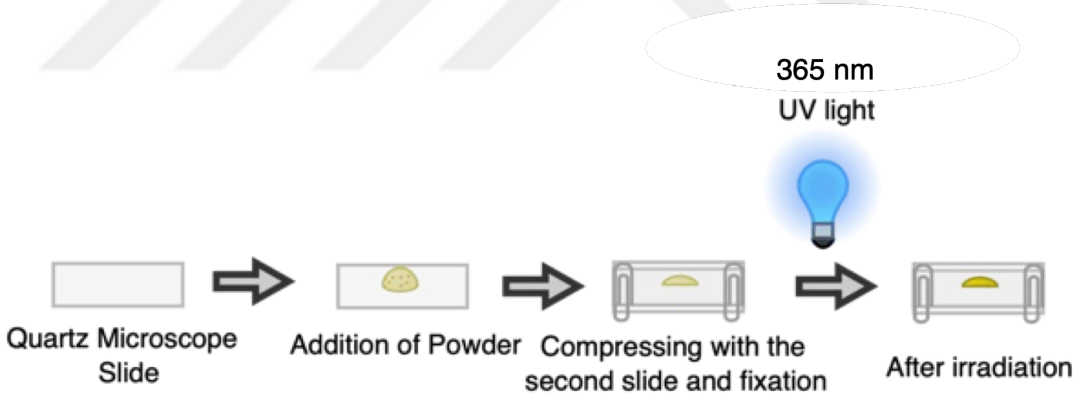

Figure 7. Illustration of the powder irradiation

Diester **11** was irradiated between quartz microscope slides for 16 h. However, in this first experiment, the appearance of the diester was not homogenous. After squeezing the slides, some parts were oil but had a thick-dense look, while some parts had a powder-like look. It was predicted that there was a solvent residue; however, to see the effect, irradiation for 16 h was completed. Every 4 h, the crude mixture was mixed to provide homogenous

light distribution. After 16 h, ^{1}H NMR analysis showed 60% conversion, and after the column chromatography, a yellowish foam-like product was collected in 38% yield. Following that, a completely solid, solvent-free diester, **11,** was irradiated for 32 h to increase the conversion. However, the conversion was recorded as 15% through ^{1}H NMR spectrum. By column chromatography, pure product **12** was isolated in 11% yield.

The difference between the two reactions of diester **11** showed us that the effect of solvent may be significant. This small amount of solvent residue might have enhanced the yield by providing atoms less limited movement compared with the solid state.

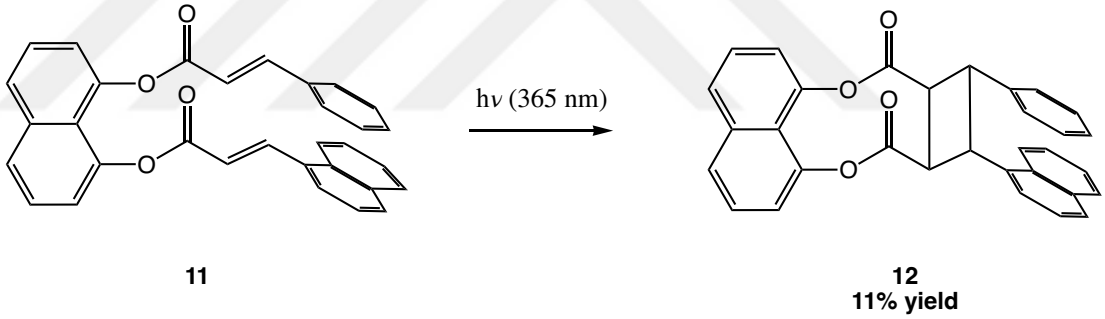

11 **12**
11% yield

Scheme 17. Irradiation of diester **11** in solid-state

Following the photochemical [2+2] cycloaddition reaction of diester **11**, to form cycloadduct **17,** diester **16** was irradiated. To be sure that there was no solvent residue in diester **16**, high vacuum was applied for a longer time. The yellow foam-like solid was relatively thin when compared with the powder of diester **11**. After squeezing the slides and irradiating the diester for 32 hours, ^{1}H NMR analysis showed 50% conversion, and after the column chromatography, a yellowish oil-like cycloadduct **17** was collected in 35% yield.

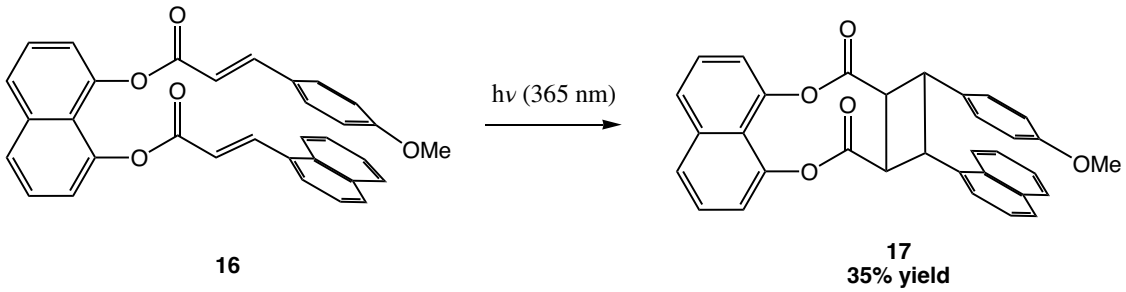

16 **17**
35% yield

Scheme 18. Irradiation of diester **16** in solid-state

Although the reaction yields are not high, the formation of [2+2] cycloaddition product showed that the template molecule provides parallelly aligned two double bonds, which are separated by the distance d smaller than 4.2 Å and greater than 3.5 Å.

1.2.4. Photochemical [2+2] Cycloaddition Reaction of Unsymmetrical Diesters in Solution

In addition to the photochemical [2+2] cycloaddition reaction of template-bound diester **11** and **16** in the solid state, the unsymmetrical diesters underwent a reaction in solution using chloroform as solvent (Scheme 19).

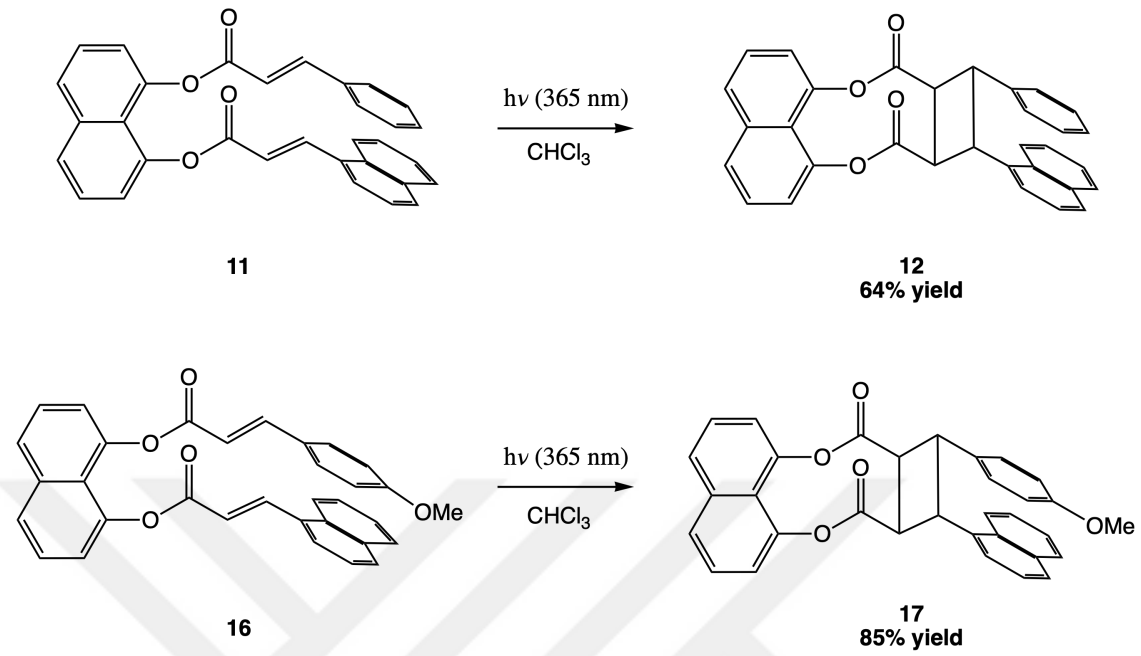

Scheme 19. Irradiation of diester **11** and **16** in solution

For solution reactions, a quartz glass test tube that transmits light of 365 nm wavelength was used.[35] To dissolve compounds **11** (23.6 mg) and **17** (18.4 mg), 3.5 mL of chloroform was used. To provide a more homogenous light distribution, reactions were mixed with a stir bar on the magnetic stirrer for 20 hours. During the reaction period, in order to monitor progress, thin-layer chromatography (TLC) was employed. However, due to the high conjugation of diester molecules, spots of starting compounds **11** and **16** glow strongly on the TLC plate under the 254 nm UV light. The conversion for compound **12** was 90%, and the conversion for compound **17** was 95% as determined based on their crude ^{1}H NMR spectra. However, as stated, the starting spots glowed strongly, and that is why the comparison of them with cycloadduct by TLC was misleading before quenching the reaction. Also, decreased conjugation in cycloadducts weakened the glow of product spots on the TLC plate.

Even though the conversions of both reactions were high, their isolation from the starting diesters was not straightforward due to the close spot on the TLC plate in tested solvent systems. Pure cycloadduct **12** was obtained in 64% yield, and cycloadduct **17** was purified in 85% yield. However, the conversion proved with ^{1}H NMR and showed that 1,8-DHN was again an efficient template for [2+2] photochemical cycloaddition reactions of naphthalene acrylic acid. Overall, our results demonstrate that the irradiation of diesters **11** and **16** proceed more efficiently and with higher isolated product yields in solution compared to solid state.

1.2.5. Template Removal from Heterodimers

The last step of the designed synthesis was template removal to get β-truxinic acid ester analogues, i.e. [2+2] cycloaddition product without template molecule. Successfully synthesized and isolated heterodimers **12** and **17,** include ester moiety. By the use of NaOMe, the template can be removed through a transesterification reaction thanks to the cleavage of a C-O single bond by methoxide ions. In other words, a nucleophilic substitution reaction occurs when the methoxide ion attacks the carbonyl carbon, which results in template removal. At the end of this reaction, in addition to the cyclobutane ring, there are possible by-products that are isolated relatively easily. One of them is the sodium salt of the 1,8-DHN, and the other possible by-product is 1,8-DHN itself. Due to the poor solubility of the salt in organic solvent, the case where sodium salt forms is the simplest one to purify. For the 1,8-DHN formation, column chromatography is needed to isolate the pure cycloadduct. At this point, the retention time of the 1,8-DHN in the column due to the high interaction with silicon dioxide can be considered as advantageous.

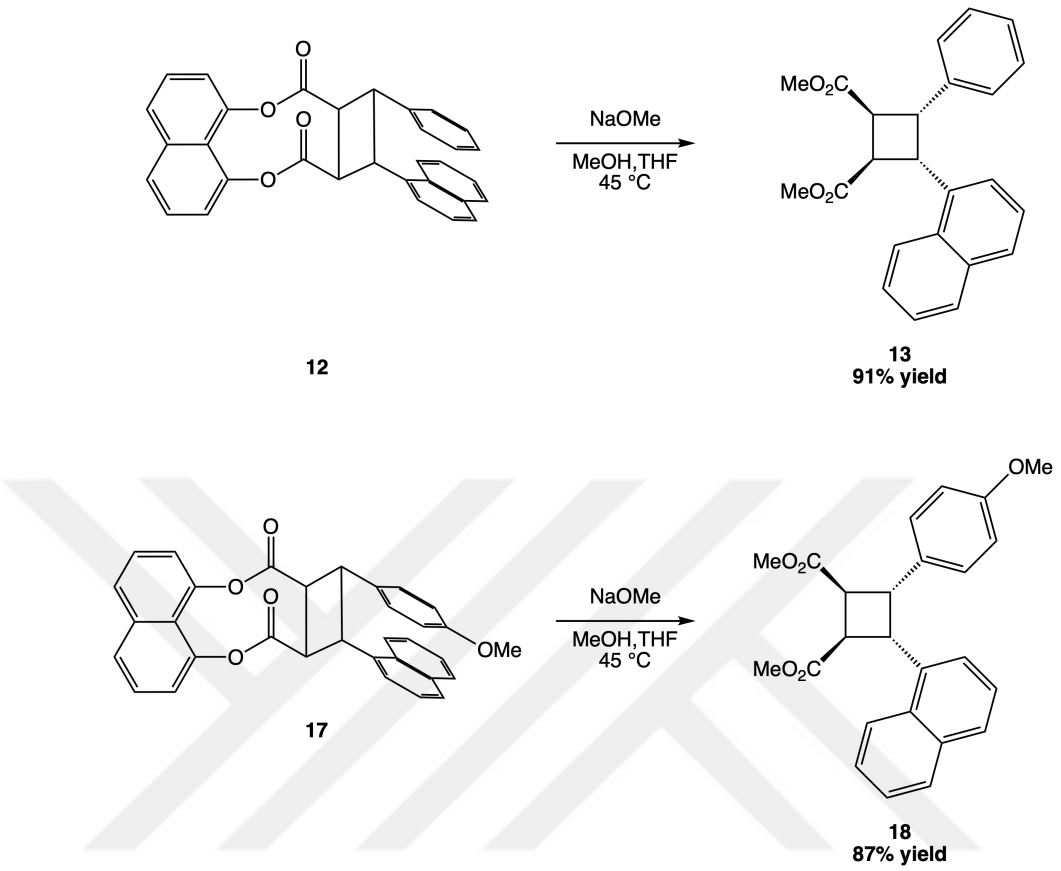

Scheme 20. Transesterification reactions of heterodimers **12** and **17**

Heterodimers **12** and **17** underwent the transesterification reaction for 3.5 hours at 45 °C when treated with NaOMe in a mixture of MeOH and THF. During the reaction, the formation of a template-removed cyclobutane ring was monitored with TLC analysis. Those analyses show that the 1,8-DHN was present in the crude mixture. Therefore, column chromatography was needed. However, decreased conjugation in template-removed cycloadducts weakened the glow of product spots on the TLC plate. That feature made monitoring the product during the column chromatography hard, especially for the small-scale reactions when the concentration of product in the test tube decreases. Despite that, targeted unsymmetrical diester products were purified with high yields: 91% yield for compound **13** and 87% yield for compound **18**. And importantly, thanks to the template

molecule, diastereocontrol was provided, and the *syn*-head-to-head dimerization product (i.e. the *β*-truxinic acid ester) was isolated as single diastereomer .

1.3. Conclusion

In this part of the thesis, a recently reported novel method for the [2+2] photocycloaddition reaction of cinnamic acids and vinylogous cinnamic acids was applied to the 1-naphthalene acrylic acid derivatives.[21,22,26] With this purpose, proper alignment between double bonds was aimed. To provide this alignment in the template-bound molecule, *trans*-cinnamic acid and its derivative were synthesized in accordance with the previous studies of the Türkmen research group. [21,22,26] And *trans*-1-naphthalene acrylic acid was synthesized in 3 steps with high yield. ^{1}H NMR studies confirmed the *trans* configurations of the olefins.

In solid state and solution, cycloadduct formations were seen and showed that the designed molecule obeys Schmidt's criteria. However, in the solution, higher conversion and yields were achieved for the given high conjugation systems.

Once again, the reported template molecule, 1,8-dihydroxynaphthalene, was also an effective template molecule for the [2+2] photochemical cycloaddition reaction but with an important difference. It was effective for high conjugation systems composed of naphthalene and phenyl-containing aryl groups. Formed cyclobutane rings with those molecules are promising for further synthesis studies of the natural products or their analogs. This methodology has easy access to the template molecule, good to high reaction yields in short synthesis pathways, and the chance for diastereocontrol. Therefore, it is effective and powerful method.

2. Investigation of an SCSC Transformation: Template-Directed Photochemical [2+2] Cycloaddition Reaction of Naphthalene Acrylic Acid

2.1. Introduction

2.1.1. Single-Crystal-to-Single-Crystal Transformation

Solid-state reactions have a broad scope.[36–38] Reactions of single crystals without dissolving them in solvents can also be classified under this scope. Unlike the solution phase, the movement of atoms in solid state and, of course, in single crystals is restricted. Mentioned single crystals may be formed by molecules of the same kind, but may also include different kinds of molecules as cocrystals.[39] To classify the transformation of those crystals as single-crystal-to-single-crystal, they should be exposed to external stimuli (solvent vapor, irradiation, temperature change, etc.) to give a reaction in the same solid phase without losing their crystallinity (Figure 8).[40]

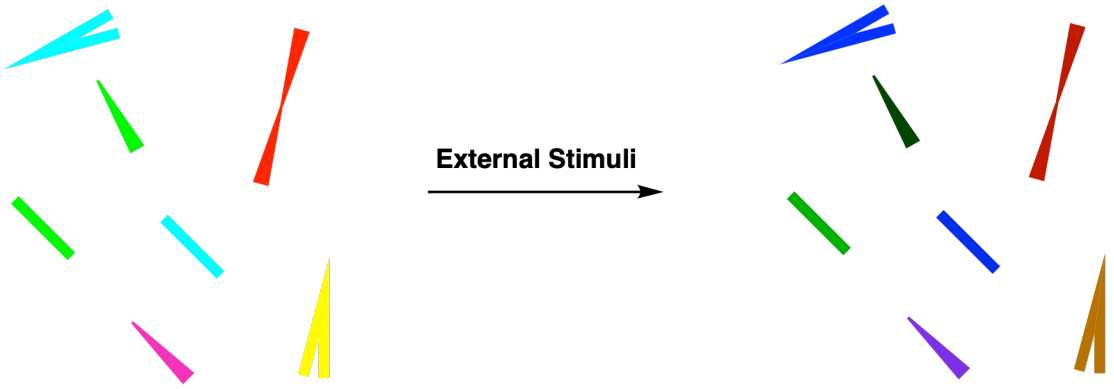

Figure 8. Illustration of single-crystal-to-single-crystal transformation

Although the movement of atoms in solid state is restricted, they are moving and releasing a strain during the transformation.[41] Therefore, the most challenging part of SCSC reactions is preserving crystallinity without any crack or crumbling at the end of the reaction. To investigate and prove crystallinity, single crystal or powder X-ray diffraction can be employed.[39] Although SCSC transformations are not easy to design, there are examples of SCSC in the literature.

Ito and co-workers synthesized compound **21**, and by rapid crystallization, they produced crystals **a** that shows blue photoluminescence under UV light (Scheme 21). When they followed another procedure for slow crystallization, they observed crystal structures different from **a**. Newly formed crystal **b** was a polymorph of crystal **a,** and crystal **b** was reported as producing yellow emission under UV light. For both **a** and **b**, the authors provided single crystal X-ray analysis. While crystal **a** is in a triclinic system, crystal **b** is in a tetragonal crystal system. Further studies showed that crystal structure **a** can transform to its polymorph **b** when researchers use a needle to pin as a mechanical stimulus. This transformation starts at the point where the needle touches first and expands. During the transformation, change in the structure occurs in the same solid phase without harming crystallinity. Therefore, it is an example of single-crystal-to-single-crystal transformation.[40]

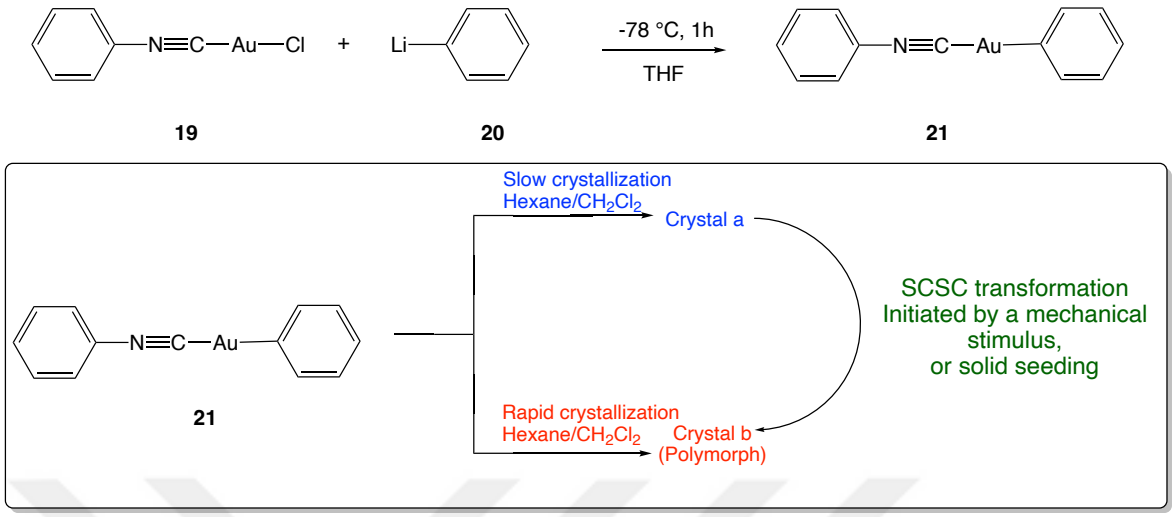

Scheme 21. Synthesis of compound **21**, 1-phenyl(phenyl isocyanide)gold(I), and phase transformation through SCSC transformation

For the photochemical [2+2] cycloaddition reactions, there are also examples of SCSC transformation. In 1998, Buchholz and Enkelmann synthesized (E)-2,6-di-tert-butyl-4- [2-(4-methylphenyl)-ethenyl]pyrylium salts. When they used perchlorate as a counterion, they could synthesize the compound **22**. The crystal of **22** reported with four crystallographically independent molecules in one unit. The distances between double bonds reported as 3.66 Å and 3.70 Å, are in agreement with the Schmidt criteria. The irradiation of those single crystals resulted in the construction of a cyclobutane ring, **23**, due to the photochemical [2+2] cycloaddition reaction (Scheme 22).[42]

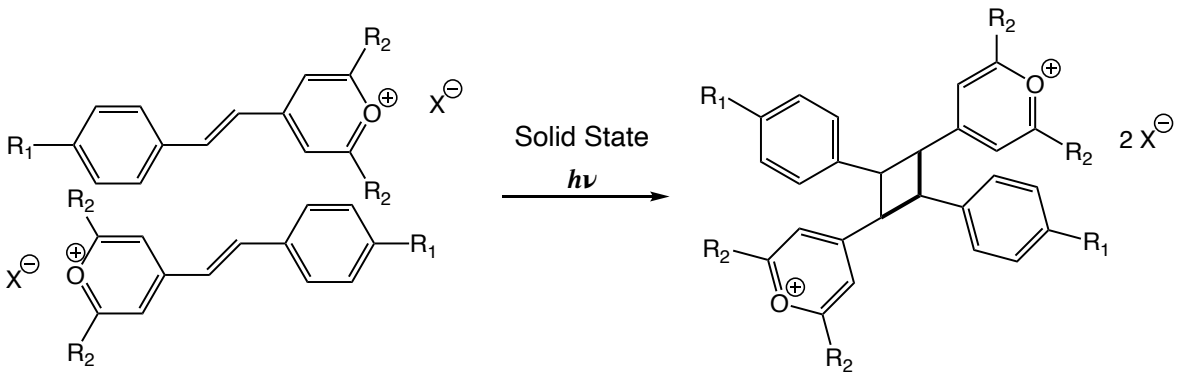

22 **23**

R_1 = Me R_2 = t-Bu X = ClO_4

Scheme 22. Dimerization of styrylpyrylium salt **22**

In 2003, Tyrk and co-workers designed a parallelly packed crystal from anthracene derivative **24** (Scheme 23). As is known, anthracene can undergo a photochemical [4+4] cycloaddition reaction when exposed to UV light, 445 nm, for the given specific example. As a result of irradiation, Tyrk and co-workers were able to report the [4+4] photodimerization product **25**. During the transformation, they monitor the change in the crystal structure with a single-crystal X-ray diffraction analysis.[41]

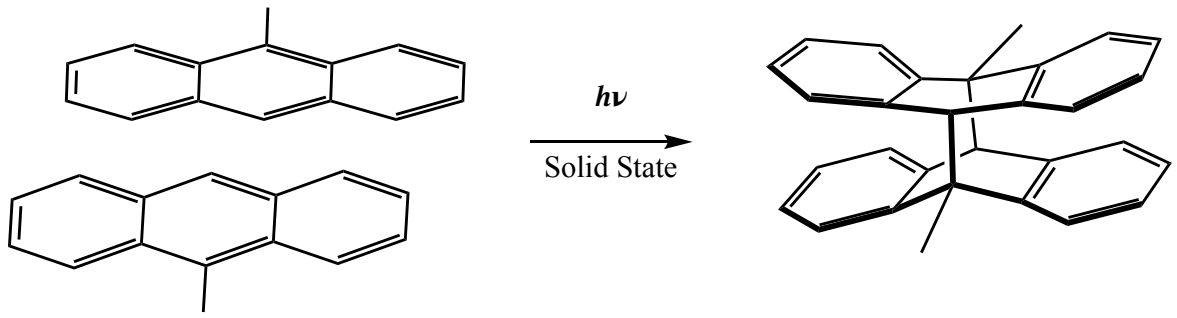

24 **25**

Scheme 23. [4+4] Photodimerization of anthracene derivative **24**

2.1.2 Usefulness of Single-crystal-to-single-crystal Transformation

As given in the examples from the literature, SCSC transformation has attracted the attention of researchers for decades. It has not just the advantages of solid-state reactions but also gives scientists a valuable chance to track the change in structure at the atomic level and real-time by single crystal or powder X-ray diffraction.[41]

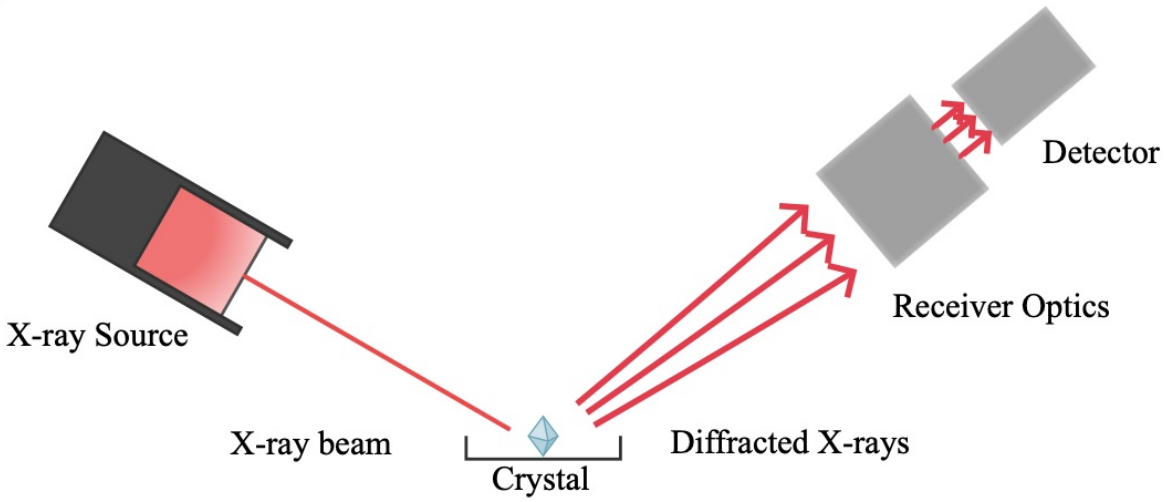

Figure 9. Illustration of components of XRD

Besides the chance for mechanistic studies, in general, during the SCSC transformation, the colors of the crystal are changing. This feature is also promising for employing SCSC transformation in sensor technology.[39] In addition to that, with SCSC transformation, there is a higher chance of constructing a structure that is not possible or easy to achieve structures in *de novo* synthesis.[43]

2.1.3. Aim of The Second Chapter of Thesis

With the aim of investigating SCSC transformation, a template-bound photochemical [2+2] cycloaddition reaction of naphthalene acrylic acid, **26**, was synthesized in four steps. By the vapor diffusion crystallization technique, transparent-white-like crystals were obtained.

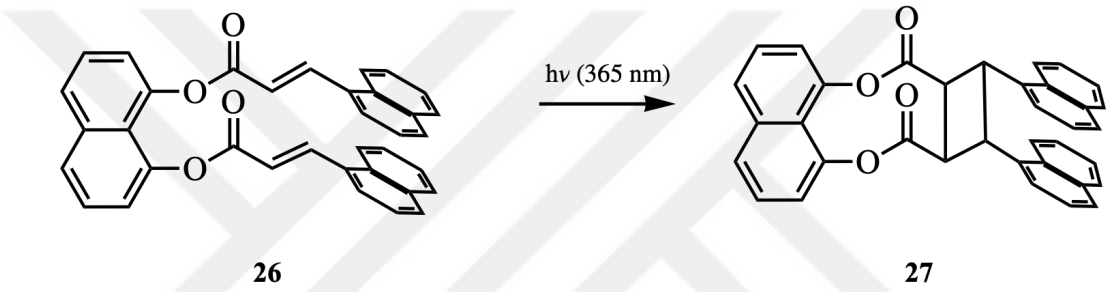

26 **27**

Scheme 24. Photochemical [2+2] Cycloaddition of diester **26**

After getting proper crystals for the irradiation with 365 nm UV light, crystals were exposed to light for 20 hours. During the transformation from molecule **26** to **27** photographs recorded the initial and final appearance of the compounds. SCSC transformation was investigated with ^{1}H NMR spectroscopic and X-ray diffraction analysis.

2.2. Results And Discussion

2.2.1 Synthesis and Crystallization of Template-Bound Symmetrical Diester

In the second part, 1,8-DHN bound naphthalene acrylic acids were synthesized by following the steps in Scheme 25.

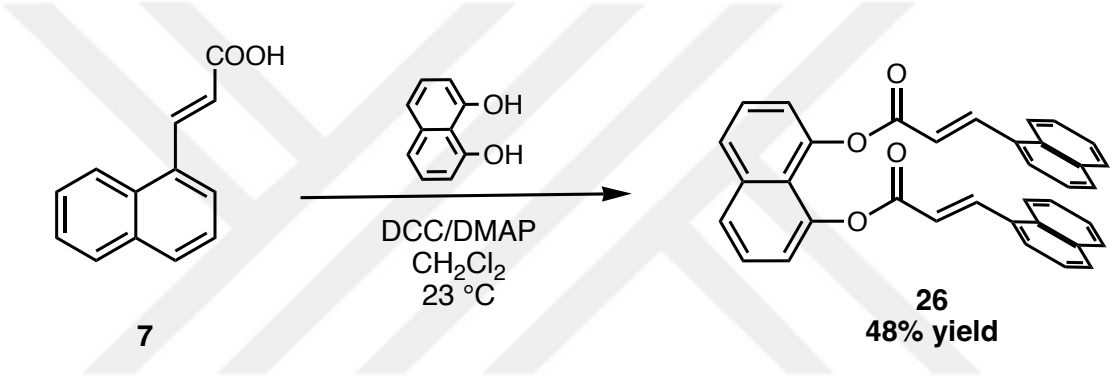

Scheme 25. Synthesis pathway of symmetrical diester **26**

Compound **7** was synthesized as described in the first part of this thesis. After the synthesis and purification of 3-(1-Naphthyl)acrylic (compound **7**), Steglich esterification was employed to synthesize the symmetrical diester of naphthalene acrylic acid. The specialized reagents DCC (*N*,*N*′-dicyclohexylcarbodiimide) and DMAP (4-dimethylaminopyridine) were used during the Steglich esterification, and the conditions were mild when compared with Fischer esterification. In Fischer esterification, required the use strong acid along with water formation make this reaction hard to apply.[44] However, the Steglich esterification is carried out at room temperature, and water formation is not an issue. The only drawback was the formation of the by-product.[45]

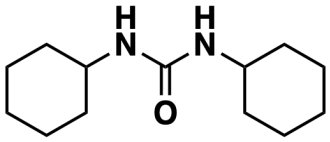

Dicyclohexylurea

Figure 10. Structure of DCU

Due to the lack of conjugation, DCU is not UV active, and therefore, during the TLC analysis under 254 nm UV light, it is not possible to track it.[46] During the isolation of compound **26**, this feature of DCU created a challenge. However, it was occupied by using large size column and a 1:1 Hexane: DCM solvent system. This method prevented the DCU interference with the collected fragments for compound **26** during the column chromatography.

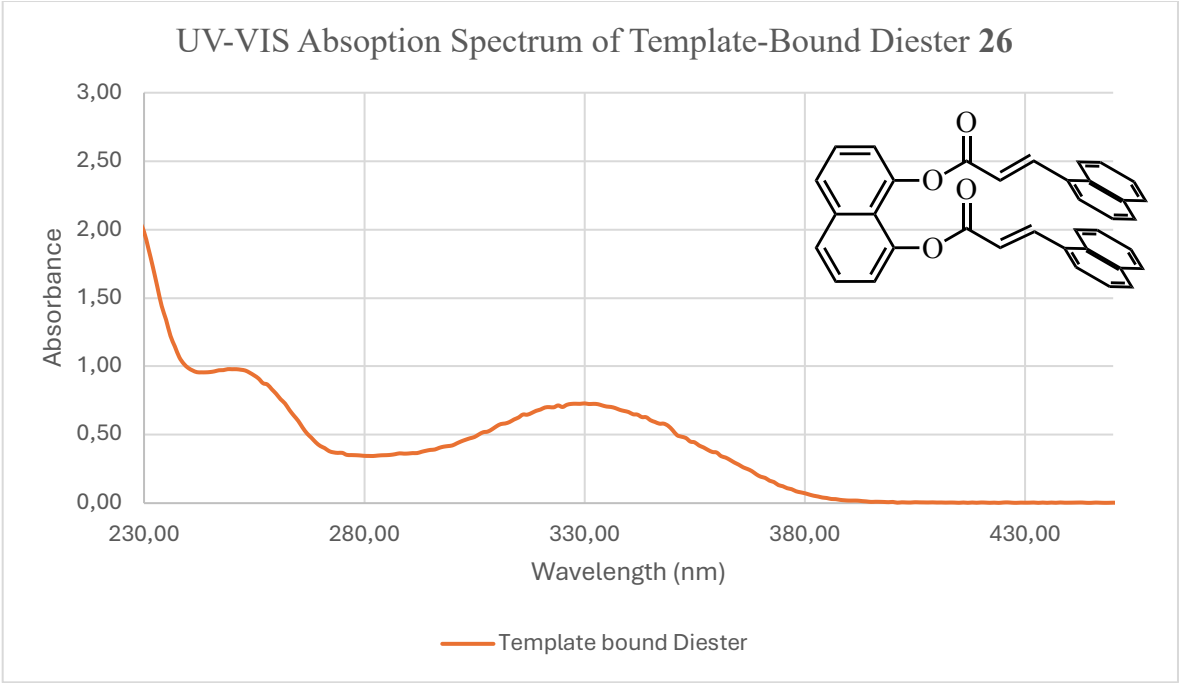

Figure 11. UV-Vis absorption spectrum of template-bound diester **26** in DCM solvent

The conjugation of symmetrical diester **26** was higher than the unsymmetrical diester **11** and **16** due to the presence of two naphthalene rings. UV-Vis absorbance study with pure symmetric *trans*-diester in DCM showed that the absorption band starts around 400 nm. Because of that feature, *cis*-*trans* isomerization, even at the laboratory lighting, was fast. As stated in the first chapter, from the ^{1}H NMR, it is possible to trace the olefin configurations of the products. In Figure 12**,** the ^{1}H NMR spectrum of one of the isolated fragments of diester **26** can be seen. Doublets at 8.82 ppm and 6.74 ppm belong to the *trans*-diester **26** with a 15.8 Hz coupling constant. As known for the vinyl *trans* protons, the coupling constant *J* is in the range of 11-18 Hz, and that information proves the *trans* configuration. For the doublet at 6.62 ppm, coupling constant *J* was equal to 12.2 Hz. Because it is between 6-15 Hz, it belongs to the *cis* configuration.[33] Removal of the *cis* diester **26** from the *trans* conformation was achieved by dividing the tubes collected during the column into different fragments and analyzing them ^{1}H NMR to detect the purity or by the crystallization of the *trans* isomer.

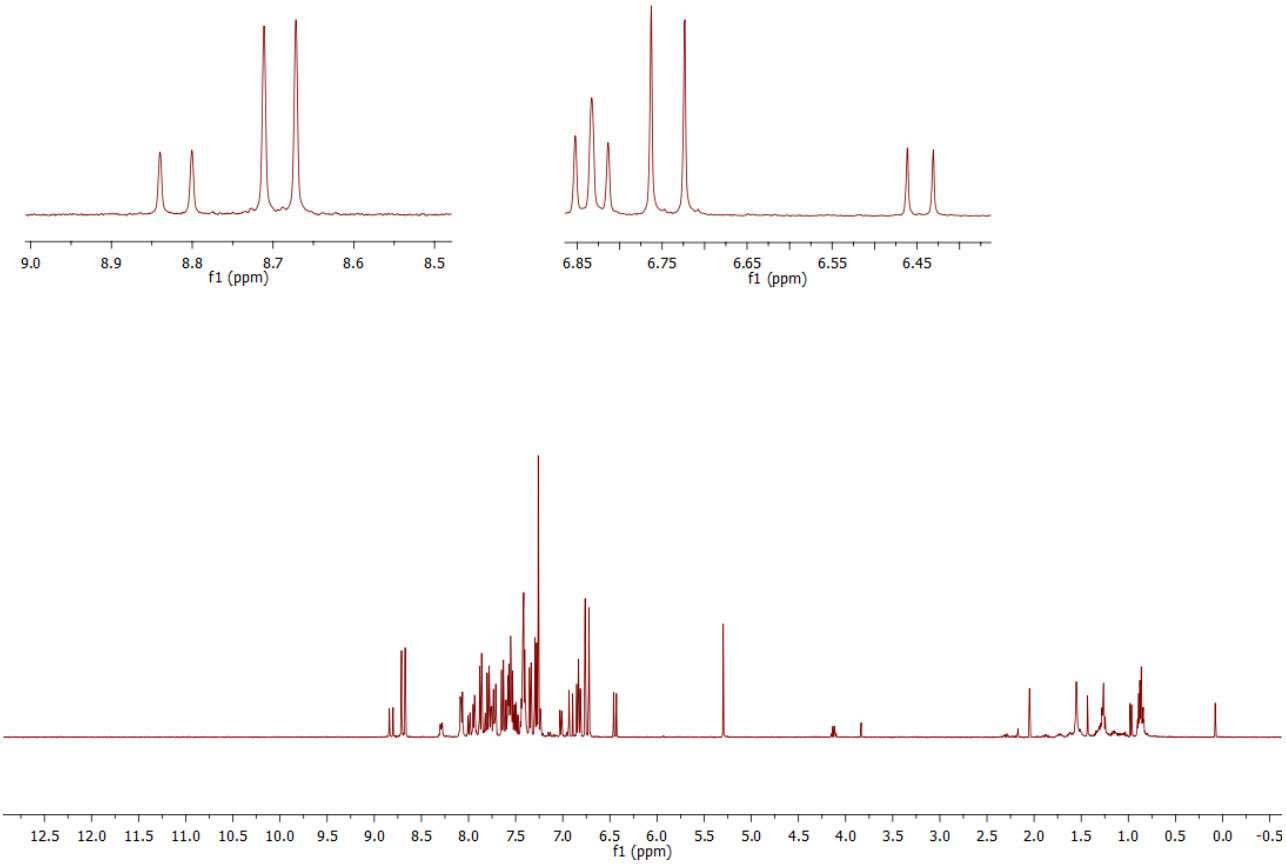

Figure 12. ^{1}H NMR Spectrum of *cis*- and *trans*-diester **26**

In addition to that, cycloadduct formation was also possible. Therefore, isolation was applied under the hood when lights were off, and the purified diester was protected from light, like in previous examples.

The synthesized and isolated diester **26** had a yellowish-white color. This solid compound underwent photochemical [2+2] cycloaddition reaction in solid phase: powder form, as a single crystal, and in solution under 365 nm UV irradiation.

For the single-crystal reaction, the vapor diffusion technique was employed to reach proper crystals.

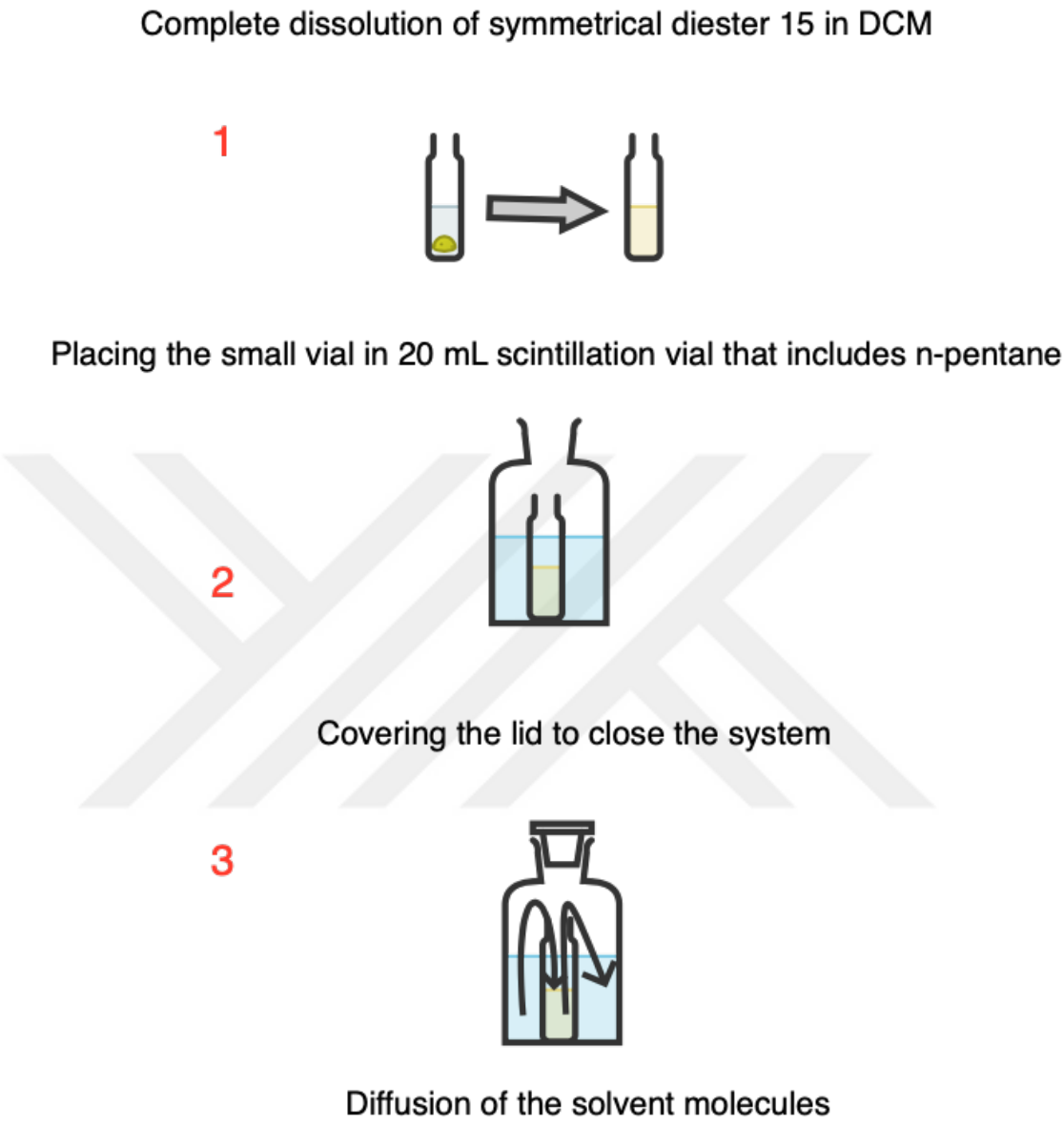

Figure 13. Vapor diffusion technique with DCM/*n*-pentane

With this crystallization technique, proper single crystals were obtained. Formed single crystals had different sizes and shapes, and their look was white-transparent, like in Figure 14. Formed crystals of symmetric diester were stored in an aluminum-foil-covered scintillation vial at +4 °C.

Figure 14. Single crystals of diester **26**

2.2.2. Template-Bound Photochemical [2+2] Cycloaddition Reactions of Symmetrical Diester of 1-Naphthalene Acrylic Acid in Different Phases

Template-bound symmetrical diester **26** gave [2+2] cycloadduct **27** upon irradiation both in solution and in solid state (Scheme 26).

$CHCl_3$ was used as solvent for the solution reactions, and a quartz glass test tube that transmits light of 365 nm wavelength was used.[35] To provide a more homogenous light distribution, reactions were mixed with a stir bar on the magnetic stirrer for 9 h. During the reaction period, in order to monitor progress, thin-layer chromatography (TLC) was employed. However, due to the high conjugation of diester molecules, spots of starting compound **26** glow strongly on the TLC plate under the 254 nm UV light. Homodimer **27** had a lower intensity. Therefore, again, the TLC analysis was not straightforward.

.

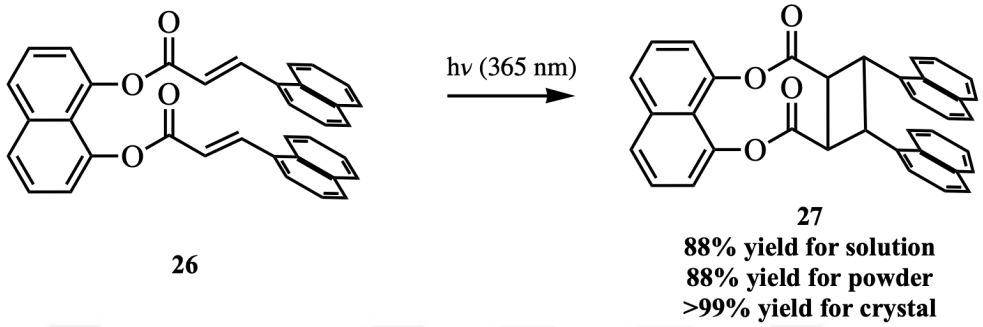

Scheme 26. Homodimerization of diester **26** in different phases

At the end of 9 h, the reaction was stopped by evaporating the solvent. Care was given to not wait after turning the UV light off to prevent the effect of laboratory lighting on the results. The conversion was 95%, and with the purification by column chromatography, 88% yield was achieved for the cycloadduct **27**. It was yellow-colored, solid material.

By taking the UV-Vis absorption spectrum of the diester **26** into account to investigate the effect of daylight on the reaction, another experiment in $CHCl_3$ was designed. 33.1 mg (0.063 mmol) of diester **26** was dissolved in 1.0 mL $CDCl_3$ in an NMR tube and placed in front of the window from inside of the laboratory. The % conversion was followed by ^1H NMR spectroscopy every day for 15 days (360 h). At the end of 15 days, %96 conversion was seen. The detailed change of conversion values with respect to number of days can be seen in Figure 15. Due to the difference between the flux of the 365 nm (36 Watt) UV light and daylight, the reaction under the lamp was faster.

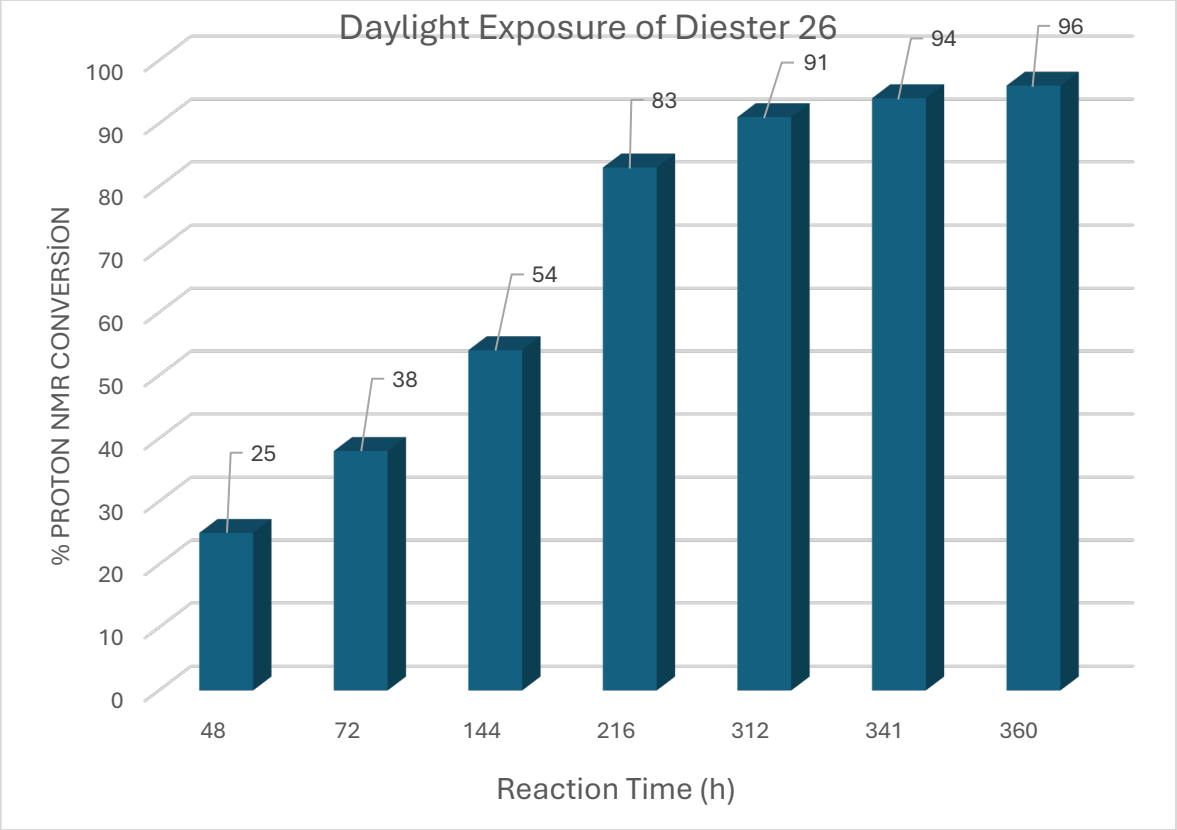

Figure 15. Daylight exposure and % conversion of diester **26** to cycloadduct **27**

After finishing our studies on the cycloaddition reactions in solution, the powder of diester **26** was irradiated under 365 nm UV light. As in the first chapter and solution irradiations of homodimer **26**, the experimental set-up was also the same for homodimerization and consisted of a nail dryer equipped with four 9-Watt fluorescent bulbs (UVA, 365 nm), quartz microscope slides, and paper clips to fix the slides. Yellow powder of diester **26** was placed between those quartz microscope slides and irradiated for 16 h. Every 4 h, crude solid was mixed to provide homogeneous light distribution. It is noted that as time went by, the color became orange. After 16 h, ^{1}H NMR analysis showed 98% conversion, and after purification by column chromatography, a yellowish solid homodimer

27 was collected with 88% yield. After full characterization, the powder of compound **27** was crystallized using the same technique as described for the diester **26**. Formed single crystals were needles and slightly yellowish-transparent.

2.2.3. Irradiation Studies on Single Crystal of Template-Bound Symmetrical Diester of 1-Naphthalene Acrylic Acid

The photochemical [2+2] cycloaddition reaction of diester **26** was also run with single crystals. For this purpose, single crystals were gently picked and placed on the quartz microscope slide; however, this time, the second slide was not used to squeeze the materials to not to distort the crystals' shapes and not to turn them into powder (Figure 16).

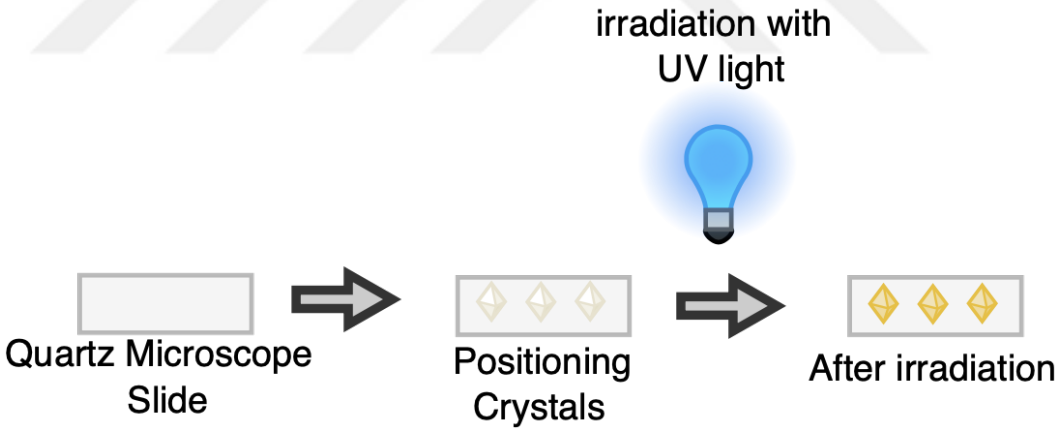

Figure 16. Illustration of the irradiation of the crystal

The literature review was conducted before the irradiation studies of single crystals. Those studies on single crystal reactions gave insight into reactions and created three expectations. A possible jump of the crystals due to the movement of the molecule was among the expectations.[47] Again, due to this movement of molecules or atoms, loss of crystal form and crumbling were also possible. . A previous study by Türkmen and co-workers can

be examined as one of the examples of crumbling of the crystals during the reaction (Scheme 27).[21]

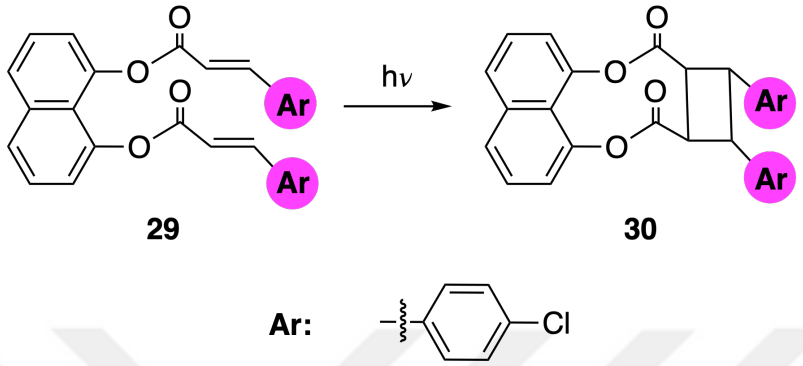

Scheme 27. Cycloadduct formation from diester **29**

A third possibility was recording single-crystal-to-single-crystal transformation. To investigate the reality, the following reactions were run. In Figure 17 shown below, a picked single crystal of compound **26** was observed during 20 h of irradiation. Every 4 h, the side of the crystal that directly faced the lamp was changed to provide equal light distribution to every side of the crystal.

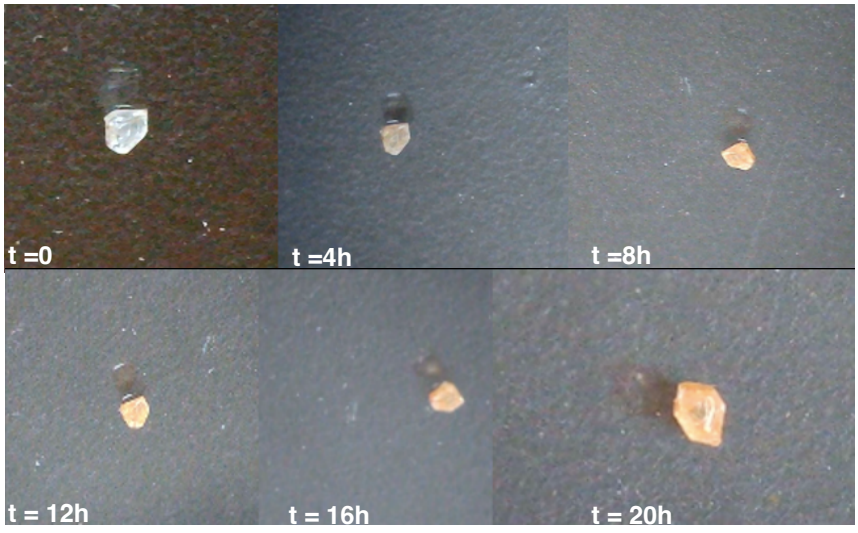

Figure 17. Irradiation of single crystal for 20 hours

As stated, making the crystal upside-down to guarantee equal light distribution caused a change in the position of the crystal. However, there was no movement or crumbling and cracks. The only change in the look was being orange within the time. In addition to that, at the end of 20 h, it was not transparent anymore. ^{1}H NMR study at the end of 20 h showed that the conversion of crystal to cycloadduct **27** was achieved with full conversion.

In order to follow the conversion of the reaction with the irradiation time, single crystals of **26** were picked and irradiated for 1, 5, 10 and 20 h. The change in the look of the crystals was recorded by the microscope, like in the previous Figures 17 and 18. Again the increase in the intensity of the orange color and decreasing transparency were the changes.

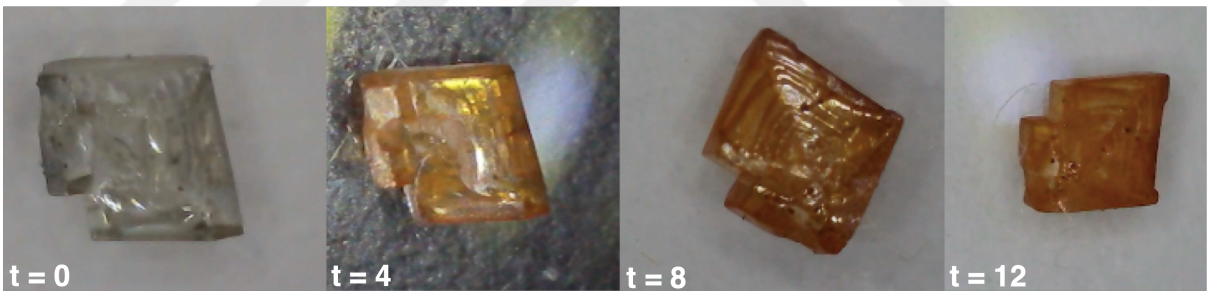

Figure 18. Change of the crystal during the irradiation

To follow the reaction %conversion with the irradiation time, single crystals of **26** were picked and irradiated for 1,5,10 and 20 hours. The change in the look of the crystals was recorded by the microscope, like in the previous figures 17 and 18. Again the increase in the intensity of the orange color and decreasing transparency were the changes.

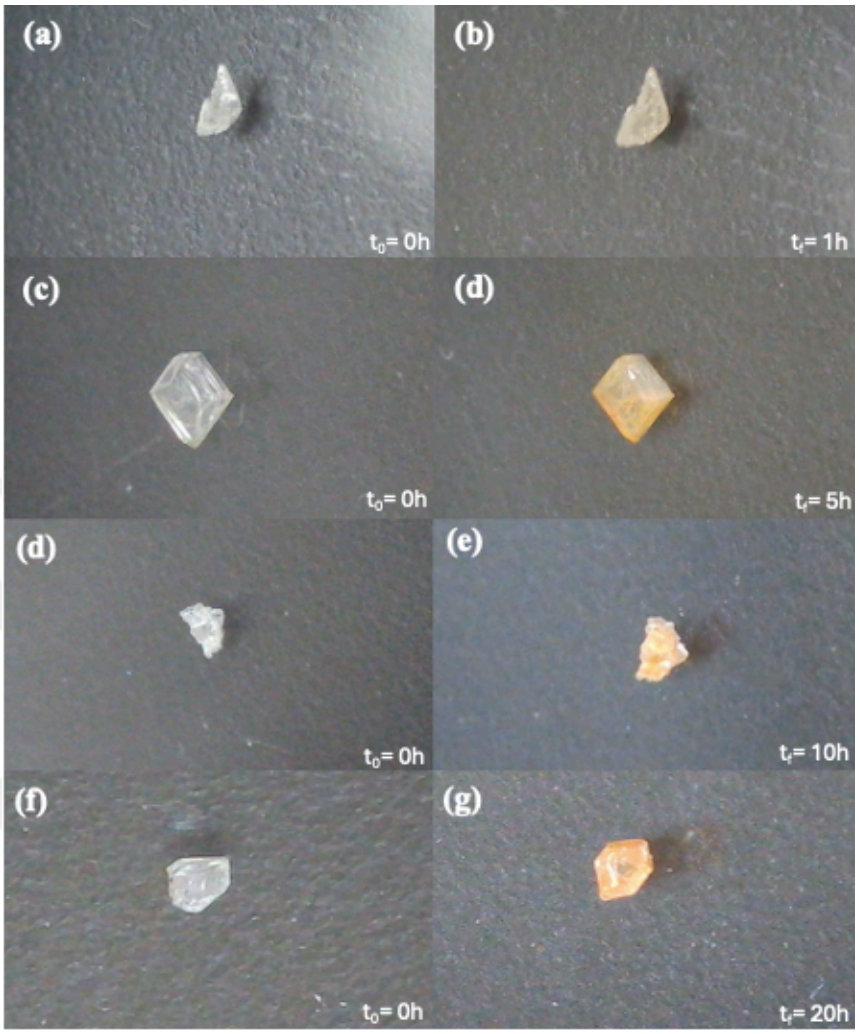

Figure 19. Irradiation of single crystals of diester **26** for different times

At the end of each period, the ^{1}H NMR spectrum was recorded to see the formation of the product in a single crystal and calculate the %conversion based on the spectrum.

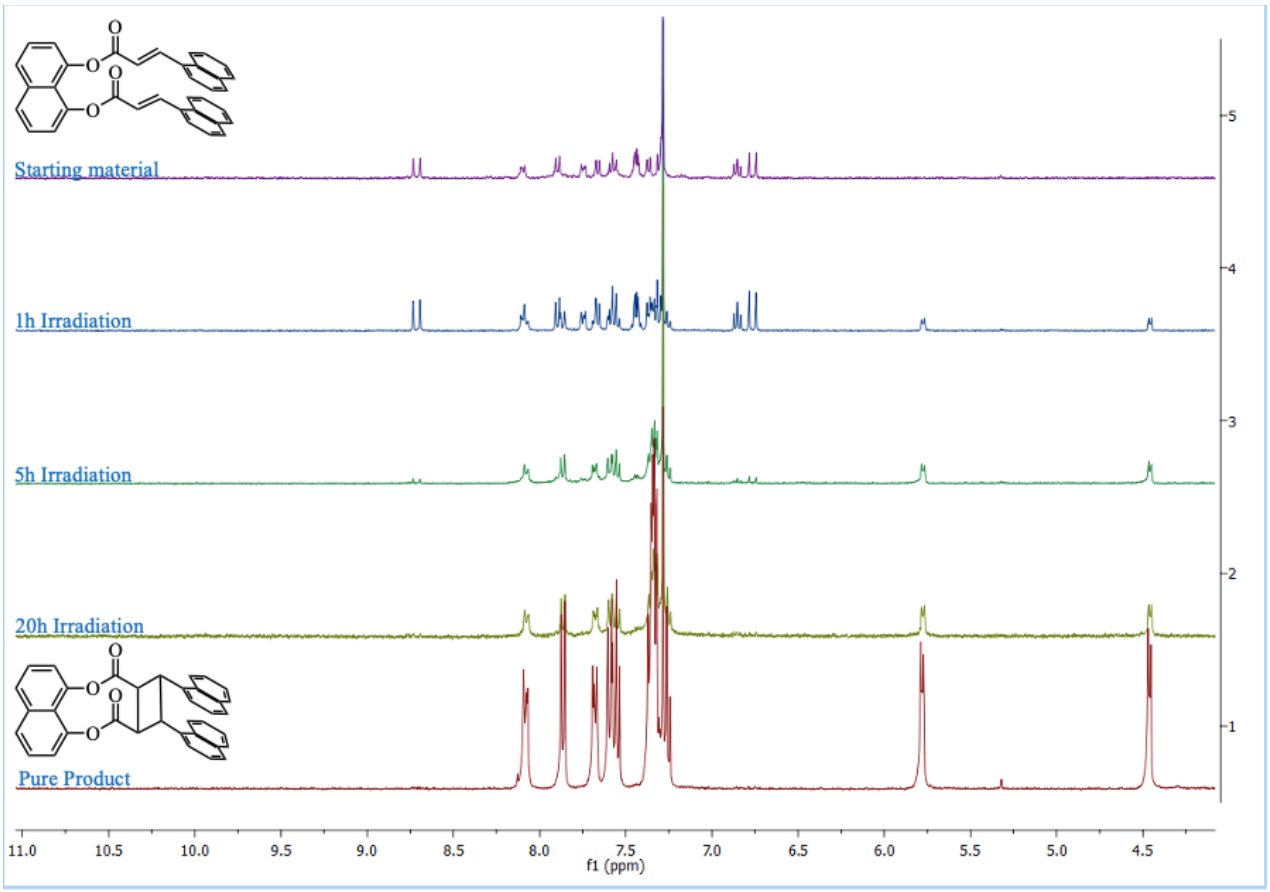

Figure 20. Stacked spectra of single crystals of **26** in $CDCl_3$

In the ^1H NMR spectrum of the starting material, the alkene peaks are clearly visible at 8.61 (2H, d, J = 15.8 Hz) and 6.66 ppm (2H, d, J = 15.8 Hz). And for the pure product, peaks at 5.68 (2H, m) and 4.36 ppm (2H, m) are highly characteristic. For the %conversion calculation, one of the alkene peaks of the starting diester and one of the multiplets for the cycloadduct were used, and both were responsible for two protons. With the necessary calculations, it was seen that for the 1-h irradiation, the conversion was 33%. For 5, 10, and 20 h, conversion values were 85, 92, and 100%, respectively.

2.2.4. SC-XRD and IR Studies of the Template-Bound Photochemical [2+2] Cycloaddition Product

For the XRD analysis, a single crystal of diester **26**, recrystallized cycloadduct **27** from the powder, and an irradiated single crystal of diester **26** were sent to SC-XRD studies. For the diester **26**, SC-XRD studies showed that it has a monoclinic structure with the Z value equal to 2, which indicates that the unit cell has two repeating units.

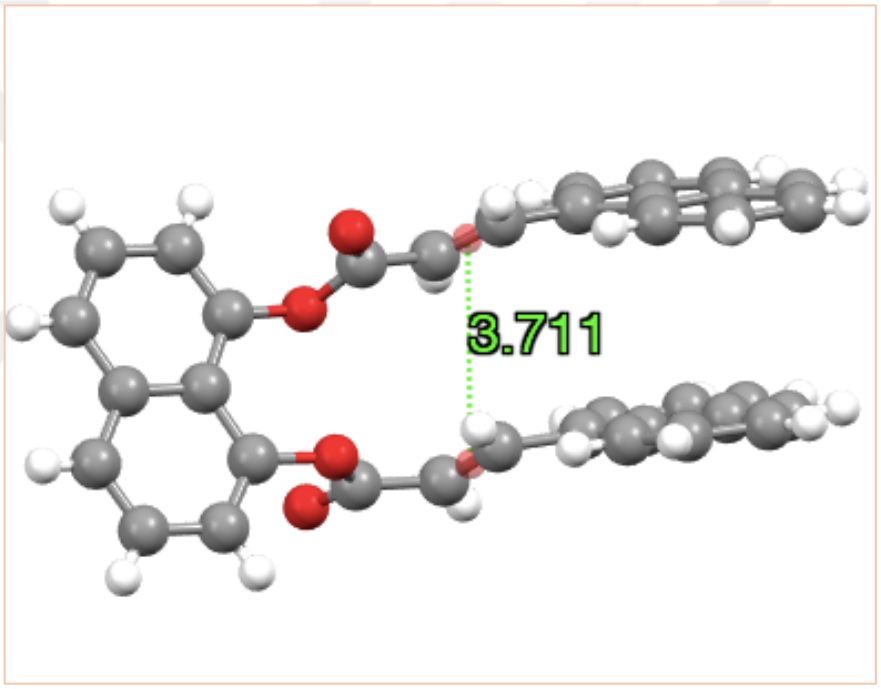

Figure 21. SC-XRD study of diester **26**

The single crystal XRD analysis by Prof. Onur Şahin from Sinop University also provided the distance between two parallelly aligned double bonds is 3.711 Å, which obeys the Schmidt criteria. And explains the success of photochemical [2+2] cycloaddition reaction. In addition to that, the face-to-face positioning of two naphthalene units supported the π-stacking, which contributes to the stabilization of the compound **26**.[48,49] From the SC-

XRD structure, it is also clear that C=O oxygen atoms of ester groups do not point in the same direction. After that study, the recrystallized cycloadduct **27** was also studied by SC-XRD. For the homodimer, SC-XRD studies showed that it has a monoclinic structure with the Z value equal to 4, which indicates that the unit cell has four repeating units.

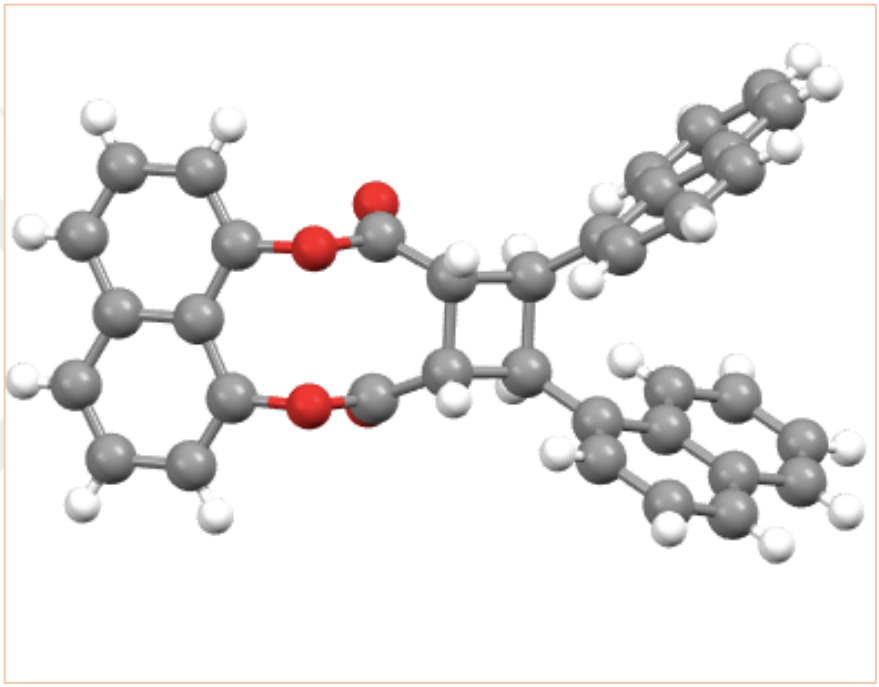

Figure 22. SC-XRD study of recrystallized cycloadduct **27**

The solved structure of recrystallized cycloadduct **27** showed that [2+2] cycloadduct formed successfully, as NMR analysis showed earlier.

One of the noteworthy differences between the two solved structures is the position of the oxygen atoms. In the diester's structure, oxygens are pointing in different directions; however, in the cycloadduct's structure, they are pointing in the same direction. When bond length was measured with mercury software, there was no significant differences.

Another difference was the distance between two naphthalene molecules. When it is measured by referencing the shared carbon atom, for diester **26**, the distance is 3.793 Å, and for the cycloadduct **27**, it is 3.953 Å. It was also longer for the cycloadduct.

In addition to the diester **26**, the irradiated single crystal was also investigated with SC-XRD; unfortunately, diffraction could not be obtained. The reason for that might be the opaque feature of the compound **27** after the irradiation.

After the XRD studies, the IR spectra of diester **26** and cycloadduct **27** were recorded in solid state.

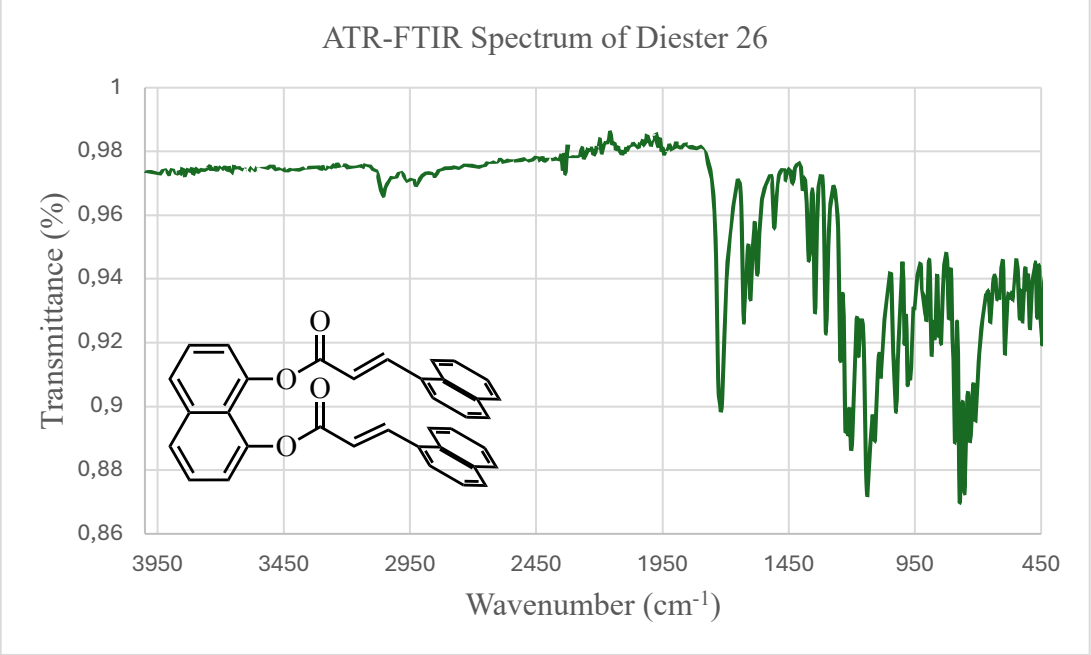

Figure 23. The IR spectrum of diester **26**

When the IR spectrum of diester **26** is investigated, between 3100 and 3010 cm^{-1}, the stretches of C-H bonds of the aromatic ring are visible. At 1628 cm^{-1}, it is possible to detect

the stretch of the C=C bond of alkene. And the ester's C=O stretch is present at 1717 cm^{-1}. Aromatic C-H bending and aromatic C=C stretching are present in 860 – 680 and 1700 – 1500 cm^{-1}, respectively.

After single crystal irradiation with 365 nm UV light, the IR spectrum of irradiated crystals was recorded by directly placing the crystal onto the ATR diamond.

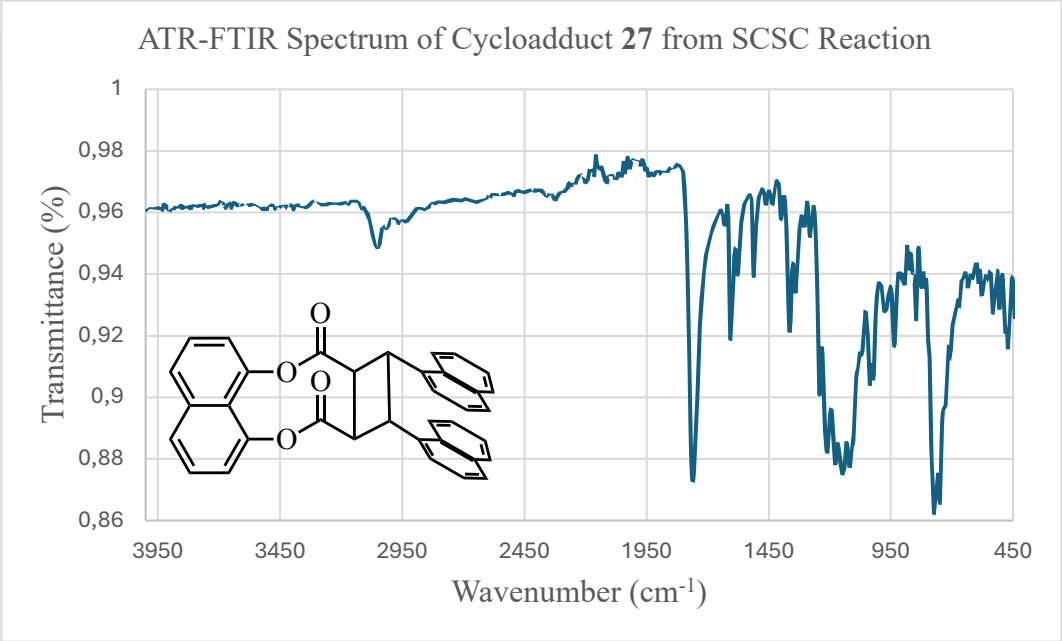

Figure 24. IR spectrum of cycloadduct **27** after SCSC reaction

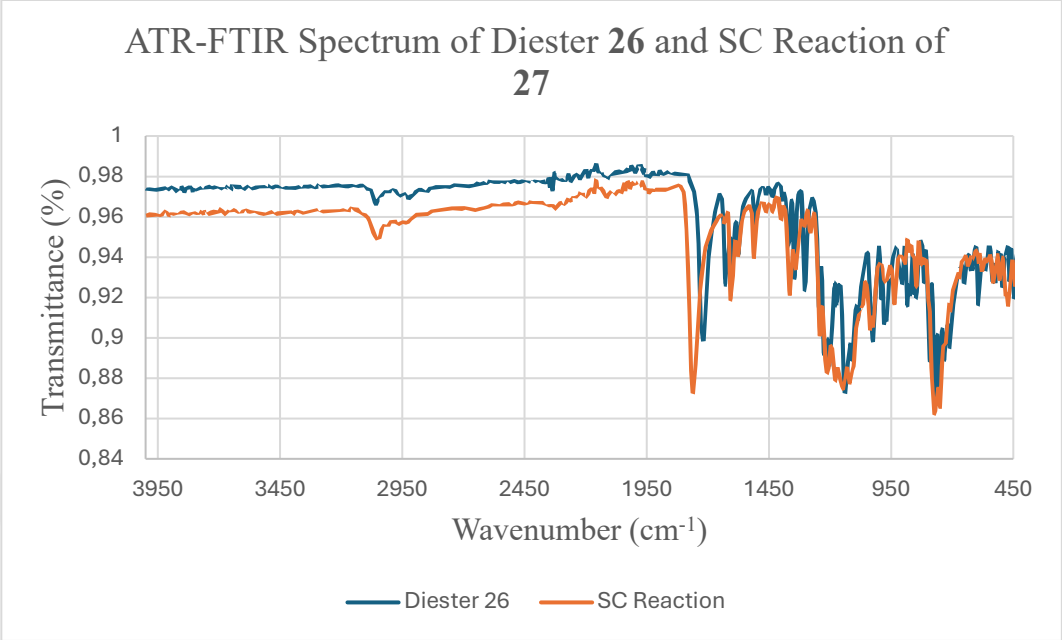

Figure 25. IR spectrum of diester **26** and cycloadduct **27** from SC reaction

As in diester **26**, between 3100 and 3010 cm^{-1}, the stretches of C-H bonds of the aromatic ring are visible. The 1628 cm^{-1} peak disappears due to the cycloadduct formation. The C=O stretch of ester is present at 1761 cm^{-1}. Aromatic C-H bending and aromatic C=C strecthing are present in 860 – 680 and 1700 – 1500 cm^{-1}, respectively. The disasppearance of the signal at 1717 cm^{-1}, which belongs to the reactant **26**, and appearance of the new C=O stretching signal at 1761 cm^{-1} confirms that the [2+2] cycloaddition took place successfully in the single crystal. However, when the IR spectrum of a powder sample of cycloaddition product **27**, which was purified after column chromatography, was recorded, the C=O stretch of the ester appeared as two separate peaks.

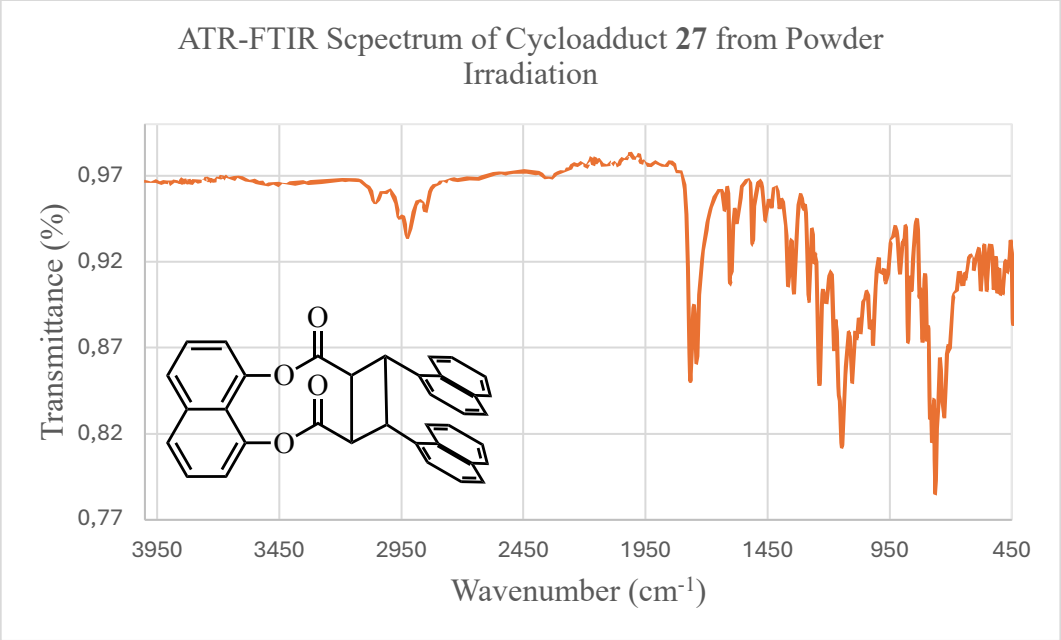

Figure 26. IR spectrum of cycloadduct **27** after powder irradiation reaction

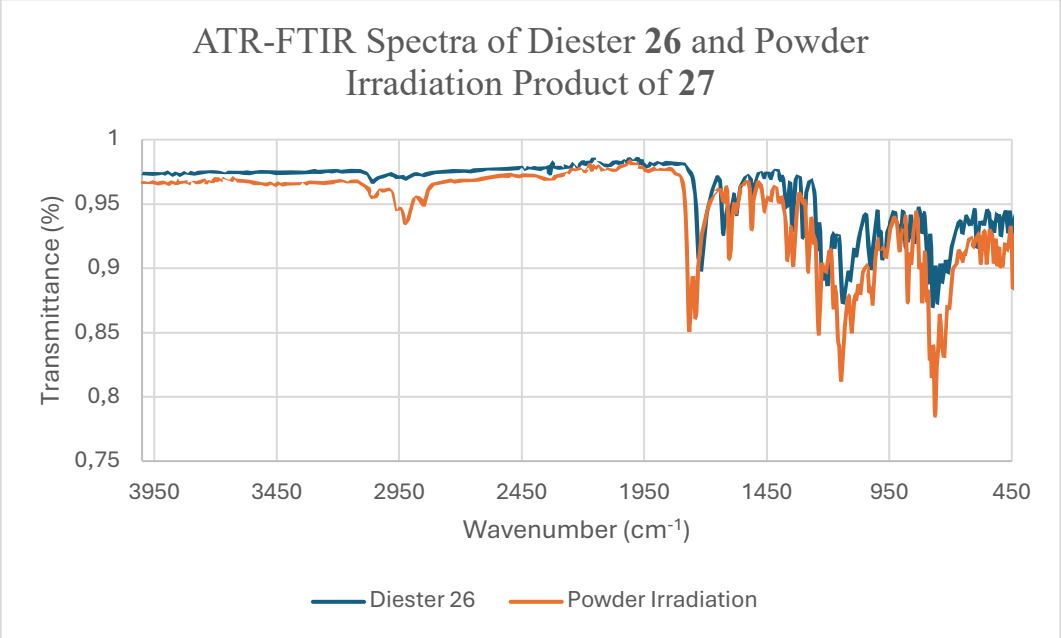

Figure 27. The stacked IR spectra of diester **26** and cycloadduct **27** from powder irradiation reaction

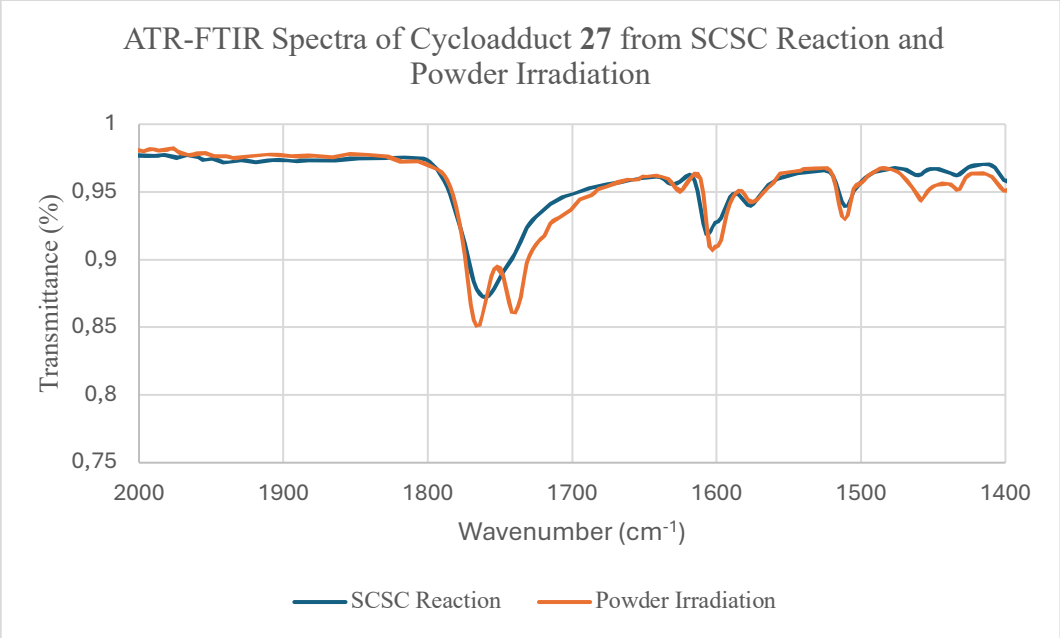

Figure 28. The stacked IR spectra of cycloadduct **27** after SC reaction and powder irradiation reaction

For the purified cycloadduct **27** after powder irradiation, in 1765 and 1740 cm^{-1}, the C=O stretching signal of the ester appeared (Figure 26 and 27). The difference between the spectrum of single crystal reaction and powder form from the purified product is clearer when the wavenumber is limited from 2000 to 1400 cm^{-1} (Figure 28).

To investigate the effect of recrystallization on purified product **27**, vapor diffusion crystallization was applied to the powder. The IR spectrum of these crystals was also recorded. The region responsible for the ester stretching signal of the C=O bond is clearer when the wavenumber is limited from 2000 to 1500 cm^{-1} (Figure 29). In both spectra, there are two separate peaks for the ester stretch of the C=O bonds. Those two separate peaks for the carbonyl groups may represent the symmetric and asymmetric stretching. In the single crystal reaction, we cannot see this splitting for the C=O bond vibrations. These observations

suggest that the conformations of cycloadduct **27** in the crystal right after the irradiation of a single crystal and in the samples which contain purified product may be different.

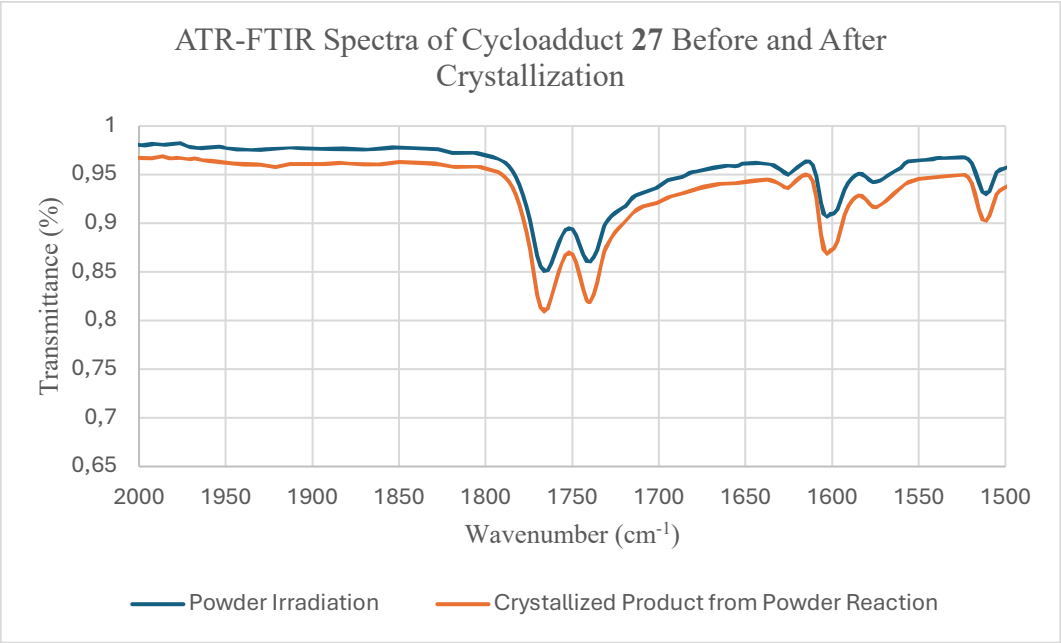

Figure 29. The stacked IR spectrum of cycloadduct **27** before and after the crystallization

In summary, the product of powder irradiation provides two peaks for C=O stretching even after recrystallization of **27**. However, only one stretching peak for C=O bond appeared in IR spectrum of the irradiated single crystal. This situation can be interrupted by the intermolecular arrangement of two samples of **27** being different. Single-crystal irradiation could result in another crystal structure of **27** and eliminate the possibility of being single-crystal-to-single-crystal transformation. This kind of difference, supported by IR spectra, can be used in explaining crystal polymorphism. Because in crystal polymorphism, intermolecular arrangements are different between the crystals of the same molecule.[50] This affects most of the characteristics of the crystals, such as optical properties, hardness, melting

point, and so on, and characterization of polymorphs can be done with IR spectroscopic imagining.[51]

2.2.5. Template Removal from Homodimers

The template removal to get β-truxinic acid ester analogues, i.e. [2+2] cycloaddition product without template molecule, was successfully done by the use of NaOMe. The template was removed through a transesterification reaction. In this reaction product of powder irradiation, **27**, was used. Thanks to the cleavage of a C-O single bond by methoxide ions, the template was removed. During the reaction, the formation of a template-removed cyclobutane ring **35** was monitored with TLC analysis. Those analyses show that the 1,8-DHN was present in the crude mixture. Therefore, column chromatography was applied, and compound **35** was purified in %75 yield.

As in the first chapter, thanks to the template molecule, diastereocontrol was provided, and the *syn*-head-to-head dimerization product (i.e. the *ß*-truxinic acid ester) was isolated as single diastereomer . The ^{1}H NMR analysis also confirmed the formation of *ß*-truxinic acid ester with its unique splitting pattern for the protons of cyclobutane ring.

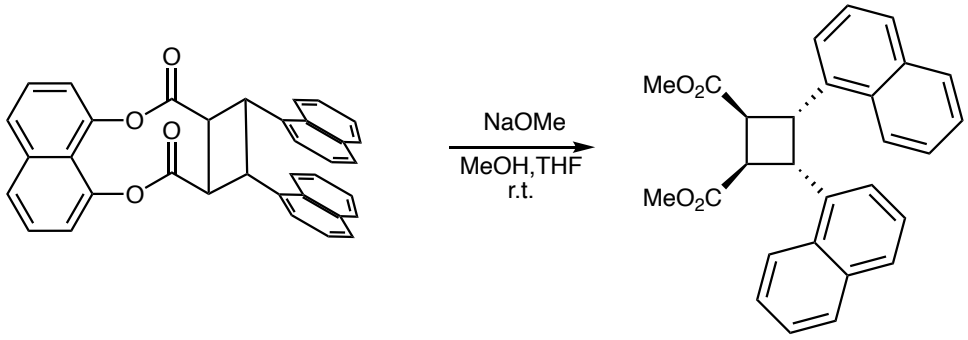

27

35
75 % yield
***β*-truxinic**
acid ester analogue
head-to-head

Scheme 28. Template removal from cycloadduct **27**

2.2.6. Photochemical [2+2] Cycloaddition Studies Without Template Molecule

In the last part of the project, possible homodimerization of molecules **6** and **7** without the template molecule was investigated. Before designing the experiment, UV-Vis spectra of two compounds were recorded in MeOH. This analysis shows that compounds **6** and **7** have a close absorption trend. Both compounds have absorption band that start around 380 nm.

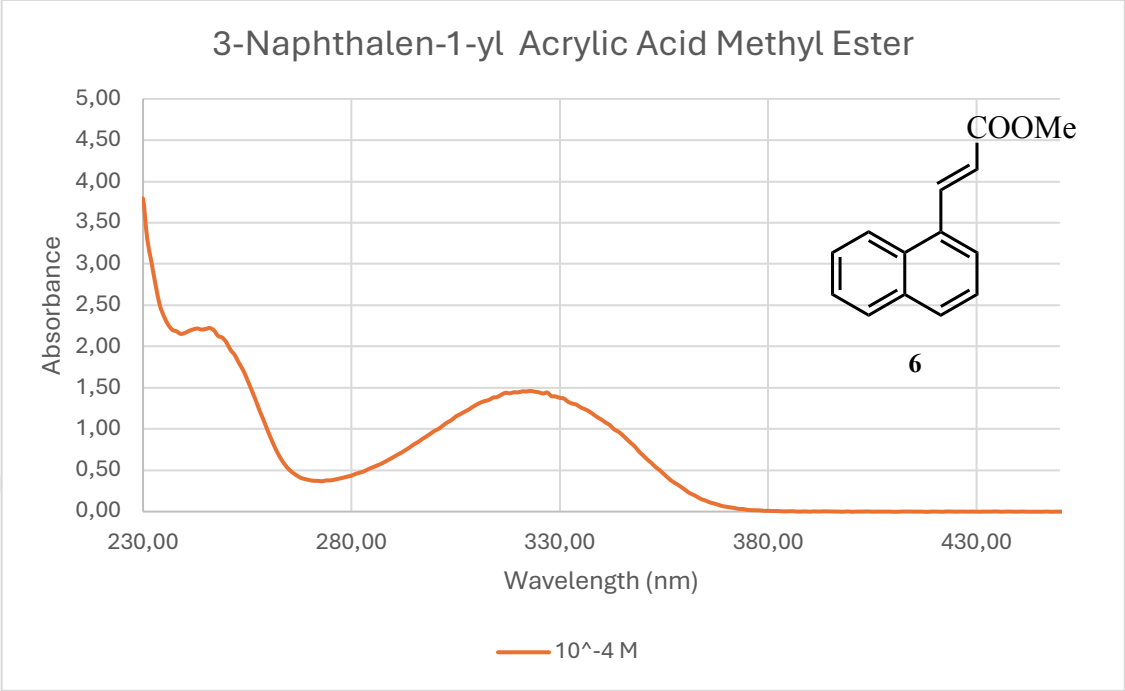

Figure 30. UV-Vis absorption spectrum of compound **6** in MeOH

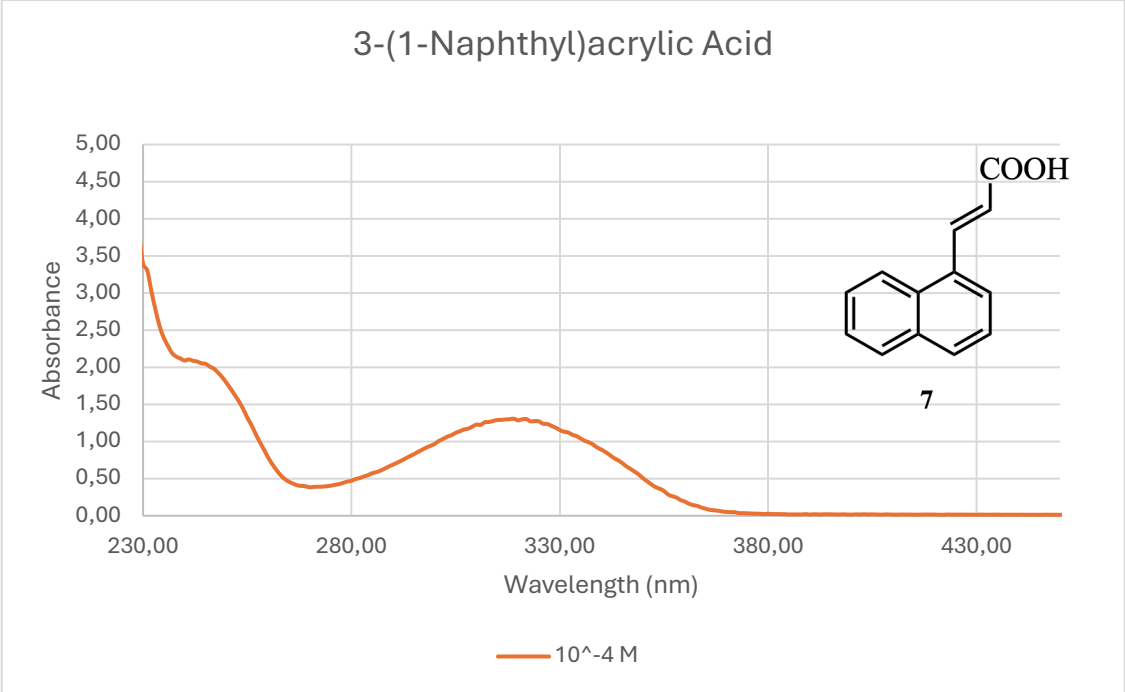

Figure 31. UV-Vis absorption spectrum of compound **7** in MeOH

Initially, the effect of daylight was investigated. For compound **6**, 5.7 mg was dissolved in 0.8 mL $CDCl_3$ in an NMR tube. As a first step, initial ^1H NMR was recorded, and it was seen that *trans:cis* ratio was 98:2. For compound **7**, 10.0 mg was dissolved in 0.8 mL DMSO-d_6. Initial ^1H NMR analysis showed that it was pure *trans* product. After that, both NMR tubes were placed in front of the window, where they could be exposed to the daylight. From day 1 to 11, the change was followed by the ^1H NMR. During this period, cycyloadduct formation was not seen for both compounds. However, *cis-trans* isomerization was seen, and the ratio for both compounds stopped increasing after day 9.

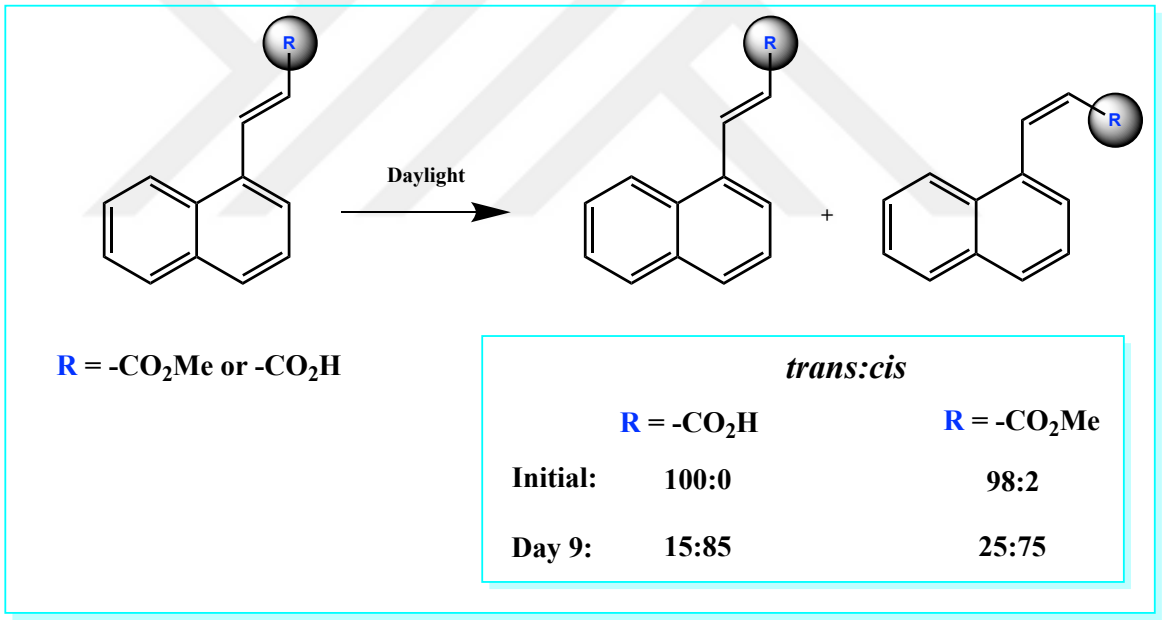

Scheme 29. Isomerization of compounds **6** and **7**

After the effect of daylight exposure, another experiment was designed to see the effect of different wavelengths. With this aim, two light sources with different λ_{max} were used: 365 (4 ×9 Watt) and 395 (46.65 Watt) nm. Because compound **6** was in oil form, it was possible to drop it on the quartz microscope slide and irradiate it with the UV light. In

addition to the irradiation in that neat form, compound **6** was also dissolved in $CDCl_3$ in an NMR tube and irradiated under both wavelengths. For both phases and wavelengths, homodimerization was seen. However, it was not diastereoselective (Scheme 30).

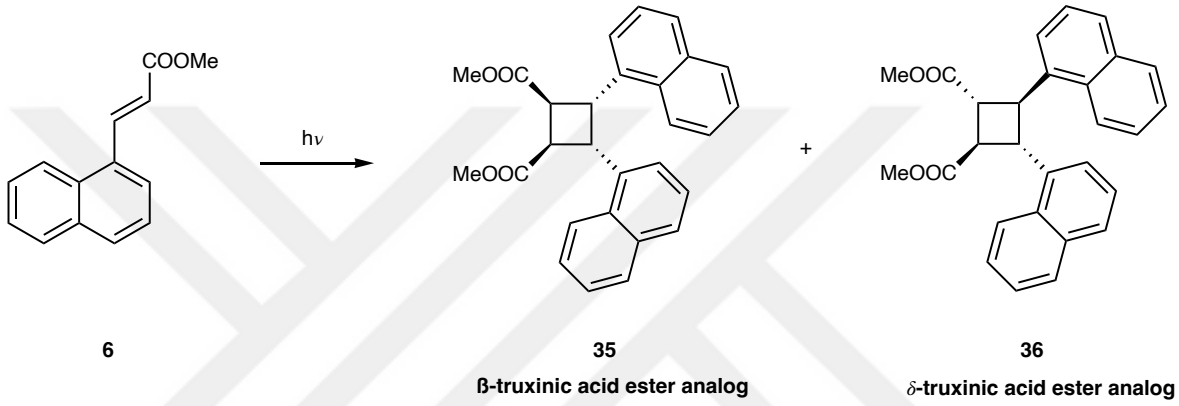

Scheme 30. Homodimerization of compound **6**

As mentioned, template molecule **4** provides the *syn*-head-to-head dimerization product as single diasteromer like the *ß*-truxinic acid ester **35** that was isolated as a single diastereomer after the template removal of **27**. However, the irradiation study of compound **6**, gave the mixture of ß and δ diastereomers as showed by ^{1}H NMR spectroscopy. In addition to that these light sources with given λ_{max} values may have crosssections in the 380 nm-280 nm range where compound **6** absorbs based on the UV-Vis study. Because at 395 nmr compound **6** does not absorps the light in solution of MeOH. Summarized results can be seen in the below Tables 2 and 3.

Table 1. Irradiation of compound **6** under UV light with λ_{max} 365 nm

365 nm	Time (h)	Amount (mg)	Diastereomeric Ratio (ß/ δ)		yield(%)
			Before Column	After Column	
Neat	16	21.6	1.00/0.34	1.00/0.29	64
Solution	28	17.0	≅ 1.0	No column	-

Table 2. Irradiation of compound **6** under UV light with λ_{max} 395 nm

395 nm	Time (h)	Amount (mg)	Diastereomeric Ratio (ß/ δ)		yield(%)
			Before Column	After Column	
Neat	16	17.4 mg	1.00/0.45	1.00/0.40	80
Solution	28	15.4 mg	1.00/3.61	1.00/3.29	77

With respect to Tables 2 and 3, it can be said that the ratio of delta isomers increases in the solution irradiations. Results can be interrupted as, in neat form, due to the being oil-like, there is still movement of molecules, giving rise to little delta isomer, *anti*-head-to-head dimerization product. However, in solution, molecules can move freely, and it affects delta isomer formation; therefore, it has a greater ratio.

For the visible light irradiation of compound **6**, $Ir(ppy)_3$ photocatalyst and blue light (450 nm, LED) were used.[52] At the end of the 8 hours, the major product was the δ-truxinic acid ester analog, **36**. However, compound **35** was also present in the medium. According to the ^1H NMR studies, the ratio was 1.00:0.16 (δ: ß). By taking advantage of the R_f difference of the compounds, the isolation with the column chromatography was achieved. The δ-truxinic acid ester analog was isolated in a 39% yield.

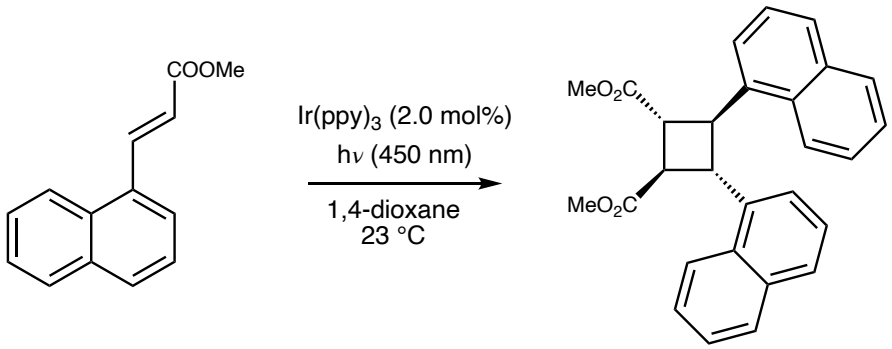

6

36
***δ*-truxinic acid ester analogue**
39% yield

Scheme 31. Homodimerization of compound **6** catalyzed by the iridium photocatalyst

As a last step, the powder of compound **7** was irradiated. The experimental setup was also the same as the heterodimerization and consisted of a nail dryer equipped with four 9-Watt fluorescent bulbs (UVA, 365 nm), quartz microscope slides, and paper clips to fix the slides. 20.4 mg of compound **7** was irradiated for 20 h. In every 4 h, the crude mixture was mixed to provide homogeneous light distribution. At the end of the reaction period, to see %conversion, ^{1}H NMR was recorded. Because compounds **7** and **36** were not fully soluble in the $CDCl_3$, deuterated acetone was used for ^{1}H NMR analysis. At the end of the 20 h, the %^{1}H NMR conversion was 88%. And the single diastereomer, ß, was isolated in 78% yield. This homodimerization shows that compound **7**, also obeys Schmidt criteria for this photochemical [2+2] cycloaddition reaction.

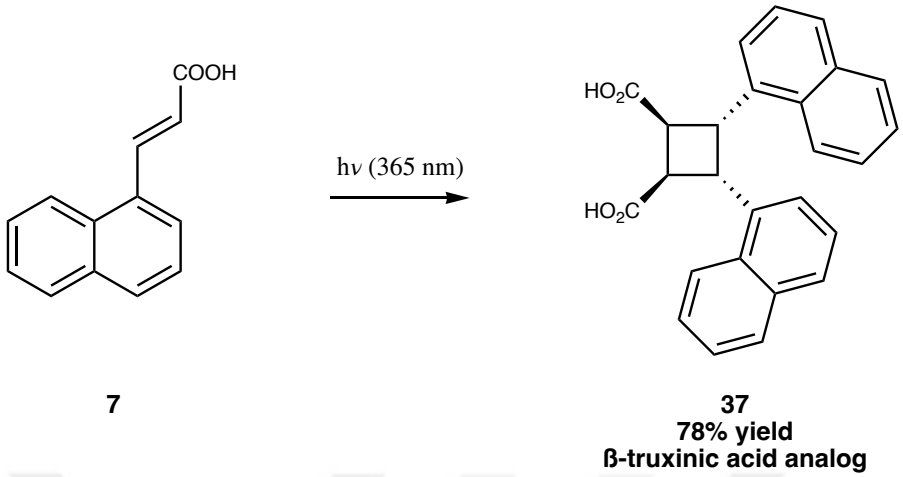

Scheme 32. Homodimerization of compound **7** in solid state

2.3. Conclusion

In the second part of the thesis, homodimerization of template-bound naphthalene acrylic acid was studied. This study brought us to the investigation of single-crystal-to-single-crystal transformation. SC-XRD studies provided the structures of the diester **26** and recrystallized cycloadduct **27**. However, SC-XRD data could not be provided for the irradiated single crystal. But, with further ATR-IR studies, it was seen that a crystal polymorphism could be the issue due to the differences recorded in the irradiated crystals' IR spectrum and powder irradiation product of **27**.

In addition to the SCSC investigation, with the irradiation experiment of compound **6**, it was seen that without template molecule **4**, reactions cannot yield a single diastereomer. This control can be provided with the 1,8-dihydroxynaphthalene to give a *syn*-head-to-head dimerization product.

3. Experimental Part

3.1 Materials and Methods

During the synthesis, when the procedure requires, reactions were run under nitrogen gas to provide an inert atmosphere in oven-dried glassware. In addition, further deoxygenation procedures were applied for DMF in Heck cross-coupling reaction by purging nitrogen through the solvent. TLC (thin-layer chromatography) was used to monitor the process at every step of the reactions. For this purpose, aluminum-backed TLC plates from Silicycle ultrapure silica gels (F-254 indicator) were used. 254 nm UV light and $KMnO_4$ stain were employed to visualize spots on the TLC plate. Flash column chromatography was used for purification, and flash silica gel, which had particle size 40-63 μm (230-400 mesh), was used. *n*-Pentane was employed as a solvent in addition to DCM for crystallization. 1,8-Dihydoxynaphthalene was commercially available from abcr and did not require any further purification. Other commercially available chemicals were used during the study, such as *trans*-cinnamic acid from Across, oxalyl chloride from abcr, and KOH from Carlo-Erba. In addition to those chemicals, others from the various brands, such as Aldrich and TCI, were used without applying any purification beforehand. Characterization processes were carried out by NMR, ATR-IR, Q-TOF/LCMS, UV-Vis and melting point detection. For the NMR, Bruker Avance III 400 (^{1}H NMR 400 MHz, ^{13}C NMR 100 MHz) spectrometer was used at the National Research Center and Institute of Materials Science and Nanotechnology (UNAM). The instrument was calibrated for both ^{1}H and ^{13}C NMR. For ^{1}H NMR, either internal standard TMS 0.0 ppm or the solvent residue was used ($CHCl_3$ in $CDCl_3$ 7.26 ppm, $(CH_3)_2CO$ in $(CD_3)_2CO$ in 2.05 ppm, DMSO in DMSO-*d*$_6$ 2.50 ppm). For ^{13}C NMR, the solvent signal was used ($CDCl_3$ at 77.16 ppm, $(CH_3)_2CO$ in $(CD_3)_2CO$ at 206.26 ppm and

DMSO-d_6 at 39.52 ppm). While reporting the NMR spectra, chemical shifts, integrals, coupling constants, and multiplicities were used (s = singlet, brs = broad singlet, d = doublet, dd = doublet of doublets, t = triplet, q= quarted, m = multiplet). UNAM also provided the mass spectrometer, Agilent Technologies 6224 Q-TOF/LCMS. ATR-IR and UV-Vis measurements were taken with Bruker Alpha Platinum and Carry 300 UV-Vis from Agilent Technologies, respectively, in the Bilkent Univeristy Department of Chemistry. Prof. Dr. Onur Şahin did the crystallographic analyses at the Sinop University. For the irradiations, 365 nm UV-A light (36 Watt), 395 nm UV light (46.65 Watt) and 450 nm blue LEDs were used. Photographs were taken with Wifi X 200 4K optical microscopes.

3.2 Reaction Procedures of Chapter 1

3.2.1 Compound 5

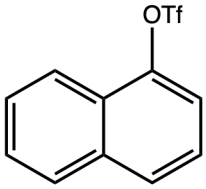

5

This compound was prepared following the procedure reposted in the literature.[53] In a 100 mL oven-dried round-bottomed flask, after three times of vacuum-nitrogen cycle, 1-naphthol (500 mg, 3.47 mmol) was added. Then, 5.0 mL of anhydrous DCM was added. After 5 min, the reaction flask was inserted in an ice bath when the solid dissolved completely, Et_3N (422 mg, 580 µL, 4.16 mmol) was added slowly. Afterward, 2.0 mL of anhydrous DCM and trifluoromethane sulfonic anhydride (1.08 g, 640 µL, 1.67 mmol) were added in 10 min slowly. After ca. 10 min, the ice bath was removed, and the reaction was

stirred for 3 h at room temperature 23 °C. The reaction was quenched with 5 mL of deionized water. During the work-up, 10 mL of DCM (3 times) was used to wash the aqueous phase. Anhydrous Na_2SO_4 was used to dry the combined organic phase; after the removal of the salt by filtration, the solvent was evaporated by a rotary evaporator. Purification was done with flash column chromatography (SiO_2; EtOAc: hexanes = 1:2), the product was obtained as a colorless oil (906 mg, 95% yield).

TLC Visualization: UV active; stains with $KMnO_4$ solution.

^{1}H NMR (400 MHz; $CDCl_3$) δ: 8.13 (1H, d, *J* = 8.3 Hz), 7.91 (1H, d, *J* = 8.0 Hz,), 7.86 (1H, d, *J* = 6.8 Hz), 7.66 (1H, t, *J* = 7.6 Hz), 7.60 (1H, t, *J* = 7.5 Hz), 7.50-7.45 (2H, m).

The ^{1}H NMR spectral data are in agreement with the data reported in the literature.[53]

3.2.2 Compound 6

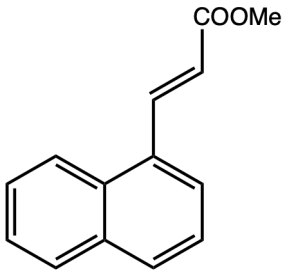

6

The oven-dried 25 mL Schlenk flask was used, and the vacuum-nitrogen cycle was followed three times. At 23 °C and continued N_2 flow, compound **5** (100 mg, 0.36 mmol) was dissolved in 3.0 mL of deoxygenated DMF. Afterward, methyl acrylate (156 mg, 164 µL, 1.81 mmol) was added to the reaction medium. The wall of the flask was washed with 1.0 mL solvent after adding Et_3N (183 mg, 252 µL, 1.81 mmol) slowly. Lastly, $PdCl_2(PPh_3)_2$

(25.4 mg, 0.032 mmol) was added, and the flask wall was washed with 1.0 mL of DMF. The Schlenk flask was then sealed with a glass stopper. Then, the Schlenk flask was heated gradually at the top of the oil bath. After 10 min, it was dipped into the 80 °C pre-heated oil bath. The reaction mixture was stirred at this temperature for 24 h. At the end of the reaction period, 5 mL of deionized water was used to quench the reaction when the reaction was cooled down to room temperature. Then, the mixture was transferred into the separation funnel, and 5 mL of deionized water and 5 mL of brine were added to the separation funnel. The product was extracted three times with 10 mL of EtOAc. Anhydrous Na_2SO_4 was used to dry the combined organic phase; after the filtration of the salt, the solvent was evaporated by a rotary evaporator. The resulting oily brown crude was purified with column chromatography (SiO_2; EtOAc: hexanes = 1:10) to give compound **6** as a colorless oil (75 mg, 98% yield).

TLC Visualization: UV active; stains with $KMnO_4$ solution.

^{1}H NMR (400 MHz; $CDCl_3$) δ: 8.55 (1H, d, *J* = 15.8 Hz), 8.20 (1H, d, *J* = 8.4 Hz,), 7.88 (2H, app t, *J* = 7.7 Hz), 7.75 (1H, d, *J* = 7.2 Hz), 7.60-7.51 (2H, m), 7.48 (1H, t, *J* = 7.7 Hz), 6.54 (1H, d, *J* = 15.7 Hz), 3.87 (3H, s).

The ^{1}H NMR spectral data are in agreement with the data reported in the literature.[54]

3.2.3 Compound 7

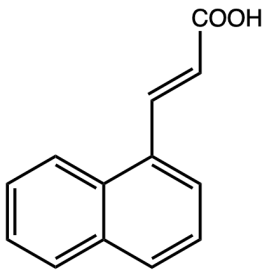

7

In a 25 mL round-bottomed flask, compound **6** (77 mg, 0.36 mmol) was dissolved in a 1:2 mixture of MeOH:THF solvent system at 23 °C. An excess of 5 M aqueous solution of KOH (3.0 mL) was gradually added to the round-bottomed flask. At the end of 4 h, TLC analysis did not show any starting material, and the reaction was stopped. The reaction flask was placed in an ice bath, and HCl (ca. 1.2 M) was added into the flask to make pH 1-2. After the pH adjustment, the product was extracted by DCM (3×10 mL). Anhydrous Na_2SO_4 was used to dry the combined organic phase; after the filtration of the salt, the solvent was evaporated by a rotary evaporator. The resulting slightly yellowish solid crude was purified by flash column chromatography (SiO_2; 1% acetic acid in EtOAc: hexanes = 1:1) to give compound **7** as a white solid (64.8 mg, 90% yield).

TLC Visualization: UV active; stains with $KMnO_4$ solution.

M.P. 211.8-212.4 °C

^{1}H NMR (400 MHz; DMSO-*d*$_6$) δ: 12.58 (1H, bs), 8.43 (1H, d, *J* = 15.7 Hz), 8.24 (1H, d, *J* = 8.3 Hz,), 8.05 (2H, t, *J* = 9.0 Hz), 7.99 (1H, d, *J* = 7.1 Hz), 7.70-7.59 (3H, m), 6.64 (1H, d, *J* = 15.7 Hz).

The ^{1}H NMR spectral data are in agreement with the data reported in the literature.[55]

3.2.4 Compound 10

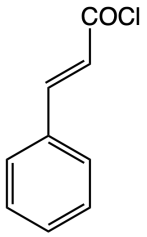

9

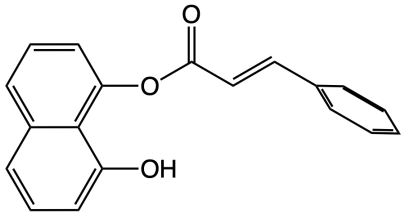

10

The synthesis of compound **10** is previously reported.[20] Initially, acyl chloride **9** was prepared by dissolving *trans*-cinnamic acid (200 mg, 1.35 mmol) in 1.0 mL of (excess) oxalyl chloride under N_2 at 23 °C. After 10 min, the round-bottomed flask was dipped into pre-heated oil bath at 60 °C and stirred for 2 h. At the end of the reaction period, unreacted oxalyl chloride evaporated under reduced pressure carefully. The resulting acyl chloride **9** (225 mg, 1.34 mmol) was obtained as a yellow solid. Then, as a next step, the monoester **10** was synthesized. An oven-dried 50 mL round-bottomed flask was cooled through the vacuum-nitrogen cycle. Under an inert atmosphere of N_2, 1,8-DHN (249 mg, 1.55 mmol) dissolved in 5.0 mL of anhydrous THF. When the solution became clear after 10 min, an ice bath was placed under the round-bottomed flask. NaH (57 mg, 1.43 mmol , 60% dispersion in mineral oil) was added carefully in small portions. After 20 min, without removing the ice bath, a solution of acyl chloride **9** (1.34 mmol, 224 mg) in 5.0 mL anhydrous THF was added into the reaction medium. After 10 min, the ice bath was removed, and the reaction mixture was stirred for 75 min 23 °C. The resulting mixture was quenched with 10 mL of saturated aqueous solution of NH_4Cl. The aqueous phase was extracted with EtOAc (3× 15 mL). The combined organic phase was dried over anhydrous Na_2SO_4. After the filtration of the salt and evaporation of the solvent with a rotary evaporator, purification by flash column

chromatography was done (SiO_2; EtOAc: hexanes = 1:5) to provide compound **10** as an orange solid (305 mg, 78% yield).

TLC Visualization: UV active; stains with $KMnO_4$ solution.

^{1}H NMR (400 MHz; $CDCl_3$) δ: 7.88 (1H, d, *J* = 15.9 Hz), 7.64 (1H, dd, *J* = 8.3, 0.8 Hz), 7.54-7.52 (2H, m), 7.37-7.34 (5H, m), 7.27 (2H, t, *J* = 7.9 Hz), 7.18-7.16 (1H, m), 6.81 (1H, dd, *J* = 7.5, 1.1 Hz), 6.65 (1H, d, *J* = 15.9 Hz).

The ^{1}H NMR spectral data are in agreement with the data reported in the literature.[26]

3.2.5 Compound 11

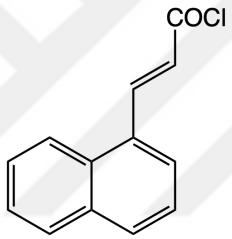

8

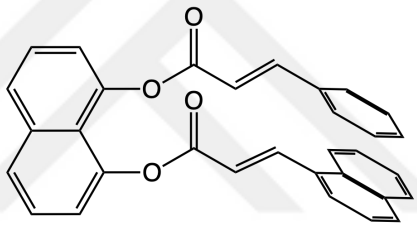

11

The applied procedure was modified from the Türkmen Research Group's previous work.[21] Initially, acyl chloride **8** was prepared by dissolving 1-naphthalene acrylic acid (**7**) (51.8 mg, 0.26 mmol) in 0.7 mL (excess) of oxalyl chloride under N_2 at 23 °C. After 10 min, the round-bottomed flask dipped into pre-heated oil bath at 60 °C and was stirred for 2 h. At the end of the reaction period, unreacted oxalyl chloride was evaporated carefully. The resulting acyl chloride **8** (56.6 mg, 0.261 mmol) was obtained as a yellow solid. Then, as the next step, diester **11** was synthesized. An oven-dried 50 mL round-bottomed flask was cooled through the vacuum-nitrogen cycle. Under an inert N_2 atmosphere, compound **10** (65.9 mg, 0.22 mmol) was dissolved in 3.0 mL of anhydrous THF. When the solution became clear after 10 min, an ice bath was placed under the round-bottomed flask. Then, acyl chloride **8**

(56.61mg, 0.26 mmol) was dissolved in 3.0 mL of anydrous THF and was added to the reaction medium. Then, NaH (0.25 mmol, 10.0 mg, 60% dispersion in mineral oil) was added in small portions. After 5 min, the ice bath was removed, and the reaction mixture was stirred overnight. It was then quenched with 10 mL of saturated aqueous NH_4Cl solution. The aqueous phase was extracted with EtOAc (3× 10 mL). Combined organic phase was dried by over anhydrous Na_2SO_4. After the filtration of salt and evaporation of the solvent with a rotary evaporator, purification by flash column chromatography was done (SiO_2; hexanes: DCM: MeOH = 8:1:1 to 7:1:1) to give compound **11** as a yellow solid (53.9 mg, 50% yield).

M.P. 147.7-148.8 °C

R_f = 0.21 (Hexanes: DCM: MeOH = 7:1:1)

TLC Visualization: UV active; stains with $KMnO_4$ solution.

^{1}H NMR (400 MHz; $CDCl_3$) δ: 8.72 (1H, d, *J* = 15.8 Hz), 8.17 (1H, d, *J* = 8.2), 7.82-7.78 (4H, m), 7.74 (1H, d, *J* = 8.2 Hz), 7.54-7.46 (5H, m), 7.24 (1H, d, *J* = 7.5Hz), 7.21 (1H, d, *J* = 7.5 Hz), 7.14-7.10 (3H, m), 7.05 (1H, t, *J* = 7.7 Hz), 6.90 (2H, t, *J* = 7.7 Hz), 6.72 (1H, d, *J* = 15.8 Hz), 6.60 (1H, d, *J* = 16.0 Hz).

^{13}C{^{1}H} NMR (100 MHz; $CDCl_3$) δ: 166.0, 165.9, 147.1, 145.4, 143.6, 137.0, 133.8, 133.7, 131.5, 131.0, 130.9, 130.5, 128.8, 128.7, 128.0, 127.1, 127.0, 126.3, 126.2, 125.4, 125.14, 123.15, 121.5, 120.8, 120.6, 119.6, 117.3.

FTIR ν_{max} (ATR, solid)/cm^{-1} 3059, 2925, 1729, 1633, 1604, 1574, 1432, 1366.

3.2.6 Compound 12

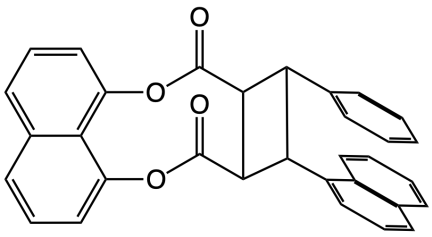

12

Diester **11** was irradiated with 365 nm (36 W) UV light in solution and solid state to get cycloadduct **12**.

Irradiation in Solution:

Diester **11** (23.6 mg, 0.050 mmol) was dissolved in 2.0 mL of $CHCl_3$ in a quartz test tube. In the nail dryer, the tube is placed with a stir bar. To control temperature, a fan is placed towards the open side of the nail dryer. Reaction was monitored by TLC. The solvent was removed at the end of 20 h, and the ^1H NMR sample was prepared. The conversion was determined as 90%. Purification was made by flash column chromatography (SiO_2; EtOAc: hexanes = 1:10 to 1:9), and compound **12** was obtained as an amorphous foam (15.1 mg, 64% yield).

Irradiation in Solid State:

Yellow-colored solid diester **11 (**18.3 mg, 0.038 mmol) was placed between two quartz microscope slides. With the help of paper clips, slides were fixed. Microscope slides were placed under UV lamps in a nail dryer (365 nm, 4×9 W). Every 4 h, solid residue is mixed with a spatula. In addition to the mixing process to ensure homogenous light

distribution, the side of the slides facing the lamp was turned every 4 h. At the end of 32 h of irradiation, the ^{1}H NMR conversion was determined as 15%. By column chromatography (SiO_2; Hexanes: DCM: MeOH = 10:1:1 to 9:1:1) compound **12** was obtained as an amorphous foam (2.1 mg, 11% yield).

R_f = 0.42 (Hexanes: DCM: MeOH = 7:1:1)

TLC Visualization: UV active; stains with $KMnO_4$ solution.

^{1}H NMR (400 MHz; $CDCl_3$) δ: 7.98 (1H, d, *J* = 8.4 Hz), 7.82 (1H, dd, *J* = 8.3, 0.8 Hz), 7.81 (1H, dd, *J* = 8.3, 0.7 Hz), 7.72-7.70 (1H, app d, *J* = 7.8 Hz), 7.62 (1H, dd, *J* = 7.5, 1.5 Hz), 7.55-7.44 (3H, m), 7.41-7.30 (4H, m), 7.25-7.23 (1H, m), 7.00-6.97 (2H, m), 6.95-6.90 (3H, m), 5.51 (1H, t, *J* = 9.5 Hz), 4.87 (1H, dd, *J* = 10.2, 4.9 Hz), 4.66 (1H, t, *J* = 9.8 Hz), 4.16 (1H, ddd, *J* = 10.6, 4.9, 0.9 Hz).

^{13}C{^{1}H} NMR (100 MHz; $CDCl_3$) δ: 170.4, 169.7, 145.54, 145.49, 138.1, 137.1, 133.7, 133.6, 131.5, 128.7, 128.0, 127.7, 127.10, 127.09, 126.9, 126.6, 126.0, 125.9, 125.0, 124.1, 123.9, 121.2, 121.1, 119.7, 45.3 (overlapping of two signals), 43.8, 42.2.

FTIR ν_{max} (ATR, solid)/cm^{-1} 2959, 2922, 2852, 1762, 1606, 1576, 1455, 1365, 1259.

3.2.7 Compound 13

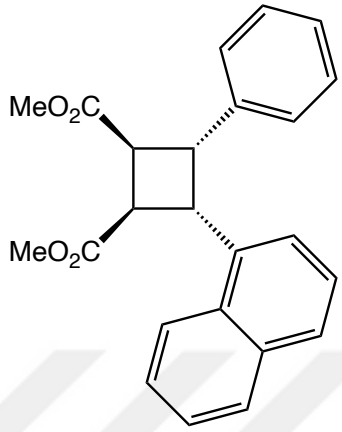

13

The applied procedure was adapted from the Türkmen Research Group's previous work.[22] Compound **12** (11.9 mg, 0.025 mmol) was dissolved in 3.0 mL of a 1:1 MeOH: THF mixture in a 20-mL scintillation vial. In the clear solution of dissolved template-bound cycloadduct **12**, 5.0 equiv. of NaOMe (6.8 mg, 0.13 mmol) was added. The vial was placed onto the magnetic stirrer at 45 °C for 3.5 h. At the end of the reaction all volatiles were evaporated under vacuum. The flash column chromatography was applied for the purification (SiO_2; EtOAc: hexanes = 1:11 to 1:5) to obtain orange-like oil product **13** (8.6 mg, 91% yield).

R_f = 0.30 (1:5 EtOAc: hexanes)

TLC Visualization: UV active; stains with $KMnO_4$ solution.

^{1}H NMR (400 MHz; $CDCl_3$) δ: 7.96 (1H, d, *J* = 8.4 Hz), 7.69 (1H, d, *J* = 8.0 Hz), 7.57 (1H, d, *J* = 8.2 Hz), 7.45 (1H, t, *J* = 7.6 Hz), 7.38 (1H, t, *J* = 7.4 Hz), 7.29-7.26 (1H, m), 7.18 (1H, d, *J* = 7.0 Hz), 6.87 (5H, app s), 5.22 (1H, t, *J* = 9.6 Hz), 4.46 (1H, dd, *J* = 9.9, 4.7 Hz), 4.28 (1H, t, *J* = 9.7 Hz), 3.81 (3H, s), 3.80-3.76 (1H, m), 3.75 (3H, s).

$^{13}C\{^{1}H\}$ NMR (100 MHz; $CDCl_3$) δ: 173.5, 172.8, 138.4, 134.3, 133.5, 131.7, 128.6, 127.8 (overlapping of two signals), 127.4, 126.6, 125.8, 125.7, 125.0, 124.2, 123.6, 52.5, 52.3, 46.1, 44.5, 42.7, 41.7.

FTIR ν_{max} (ATR, film)/cm^{-1} 2951, 2922, 2850, 1730, 1599, 1509, 1496, 1453, 1435.

3.2.8 Compound 15

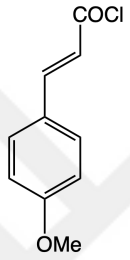

14

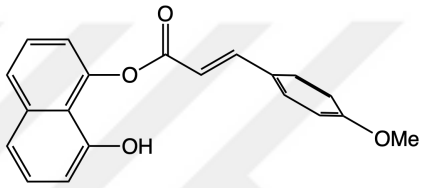

15

The synthesis of compound **15** was previously reported.[20] Initially, acyl chloride **14** was prepared by dissolving 4-methoxycinnamic acid (250 mg, 1.40 mmol) in 1.5 mL (excess) of oxalyl chloride under an inert atmosphere of N_2 at 23 °C. After 10 min, the round-bottomed flask was dipped into a pre-heated oil bath at 60 °C and was stirred for 1.5 h. At the end of the reaction period, unreacted oxalyl chloride was evaporated carefully. The resulting acyl chloride **14** (275 mg, 1.40 mmol) was obtained as a yellow solid. Then, as the next step, monoester **15** was synthesized. An oven-dried 50 mL round-bottomed flask was cooled through vacuum-nitrogen cycle. Under an inert N_2 atmosphere, 1,8-DHN (247 mg, 1.54 mmol) was dissolved in 3.0 mL of anhydrous THF. When the solution became clear after 10 min, an ice bath was placed under the round-bottomed flask. NaH (56 mg, 1.40 mmol, 60% dispersion in mineral oil) was added in small portions. After 20 min, without removing the ice bath, acyl chloride **14** (276 mg, 1.40 mmol,) was dissolved in 2.0 mL of anhydrous THF and was added to the reaction medium. After 10 min, the ice bath was

removed, and the reaction mixture was stirred for 2 h at 23 °C. It was then quenched with 10 mL of saturated aqueous solution of NH_4Cl. The aqueous phase was extracted with EtOAc (3× 10 mL). Combined organic phase was dried by over anhydrous Na_2SO_4. After the filtration of salt and evaporation of the solvent with a rotary evaporator, purification by flash column chromatography was done (SiO_2; EtOAc: hexanes = 1:11 to 1:7) to obtain compound **15** as an orange-like solid (339 mg, 76%, yield).

TLC Visualization: UV active; stains with $KMnO_4$ solution.

^{1}H NMR (400 MHz; $CDCl_3$) δ: 7.92 (1H, d, *J* = 15.9 Hz), 7.71 (1H, dd, *J* = 8.3, 0.8 Hz,), 7.56 (2H, app d, *J* = 8.8 Hz), 7.45-7.41 (2H, m), 7.34 (1H, t, *J* = 7.9 Hz), 7.25 (1H, dd, *J* = 7.6, 1.0 Hz), 6.95 (2H, app d, *J* = 8.8 Hz), 6.89 (1H, dd, *J* = 7.5, 1.1 Hz), 6.59 (1H, d, *J* = 15.9 Hz), 3.87 (3H, s).

The ^{1}H NMR spectral data are in agreement with the data reported in the literature.[26]

3.2.9 Compound 16

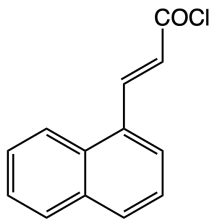

8

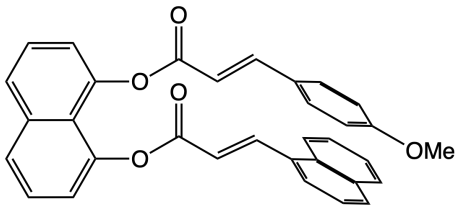

16

The applied procedure was adapted from the Türkmen Research Group's previous work.[21] Initially, acyl chloride **8** was prepared by dissolving 1-naphthalene acrylic acid (69.6 mg, 0.351 mmol) in 1.0 mL (excess) of oxalyl chloride under N_2 at 23 °C. After 10 min, the round-bottomed flask was dipped into pre-heated oil bath at 60 °C and was stirred for 2 h.

At the end of the reaction period, unreacted oxalyl chloride was evaporated carefully. The resulting acyl chloride **8** (76.1 mg, 0.351 mmol) was obtained as a yellow solid. However, 51.2 mg of compound **8** (0.236 mmol) was used in the next step where diester **16** was synthesized. An oven-dried 50 mL round-bottomed flask was cooled through vacuum-nitrogen cycle. Under an inert N_2 atmosphere, compound **15** (52.7 mg, 0.216 mmol) was dissolved in 3.0 mL of anhydrous THF. When the solution became clear after 10 min, an ice bath was placed under the round-bottomed flask. Then, acyl chloride **8** (51.2, 0.23 mmol,) was dissolved in 2.0 mL of anhydrous THF and was added to the reaction medium. Then, NaH (0.164 mmol, 6.5 mg, 60% dispersion in mineral oil) was added in small portions. After 5 min, the ice bath was removed, and the reaction mixture was stirred overnight. It was then quenched with 10 mL of saturated aqueous solution of NH_4Cl. The aqueous phase was extracted with EtOAc (3× 15 mL). The combined organic phase was dried by over anhydrous Na_2SO_4. After the filtration of salt and evaporation of the solvent with a rotary evaporator, the crude mixture looked like yellow oil. Purification with flash column chromatography was done (SiO_2; hexanes: DCM: MeOH= 11:1:1 to 7:1:1) to obtain compound **16** as a yellow solid (41.6 mg, 51% yield).

M.P. 156.7-159.9 °C

R_f = 0.155 (hexanes: DCM: MeOH = 7:1:1)

TLC Visualization: UV active; stains with $KMnO_4$ solution.

^{1}H NMR (400 MHz; $CDCl_3$) δ: 8.63 (1H, d, *J* = 15.8 Hz), 8.11 (1H, d, *J* = 8.1 Hz), 7.76-7.65 (5H, m), 7.49-7.41 (5H, m), 7.17 (1H, d, *J* = 7.3 Hz), 7.14 (1H, d, *J* = 7.5 Hz), 7.06 (1H, t, *J* = 7.7 Hz), 6.97 (2H, d, *J* =8.7 Hz), 6.66 (1H, d, *J* = 15.8 Hz), 6.38 (1H, d, *J* = 15.9 Hz), 6.28 (2H, d, *J* = 8.6 Hz), 3.62 (3H, s).

$^{13}C\{^{1}H\}$ NMR (100 MHz; $CDCl_3$) δ: 166.3, 165.9, 161.4, 146.8, 145.4, 143.3, 137.0, 133.8, 131.5, 131.0, 130.9, 129.7, 128.8, 127.1, 127.0, 126.9, 126.5, 126.3, 126.22, 126.17, 125.4, 125.23, 125.16, 123.2, 121.6, 120.8, 120.7, 119.8, 114.7, 114.0, 55.3.

FTIR ν_{max} (ATR, solid)/cm^{-1} 3061, 2961, 2933, 2911, 2835, 1714, 1629, 1601, 1573, 1510, 1463.

3.2.10 Compound 17

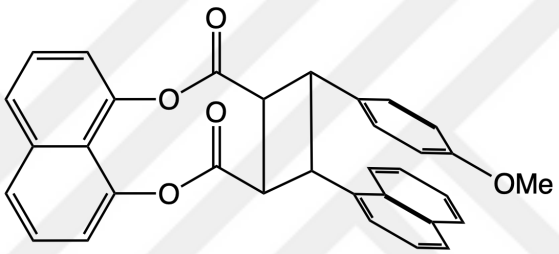

17

Diester **16** was irradiated with 365 nm (36 W) UV light in solution and solid state to get cycloadduct **17**.

Irradiation in Solution:

Diester **16** (18.4 mg, 0.036 mmol) was dissolved in 3.5 mL of $CHCl_3$ in a quartz test tube. In the nail dryer, the test tube was placed with a stir bar. In order to control temperature, a fan is placed towards the open side of the nail dyer. The reaction was monitored by TLC. The solvent was removed at the end of 20 h, and the ^{1}H NMR sample was prepared. The conversion was determined as 95%. Purification was done by flash column chromatography (SiO_2; EtOAc: hexanes = 1:15 to 1:8) to obtain compound **17** as a yellowish-orange oil (12.6 mg, 85% yield).

Irradiation in Solid State:

Yellow-colored solid diester **16** (18.3 mg, 0.036 mmol) was placed between two quartz microscope slides. With the help of paper clips, slides were fixed. Microscope slides were placed under UV lamps in a nail dryer (365 nm, 4×9W). Every 4 h, solid residue is mixed with a spatula. In addition to the mixing process to ensure homogenous light distribution, the side of the slides facing the lamp was turned every 4 h. At the end of 32 h of irradiation, the ^{1}H NMR conversion was determined as 50%. Compound **17** was purified by flash column chromatography (SiO_2; hexanes: DCM: MeOH 10:1:1 to 7:1:1) with 35% yield (6.5 mg).

R_f = 0.34 (1:2 EtOAc: hexanes).

TLC Visualization: UV active; stains with $KMnO_4$ solution.

^{1}H NMR (400 MHz; $CDCl_3$) δ: 7.90 (1H, d, *J* = 8.4 Hz), 7.75 (1H, d, *J* = 8.3 Hz), 7.74 (1H, d, *J* = 8.3 Hz), 7.66 (1H, d, *J* = 8.0 Hz), 7.57 (1H, dd, *J* = 6.9, 2.1 Hz), 7.49-7.29 (6H, m), 7.24 (1H, d, *J* = 7.5 Hz), 7.17 (1H, d, *J* = 8.4 Hz), 6.84 (2H, d, *J* = 8.6 Hz), 6.40 (2H, d, *J* = 8.6 Hz), 5.40 (1H, t, *J* = 9.4 Hz), 4.76 (1H, dd, *J* = 10.1, 4.9 Hz), 4.58 (1H, t, *J* = 9.8 Hz), 4.04 (1H, dd, *J* = 10.6, 4.9 Hz), 3.51 (3H, s).

^{13}C{^{1}H} NMR (100 MHz; $CDCl_3$) δ: 170.5, 169.8, 158.3, 145.54, 145.48, 137.1, 133.9, 133.7, 131.5, 130.3, 129.0, 128.7, 127.7, 127.1, 126.5, 126.0, 125.9, 125.1, 124.2, 123.8, 121.2, 121.1, 119.7, 113.4, 55.2, 45.8, 44.7, 43.6, 42.4.

FTIR ν_{max} (ATR, film)/cm^{-1} 3058, 2954, 2922, 2850, 1760, 1732, 1629, 1607, 1577, 1513, 1461, 1441, 1364.

3.2.11 Compound 18

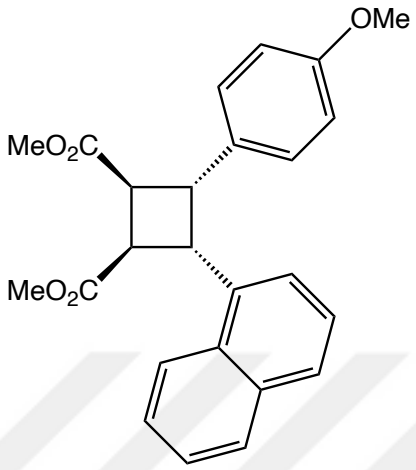

18

The applied procedure was adapted from the Türkmen Research Group's previous work.[22] Compound **17** (11.7 mg, 0.023 mmol) was dissolved in 3.0 mL of 1:1 MeOH: THF mixture in a 20-mL scintillation vial. Into the clear solution of dissolved template-bound cycloadduct, 5.0 equiv. of NaOMe (6.31 mg, 0.116 mmol) was added. The vial was placed onto the magnetic stirrer at 45 °C, and stirred for 3.5 h. Purification was done by flash column chromatography (SiO_2; 1.2:1 = hexanes: DCM). Compound **18** was obtained as a yellowish oil (8.2 mg, 87% yield).

R_f = 0.22 (1:5 EtOAc: hexanes)

TLC Visualization: UV active; stains with $KMnO_4$ solution.

^{1}H NMR (400 MHz; $CDCl_3$) δ: 7.93 (1H, d, *J* = 8.4 Hz), 7.70 (1H, d, *J* = 8.1 Hz), 7.58 (1H, d, *J* = 8.2 Hz), 7.44 (1H, t, *J* = 7.1 Hz), 7.38 (1H, t, *J* = 7.3 Hz), 7.29 (1H, t, *J* = 7.7 Hz), 7.19 (1H, d, *J* = 7.1 Hz), 6.78 (2H, d, *J* = 8.6 Hz), 6.41 (2H, d, *J* = 8.6 Hz), 5.17 (1H, t, *J* = 9.7 Hz), 4.41 (1H, dd, *J* = 9.9, 4.7 Hz), 4.26 (1H, t, *J* = 9.7 Hz), 3.80 (3H, s), 3.74 (3H, s), 3.71 (1H, dd, *J* = 10.2, 4.8 Hz), 3.56 (3H, s).

$^{13}C\{^{1}H\}$ NMR (100 MHz; $CDCl_3$) δ: 173.5, 172.8, 158.1, 134.5, 133.6, 131.7, 130.7, 128.8, 128.6, 127.4, 125.8, 125.6, 125.0, 124.2, 123.5, 113.3, 55.1, 52.4, 52.3, 45.4, 45.0, 42.9, 41.6.

FTIR ν_{max} (ATR, film)/cm^{-1} 2951, 2924, 2850, 1727, 1610, 1582, 1513, 1456.

3.3 Reaction Procedures of Chapter 2

3.2.12 Compound 26

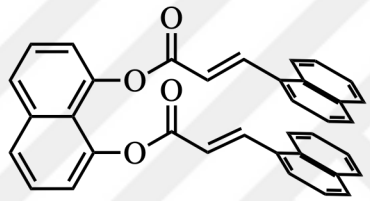

26

The applied procedure was adapted from the Türkmen Research Group's previous work.[20] An oven-dried 25 mL round-bottomed flask was cooled with three times vacuum-N_2 cycle. 1,8-DHN (50.0 mg, 0.312 mmol) was dissolved in 4.0 mL of anhydrous DCM under an inert N_2 atmosphere. Afterward, compound **7** (136 mg, 0.68 mmol) was added to the flask. To completely dissolve compound **7**, 4.5 mL of anhydrous DCM was added into the reaction medium. Sequentially, DCC (142 mg, 0.68 mmol) and DMAP (7.6 mg, 0.062 mmol,) were added to the flask. The reaction was run for 24 h under an inert N_2 atmosphere at 23 °C. The reaction mixture was quenched with 10 mL of deionized water. The aqueous phase was extracted with DCM (3×10 mL). The combined organic phase was dried over anhydrous Na_2SO_4. After the filtration of salt and evaporation of the solvent with a rotary evaporator, purification was done by flash column chromatography (SiO_2; hexanes: DCM = 1:1) to obtain compound **26** as a light yellow-white solid (77.1 mg, 48% yield).

Crystallization of Compound 26

In a 5.0 mL vial, 15.0 mg (0.029 mmol) of compound **26** was dissolved in 1.0 mL of DCM. When the solution became clear, it was placed inside a 20 mL scintillation vial that contained ca. 7.5 mL of *n*-pentane. The lid of the outer vial was closed and sealed with parafilm. To keep it under dark and far from the disturbance, it was stored inside a cabinet. Crystal formation was started to be observed within 24 h, and crystals were collected after two additional days. Single crystals had transparent-white look.

M.P. 223.5-225.2 °C (crystal)

R_f = 0.23 (1:1 DCM: hexanes).

TLC Visualization: UV active; stains with $KMnO_4$ solution.

^{1}H NMR (400 MHz; $CDCl_3$) δ: 8.61 (2H, d, *J* = 15.8 Hz), 8.01-7.98 (2H, m), 7.79 (2H, d, *J* = 8.4 Hz), 7.65-7.63 (2H, m), 7.56 (2H, d, *J* = 8.2 Hz), 7.47 (2H, t, *J* = 7.9 Hz), 7.36-7.31 (4H, m), 7.26 (2H, d, *J* = 7.2 Hz), 7.22-7.18 (2H, m), 6.75 (2H, t, *J* = 7.7 Hz), 6.66 (2H, d, *J* = 15.8 Hz).

^{13}C{^{1}H} NMR (100 MHz; $CDCl_3$) δ: 165.9, 145.5, 143.7, 137.0, 133.6, 131.3, 130.9, 130.7, 128.7, 127.1, 126.3, 126.2, 125.2, 125.0, 123.0, 121.6, 120.8, 119.6.

FTIR ν_{max} (ATR, solid)/cm^{-1} 3057, 2961, 2926, 1717, 1628, 1602, 1575, 1507, 1370, 1346.

3.2.13 Compound 27

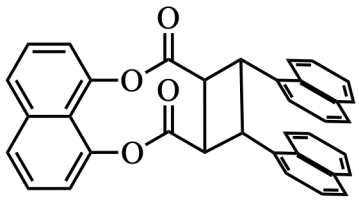

27

Diester **26** was irradiated with 365 nm (36 W) UV light in solution and solid state to get cycloadduct **27**.

Irradiation with Daylight in Solution:

Diester **26** (33.1 mg, 0.063 mmol) was dissolved in 1.0 mL of $CDCl_3$ in an NMR tube and placed in front of the window from inside of the laboratory. Conversion(%) values were determined periodically for 15 days by ^1H NMR spectroscopy. At the end of 15 days, 96% conversion was determined. The solvent was removed with a rotary evaporator, and purification was done by flash column chromatography (SiO_2; DCM: hexanes = 1:1). Compound **27** was obtained as a yellowish-white solid (18.7 mg, 56% yield).

Irradiation with 365 nm in Solution:

Diester **26** (15.8 mg, 0.030 mmol) was dissolved in 3.5 mL of $CHCl_3$ in a quartz test tube. In the nail dryer, the tube is placed with a stir bar. To control temperature, a fan was placed towards the open side of the nail dyer. Reaction monitored by TLC. The solvent was removed at the end of 9 h, and the ^1H NMR sample was prepared. Purification by flash

column chromatography (SiO_2; DCM: hexanes = 1:2 to 1:1.2) afforded compound **27** as a yellow solid (13.9 mg, 88% yield).

Irradiation in Solid State - Powder Form:

Yellowish-white solid diester **26** (8.2 mg, 0.015 mmol) was placed between two quartz microscope slides. With the help of paper clips, slides were fixed. Microscope slides were placed under UV lamps in a nail dryer (365 nm, 4×9 W). Every 4 h, solid residue was mixed with a spatula. In addition to the mixing process to ensure homogenous light distribution, the side of the slides facing the lamp was turned every 4 h. At the end of 16 h of irradiation, the conversion was determined as 98% by ^{1}H NMR analysis Purification by flash column chromatography (SiO_2; DCM: hexanes = 1:1) afforded compound **27** as a yellow solid (7.2 mg, 88% yield).

Irradiation in Solid State - Single Crystals:

Single crystals of diester **26** were gently picked and placed on the quartz microscope slide; however, this time, the second slide was not used to squeeze the materials. For 20 h, crystals were irradiated with 365 nm UV light. Every 4 h, crystals were made upside down to provide equal light distribution. At the end of the irradiation period, without applying any purification, crystals were directly dissolved in $CDCl_3$, and conversion value was calculated by ^{1}H NMR analysis.

Crystallization of Compound 27

In a 5.0 mL vial, 6.8 mg (0.013 mmol) of compound **27** was dissolved in 1.0 mL of DCM. When the solution became clear, it was placed inside a 20 mL scintillation vial that

contained ca. 7.5 mL of *n*-pentane. The lid of the outer vial was closed and sealed with parafilm. To keep it under dark and far from the disturbance, it was stored inside a cabinet. Crystal formation was started to be observed within 24 h, and crystals were collected after two additional days. Single crystals had a needle-like, yellowish-white look.

M.P. Powder likely to decompose after 178 °C, Single Crystal likely to decompose at 270 °C.

R_f = 0.62 (1:1 DCM: hexanes).

TLC Visualization: UV active; stains with $KMnO_4$ solution.

^{1}H NMR (400 MHz; $CDCl_3$) δ: 7.99-7.96 (2H, m), 7.75 (2H, d, *J* = 7.9 Hz), 7.58-7.55 (2H, m), 7.48 (2H, d, *J* = 8.2 Hz), 7.44 (2H, t, *J* = 8.0 Hz) ,7.26-7.19 (8H, m), 7.17-7.13 (2H, m), 5.68 (2H, app d, *J* = 6.2 Hz), 4.35 (2H, app d, *J* = 6.1 Hz).

^{13}C{^{1}H} NMR (100 MHz; $CDCl_3$) δ: 169.9, 145.5, 137.1, 134.4, 133.5, 131.6, 128.6, 127.6, 127.0, 126.5, 126.0, 125.7, 124.8, 123.7, 123.6, 121.1, 119.7, 45.3, 41.0.

FTIR ν_{max} (ATR, solid from powder irradiation)/cm^{-1} 3052, 2958, 2951, 2851, 1766, 1740, 1603, 1512, 1458.

FTIR ν_{max} (ATR, solid from SC irradiation)/cm^{-1} 3048, 3014, 2960, 1760, 1606, 1510, 1460.

HRMS (APCI +) Calculated for $C_{36}H_{24}O_4$ $[M+H]^+$: 521.1747 , found 521.1748

3.2.14 Compound 35

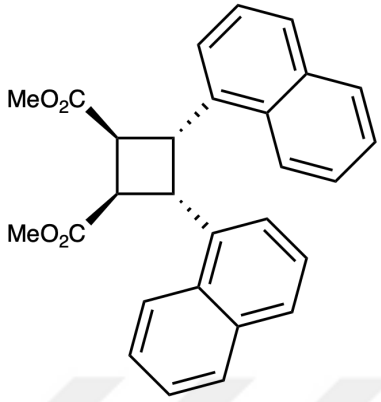

35

The applied procedure was adapted from the Türkmen Research Group's previous work.[22] 6.0 mL of 1:1 MeOH: THF mixture was added directly to a 20-mL scintillation vial that contained compound **26 (**18.2 mg,0.0349 mmol). In the clear solution of dissolved template-bound cycloadduct **26**, 2.5 equiv. of NaOMe (4.72 mg, 0.087 mmol) was added. A sonicator was used to achieve the complete dissolution of compound **26**. However, the look was cloudy. The vial was placed onto the magnetic stirrer and stirred at 23 °C for 8 h. Purification was done by flash column chromatography (SiO_2; 1:1 = hexanes: DCM) to obtain compound **35** as yellowish oil (11.2 mg, 75% yield).

M.P. 182.3 – 184.2 °C.

R_f = 0.39 (1:1 DCM: hexanes).

TLC Visualization: UV active; did not stain with $KMnO_4$ solution.

^{1}H NMR (400 MHz; $CDCl_3$) δ: 7.90 (2H, d, *J* = 8.2 Hz), 7.51 (2H, d, *J* = 8.4 Hz), 7.40 (2H, d, *J* = 8.8 Hz), 7.20-7.13 (4H, m), 7.10-7.05 (4H, m), 5.33-5.32 (2H, app d, *J* = 6.6 Hz), 4.00-3.99 (2H, app d, *J* = 6.3 Hz), 3.72 (6H, s).

$^{13}C\{^{1}H\}$ NMR (100 MHz; $CDCl_3$) δ: 173.1, 134.7, 133.5, 131.9, 128.5, 127.4, 125.7, 125.5, 124.8, 123.8, 123.6, 52.4, 43.9, 41.6.

FTIR ν_{max} (ATR, solid)/cm^{-1} 3060, 2951, 2919, 2847, 1720, 1596, 1510, 1430, 1363.

3.2.15 Compound 36

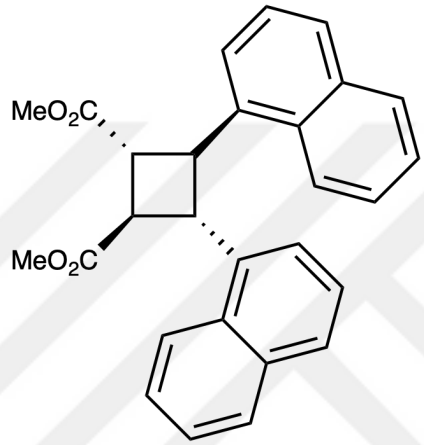

36

The applied procedure was adapted from the literature.[52] In a quartz test tube, compound **6** (20.1 mg, 0.094 mmol) was dissolved in 0.94 mL of anhydrous 1,4-dioxane under N_2 atmosphere. Afterward, tris(2-phenylpyridine)iridium(III), $Ir(ppy)_3$ (1.2 mg, 0.0018 mmol) was added. The test tube was placed into the irradiation set-up and exposed to the 450 nm UV light. At the end of 8 h, the reaction was stopped, and all volatiles were removed using the rotary evaporator. From the crude ^{1}H NMR spectrum, the ratio of *β* isomer (compound **35**) to *δ* isomer (compound **36**) was calculated as 0.16:1.00. By flash column chromatography (SiO_2; EtOAc: hexanes = 1:8 to 1:7) compound **36** was purified as yellowish-white solid (7.9 mg, 39% yield).

M.P. 197.9-199.0 °C

R_f = 0.32 (1:5 EtOAc: hexanes).

TLC Visualization: UV active; stains with $KMnO_4$ solution.

^{1}H NMR (400 MHz; $CDCl_3$) δ: 7.79 (2H, d, *J* = 8.2 Hz), 7.77-7.73 (6H, m), 7.50 (2H, t, *J* = 7.7 Hz), 7.36 (2H, ddd, *J* = 7.9 Hz), 7.21 (2H, ddd, *J* = 8.3, 6.9, 1.3 Hz), 4.75 (2H, app d, *J* = 9.5 Hz), 3.73(2H, app d, *J* = 9.6 Hz), 3.71 (6H, s).

^{13}C{^{1}H} NMR (100 MHz; $CDCl_3$) δ: 173.4, 136.7, 133.9, 132.0, 128.7, 128.0, 126.0, 125.8, 125.7, 124.1, 123.6, 52.4, 45.3, 43.9.

FTIR νmax (ATR, solid)/cm^{-1} 3050, 2954, 2923, 2850, 1723, 1597, 1510, 1445, 1435, 1397.

3.2.16 Irradiation studies of Compound 6; Formation of Compounds 35 and 36

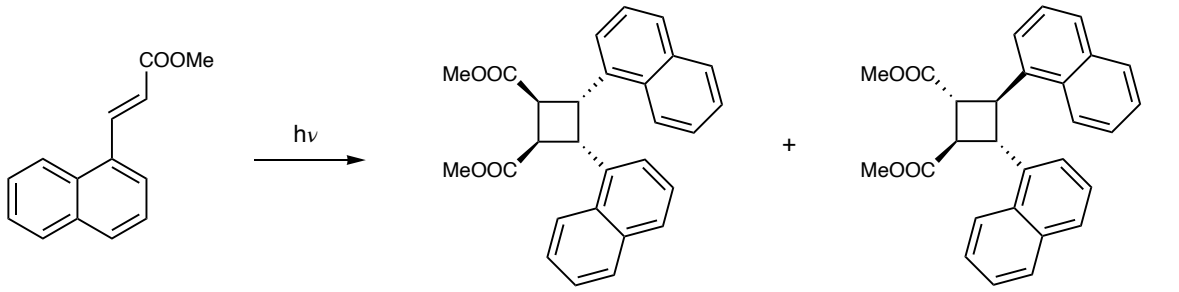

6 **35** **ß-truxinic acid ester analog** **36** **δ-truxinic acid ester analog**

In order to understant the effect of the wavelenght on the irradaition of compound **6,** another experiment was designed to see the effect of 365 nm (4×9 Watt) and 395 nm (46.65 Watt).

Neat Form / 365 nm UV light:

Onto the quartz microscope slide, compound **6** (21.6 mg, 0.10 mmol) was dropped and under 365 nm UV light, it was irradiated for 16 h. At the end of the reaction, the slide was washed with $CHCl_3$, and the solvent was removed with a rotary evaporator. The ^1H NMR spectrum of crude mixture showed that the ratio was 0.34:1.00 (δ: ß). After the purification (column chromatography (SiO_2; 1:8 = EtOAc: Hexane) the ratio was 0.29:1.00 (δ: ß). The yield of the mixture was 64%

Neat Form / 395 nm UV light:

Onto the quartz microscope slide, compound **6** (17.4 mg, 0.08 mmol) was dropped and under 395 nm UV light irradiated for 16 h. At the end of the reaction, the slide was washed with $CHCl_3$, and the solvent was removed with a rotary evaporator. The ^1H NMR spectrum of crude mixture showed that the ratio was 0.45:1.00 (δ: ß). After the purification by column chromatography (SiO_2; 1:8 = EtOAc: hexanes) the ratio was 0.40:1.00 (δ: ß). The yield of the mixture was 80% (13.9 mg).

Solution Irradiation / 365 nm UV light:

In an NMR tube, compound **6** (17.0 mg, 0.08 mmol) was dissolved in $CHCl_3$ and under 365 nm UV light, it was irradiated for 28 h. At the end of the reaction, the ^1H NMR spectrum of the crude mixture showed that the ratio was ca. 1:1. Therefore, no further purification was applied.

Solution Irradiation / 395 nm UV light:

In an NMR tube, compound **6** (15.4 mg, 0.07 mmol) was dissolved in $CHCl_3$ and under 395 nm UV light, it was irradiated for 28 h. At the end of the reaction, the ^1H NMR spectrum of the crude mixture showed that the ratio 3.61:1.00 (δ: ß). After the purification by flash column chromatography (SiO_2; EtOAc: hexanes 1:7 to 1:5) the ratio was 3.29:1.00 (δ: ß) The yield of the mixture was 77% (11.9 mg).

3.2.17 Compound 37

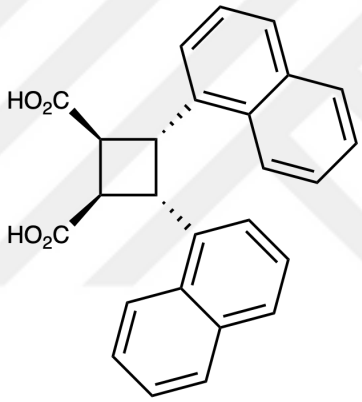

37

White-colored compound **7** (20.4 mg, 0.103 mmol) was placed between two quartz microscope slides. With the help of paper clips, slides were fixed. Microscope slides were placed under a UV lamp in a nail dryer (365 nm, 4×9 W). Every 4 h, solid residue was mixed with a spatula. In addition to the mixing process to ensure homogenous light distribution, the side of the slides facing the lamp was turned every 4 h. At the end of 20 h of irradiation, the ^1H NMR conversion was determined as 81%. By flash column chromatography (SiO_2; 1% acetic acid in EtOAc) compound **37** was purified as a white solid (15.9 mg, 78% yield)

M.P. 195 °C (decomposition)

$\mathbf{R_f}$ = 0.64 (1% acetic acid in EtOAc)

TLC Visualization: UV active; stains with $KMnO_4$ solution.

^{1}H NMR (400 MHz; $(CD_3)_2CO$) δ: 8.17 (2H, d, *J* = 7.7 Hz), 7.64-7.61 (2H, m), 7.52 (2H, d, *J* = 8.1 Hz), 7.46 (2H, d, *J* = 7.2 Hz), 7.30-7.21 (6H, m), 5.45-5.44 (2H, m), 4.22-4.21 (2H, m).

^{13}C{^{1}H} NMR (100 MHz; $(CD_3)_2CO$) δ: 174.1, 136.3, 134.5, 132.9, 129.3, 127.9, 126.4, 126.2, 125.8, 125.1, 124.8, 44.5, 42.3.

FTIR ν_{max} (ATR, solid)/cm^{-1} 3041, 2956, 2921, 2851, 1698, 1597, 1509, 1417.

4. Appendix

4.1 NMR Spectra

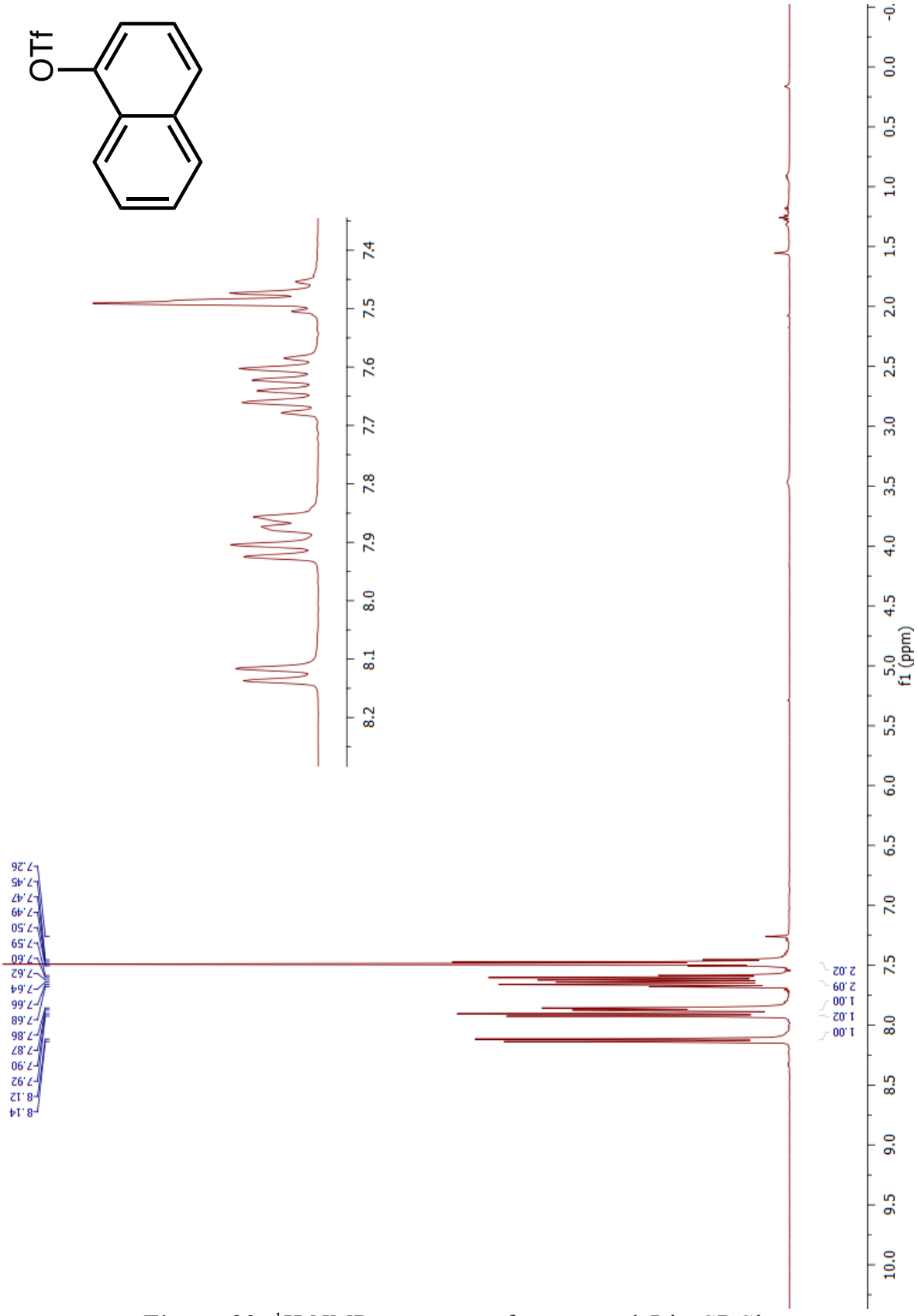

Figure 32. ^{1}H NMR spectrum of compound **5** in $CDCl_3$

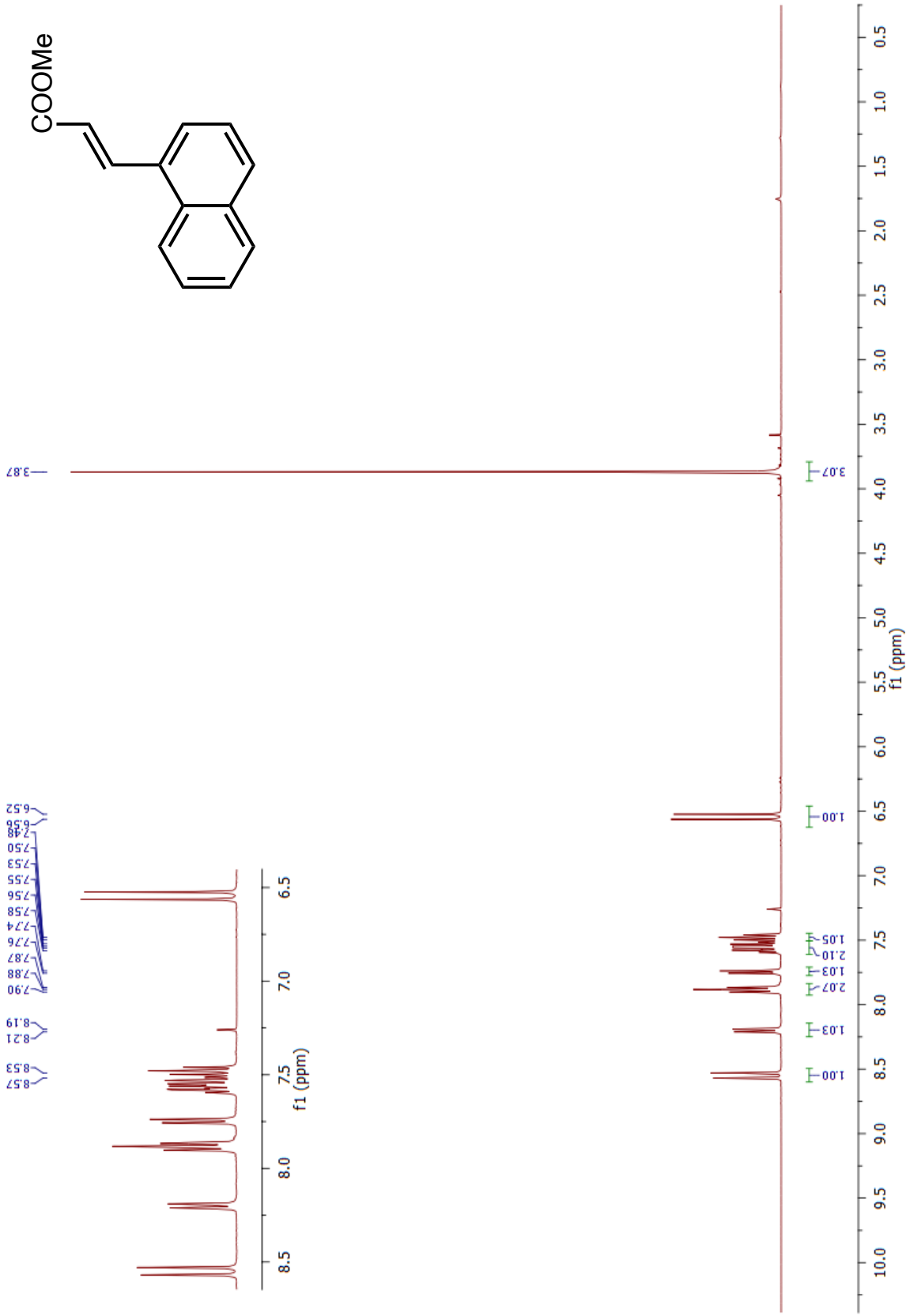

Figure 33. ^{1}H NMR spectrum of compound **6** in $CDCl_3$

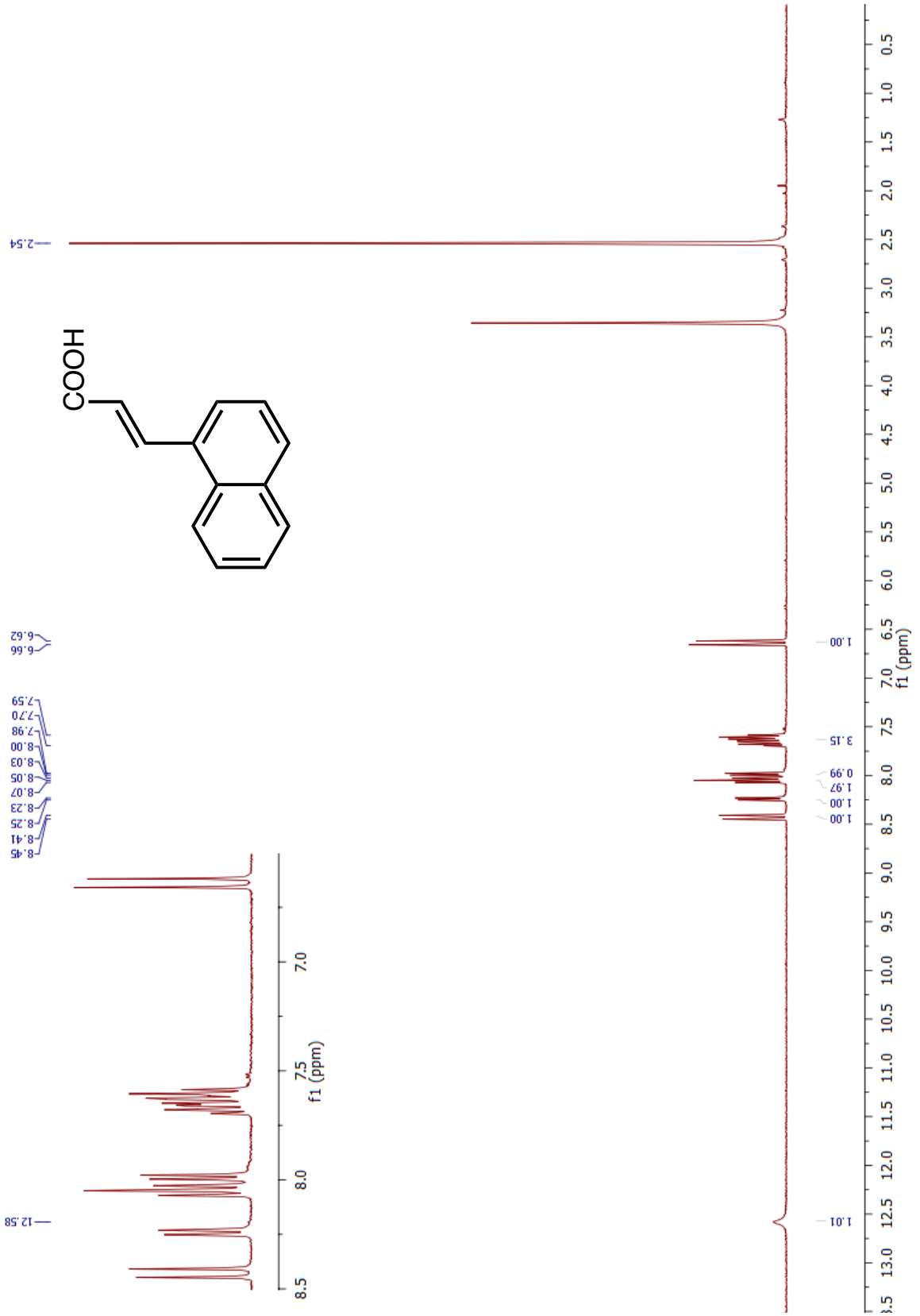

Figure 34. ^{1}H NMR spectrum of compound **7** in DMSO-d_6

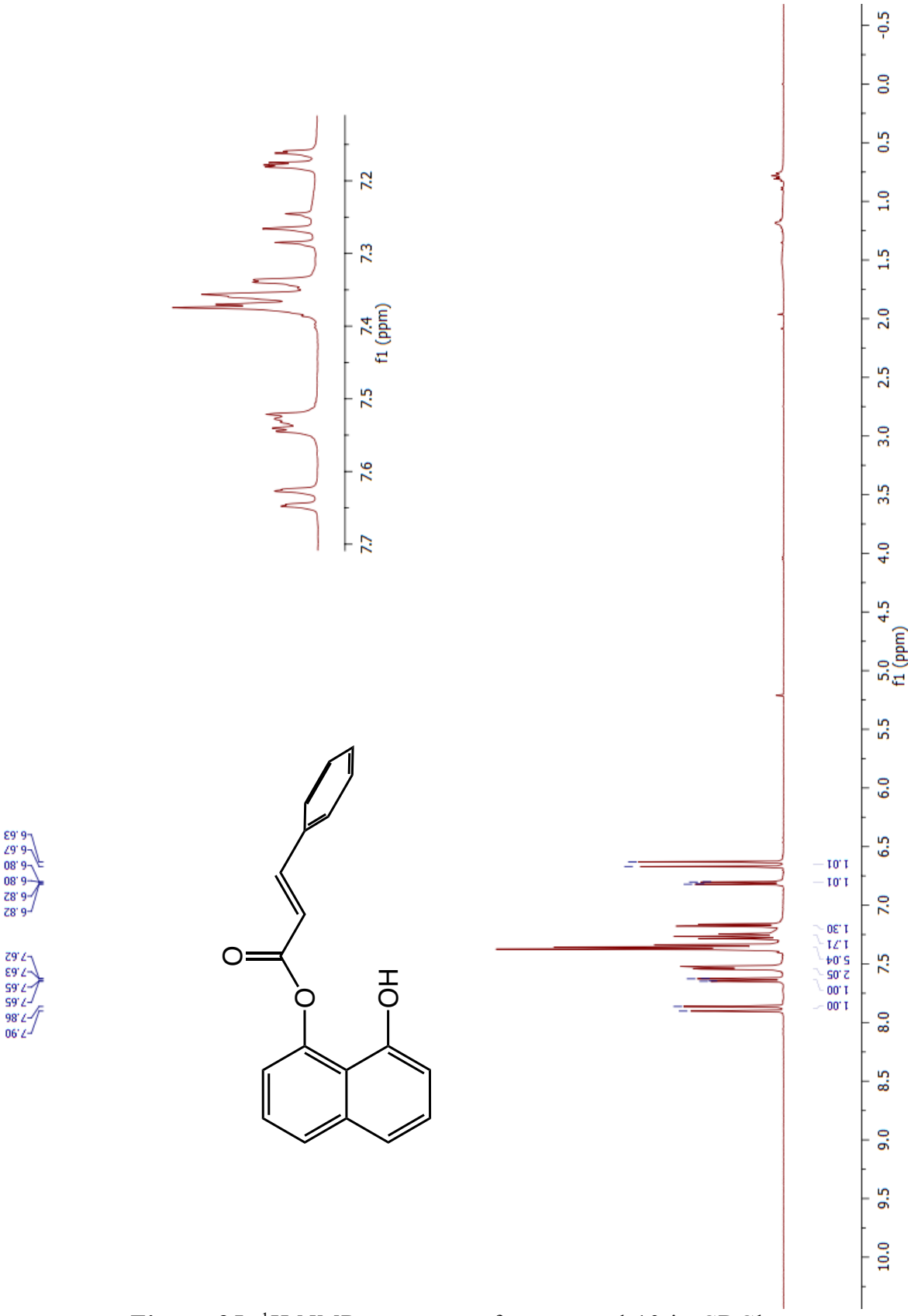

Figure 35. ^{1}H NMR spectrum of compound **10** in $CDCl_3$

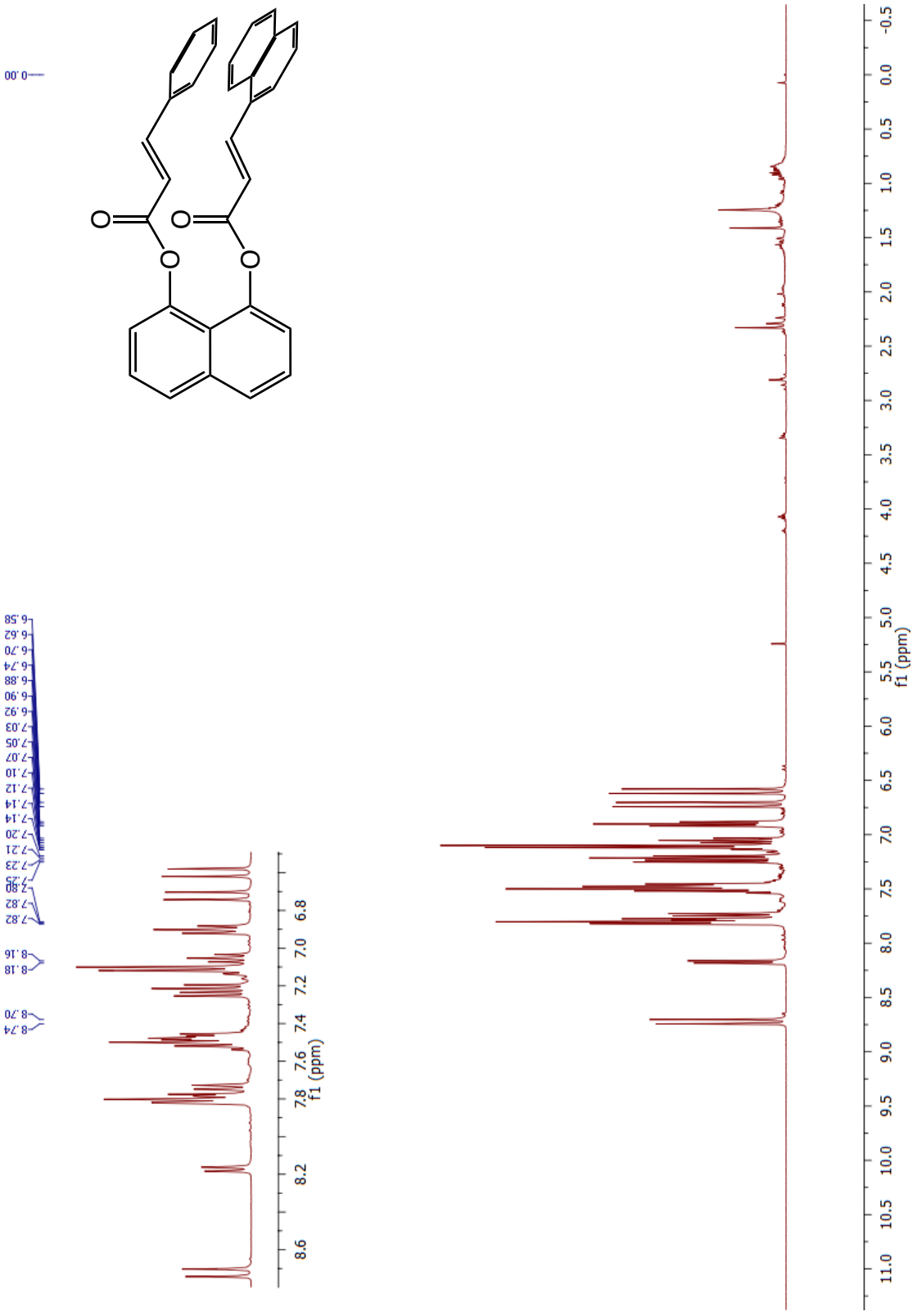

Figure 36. ^{1}H NMR spectrum of compound **11** in $CDCl_3$

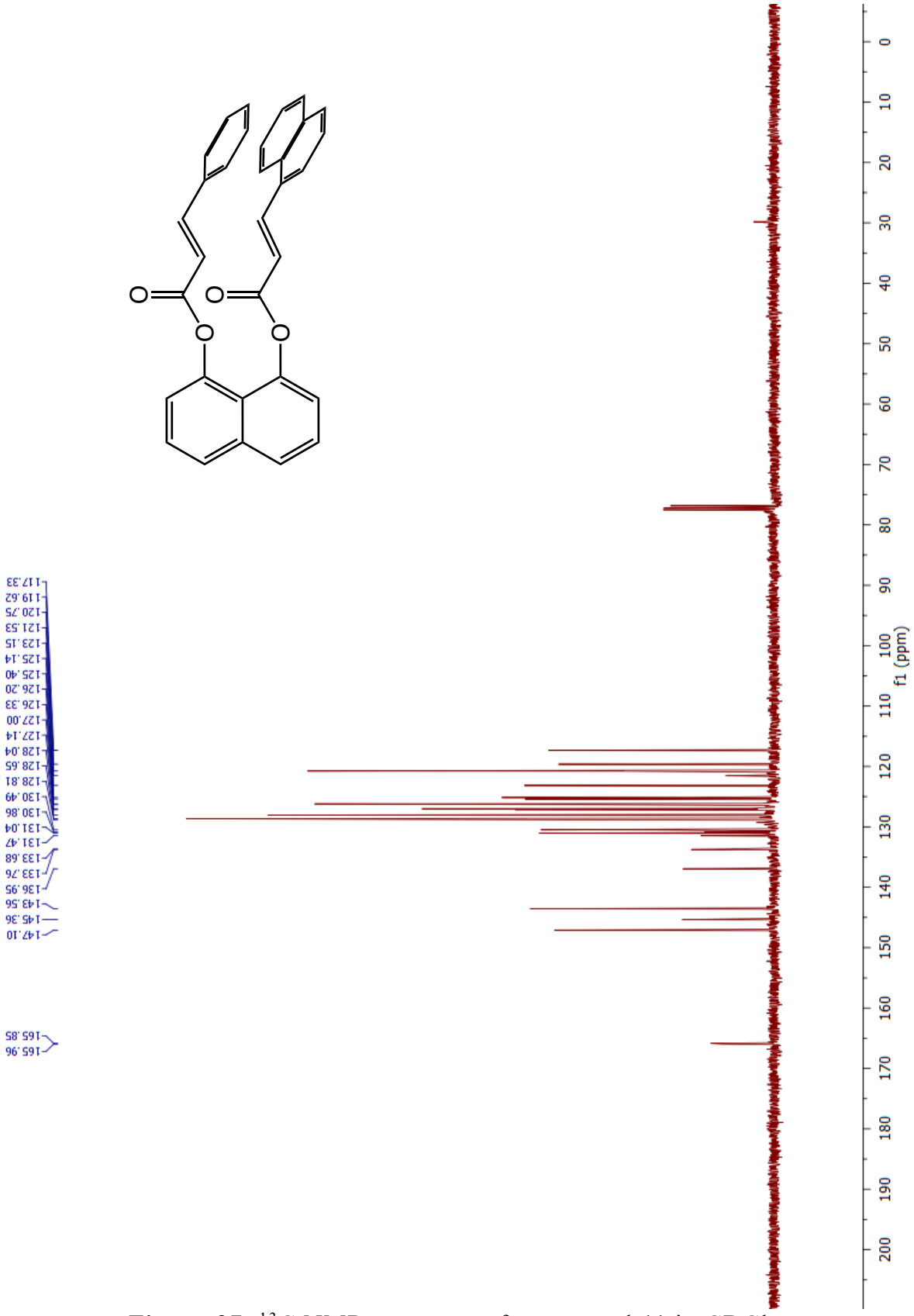

Figure 37. ^{13}C NMR spectrum of compound **11** in $CDCl_3$

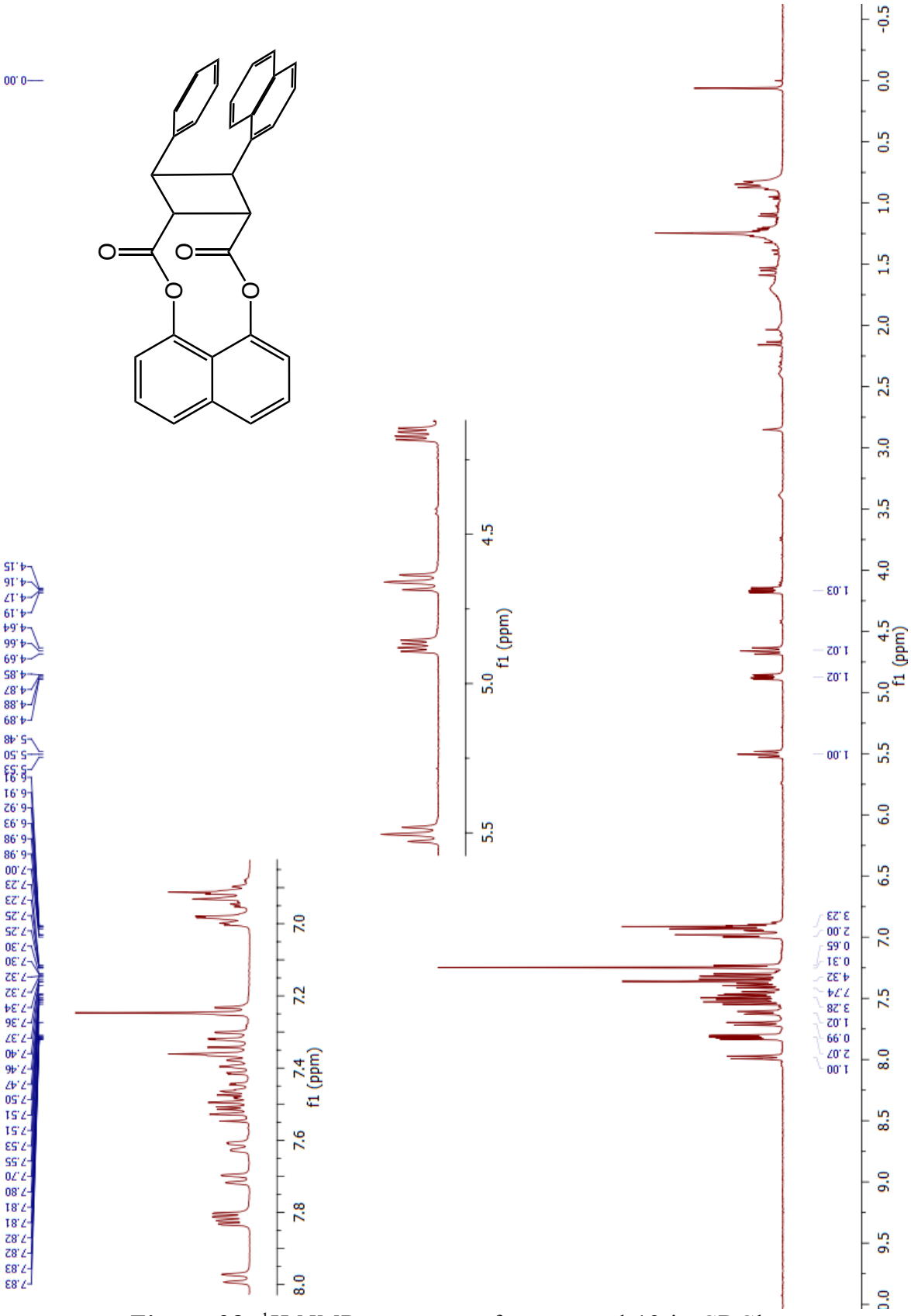

Figure 38. ^{1}H NMR spectrum of compound **12** in $CDCl_3$

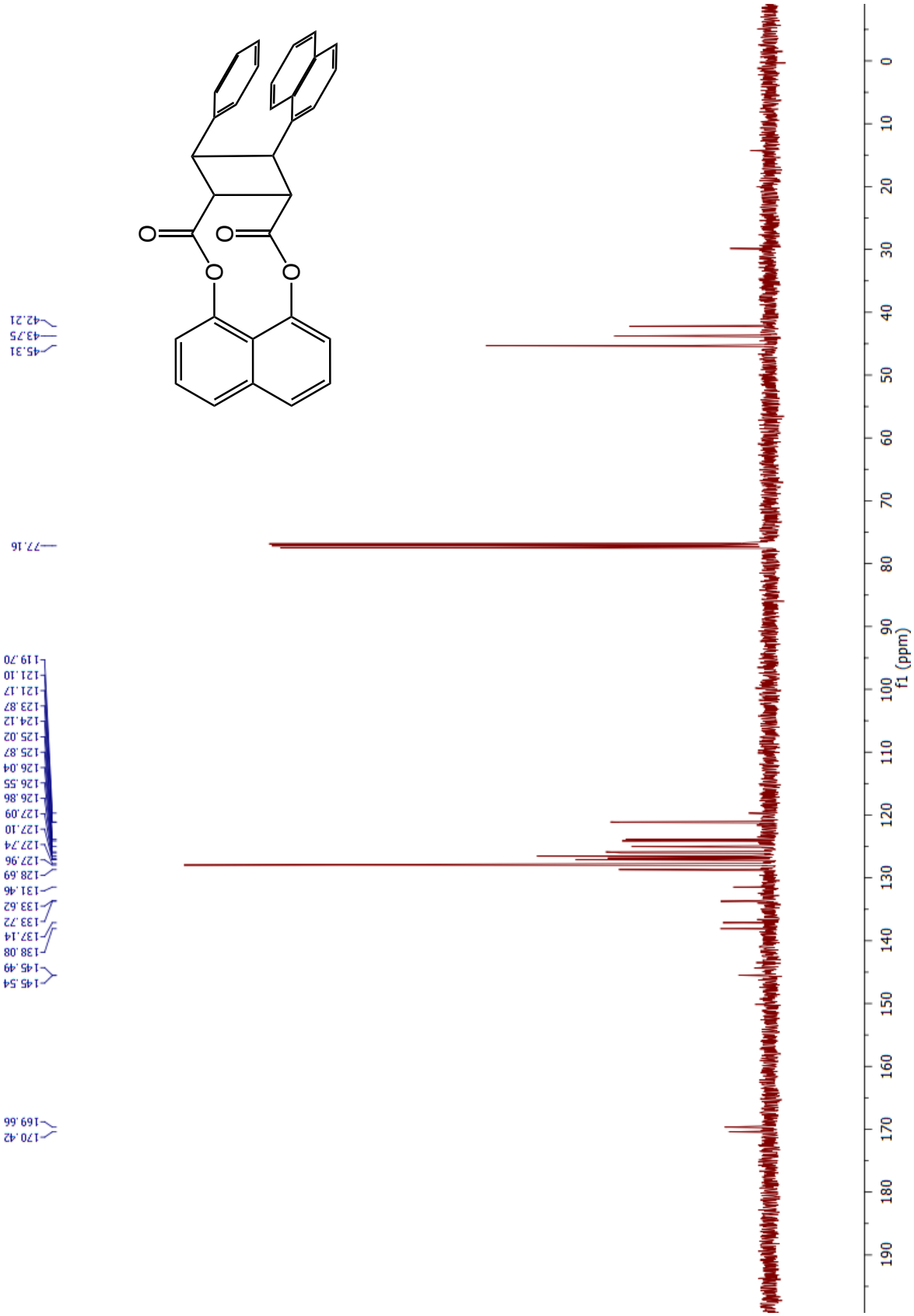

Figure 39. ^{13}C NMR spectrum of compound **12** in $CDCl_3$

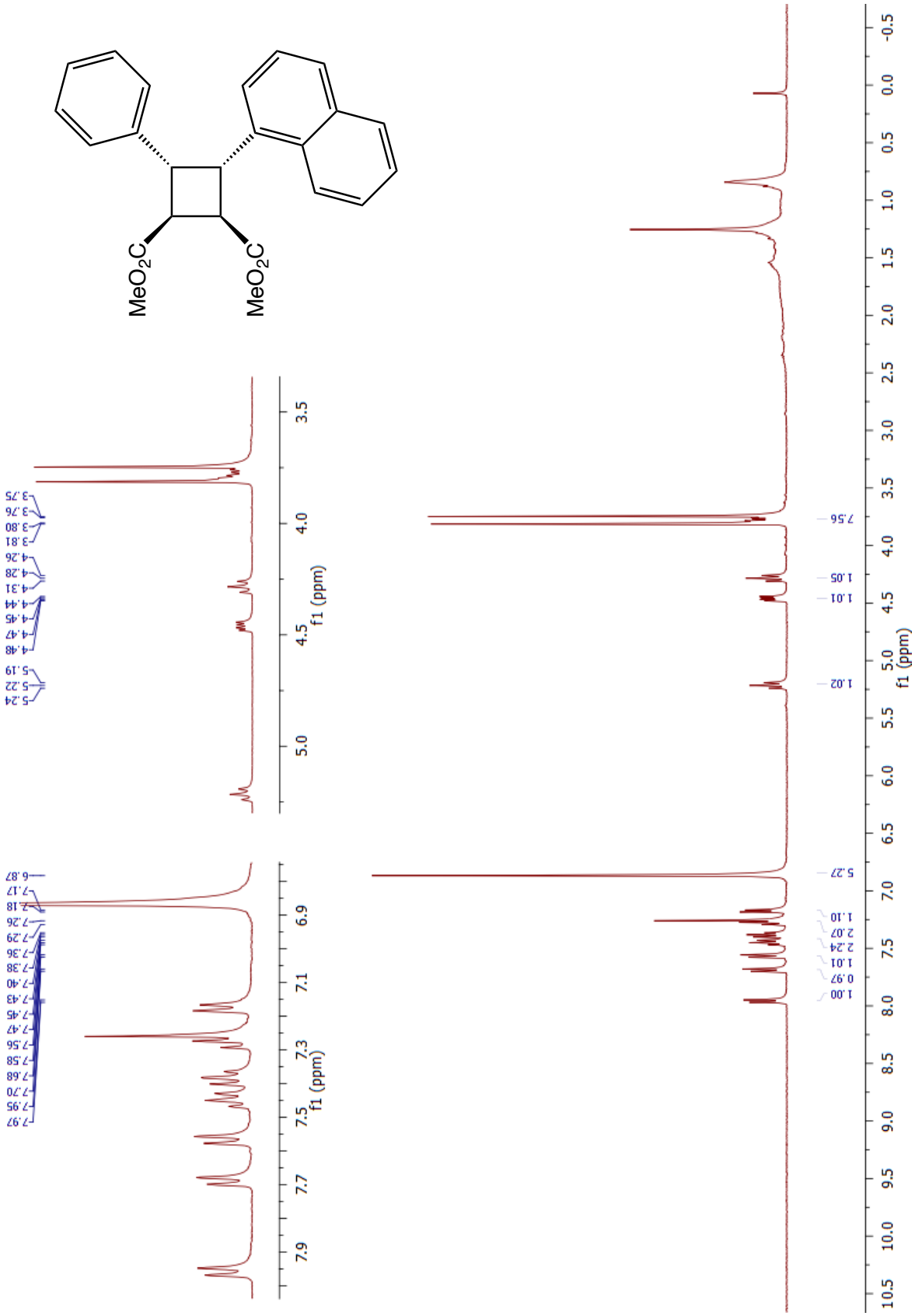

Figure 40. ^{1}H NMR spectrum of compound **13** in $CDCl_3$

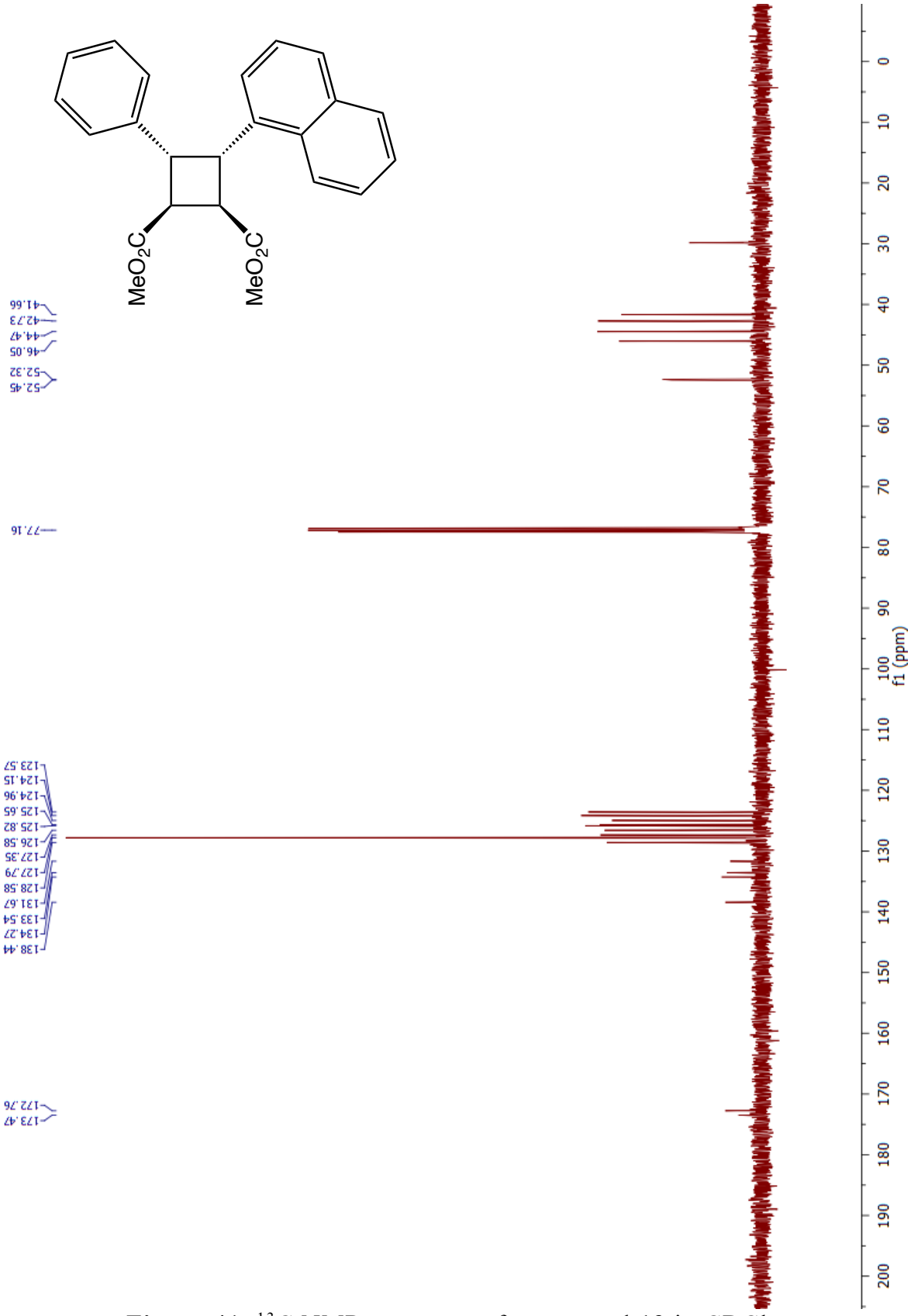

Figure 41. ^{13}C NMR spectrum of compound **13** in $CDCl_3$

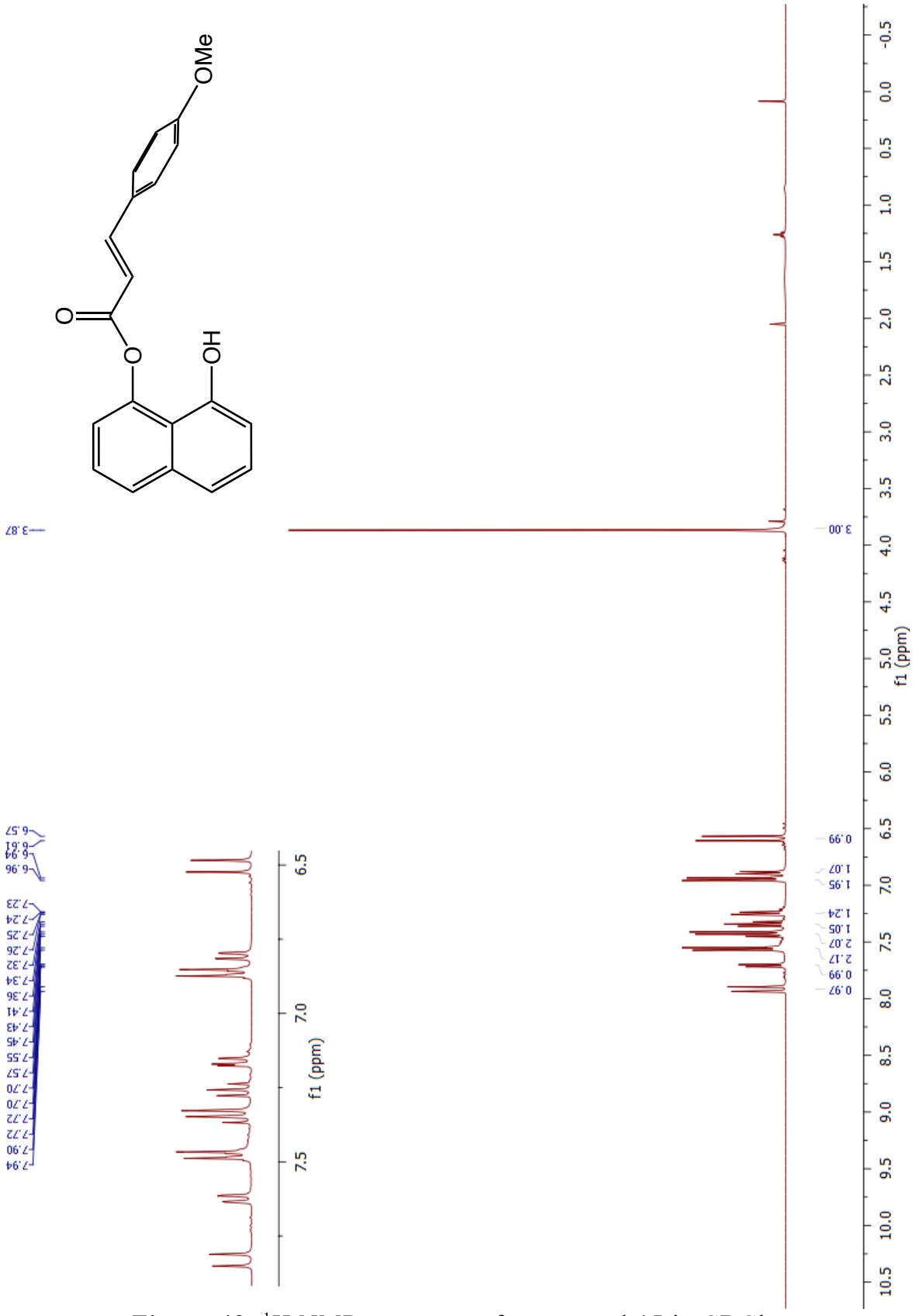

Figure 42. ^{1}H NMR spectrum of compound **15** in $CDCl_3$

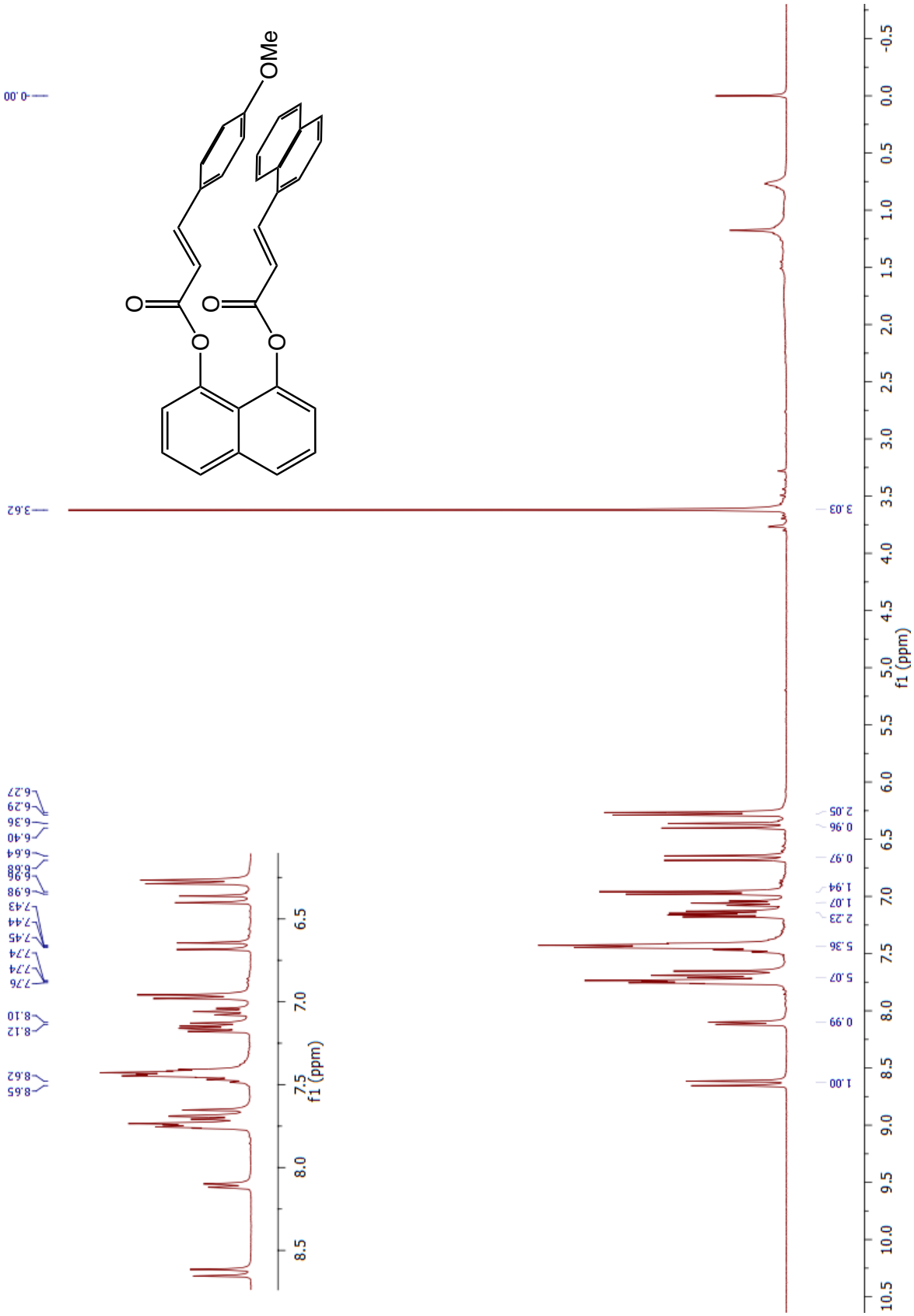

Figure 43. ^{1}H NMR spectrum of compound **16** in $CDCl_3$

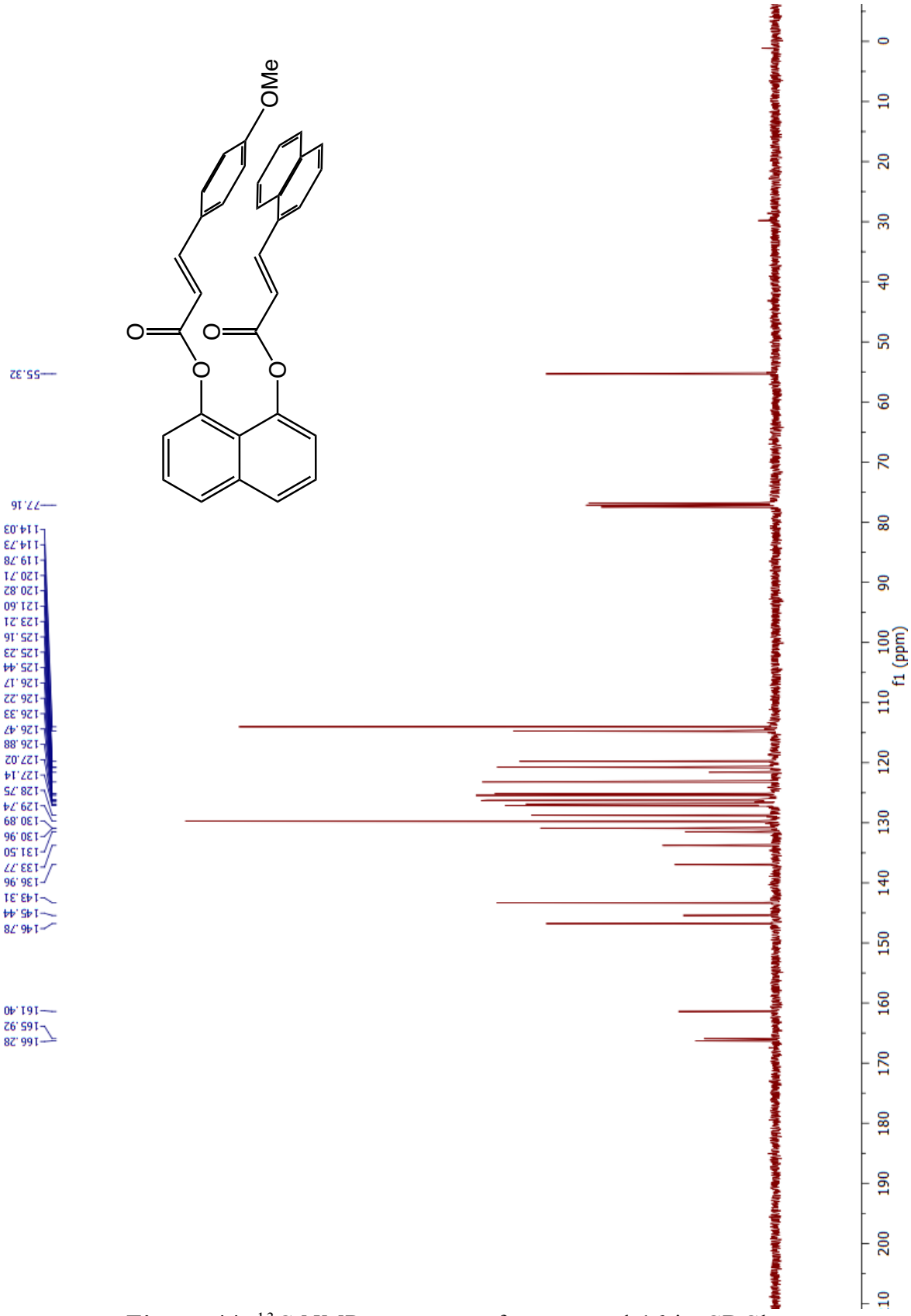

Figure 44. ^{13}C NMR spectrum of compound **16** in $CDCl_3$

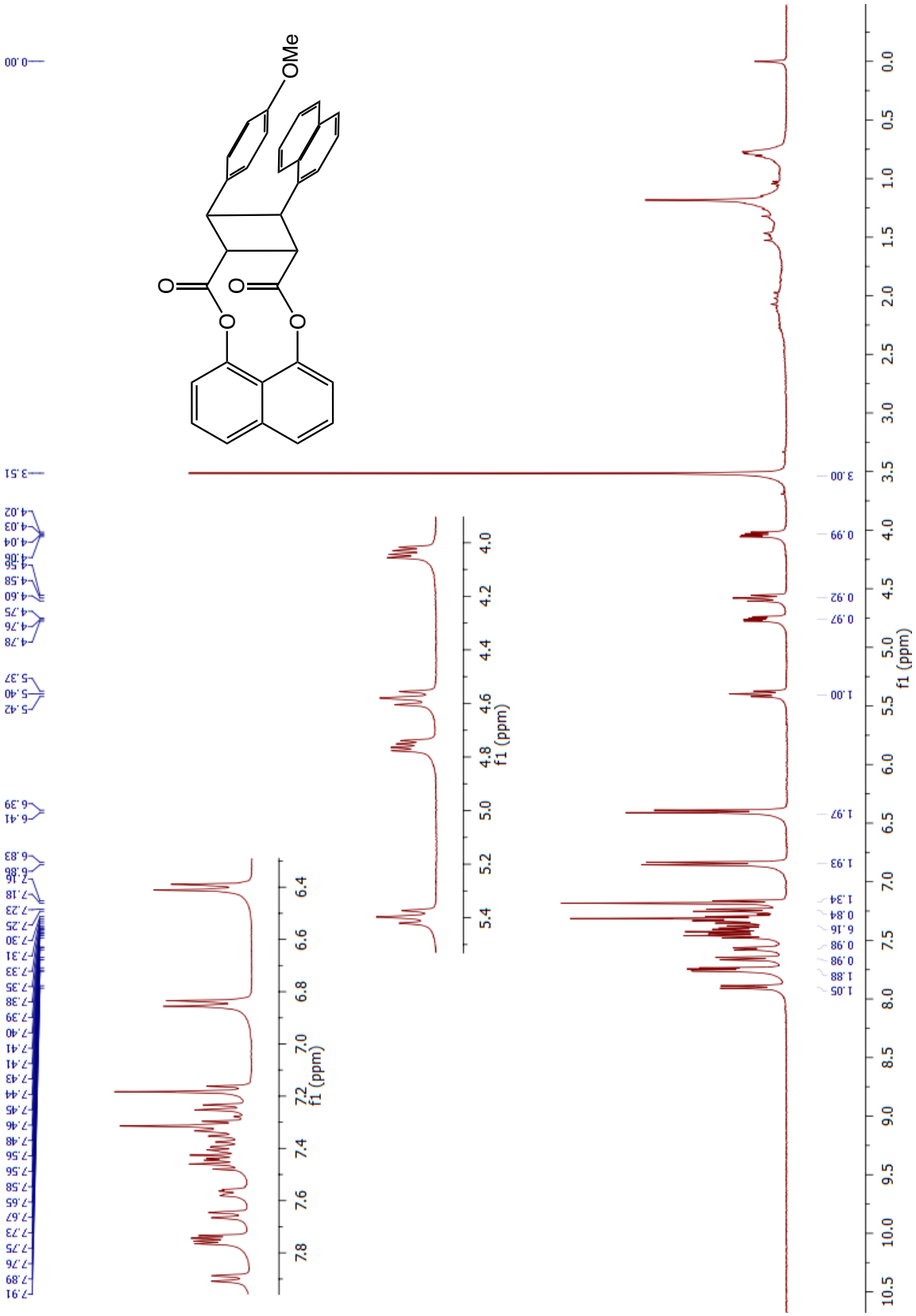

Figure 45. ^{1}H NMR spectrum of compound **17** in $CDCl_3$

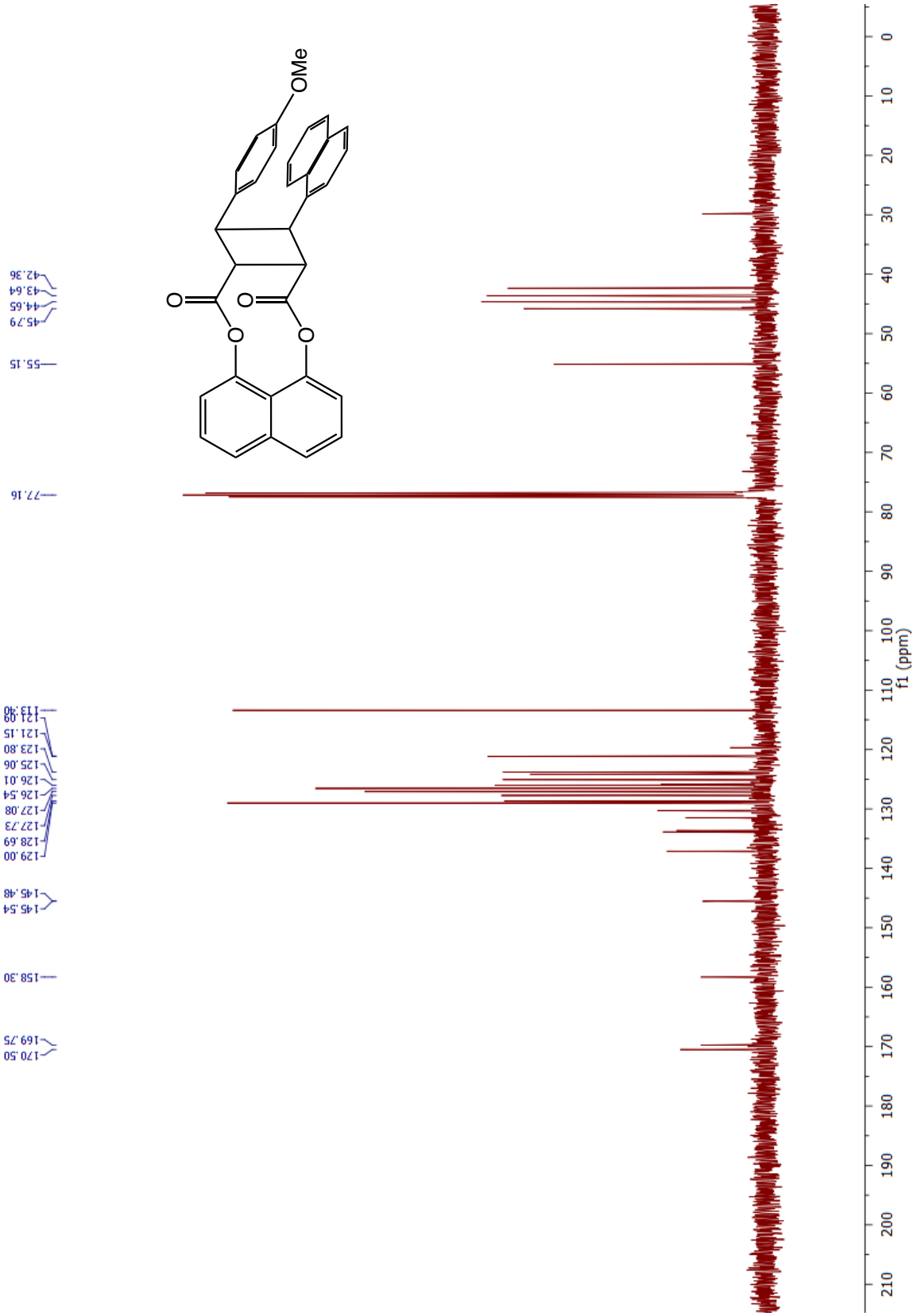

Figure 46. ^{13}C NMR spectrum of compound **17** in $CDCl_3$

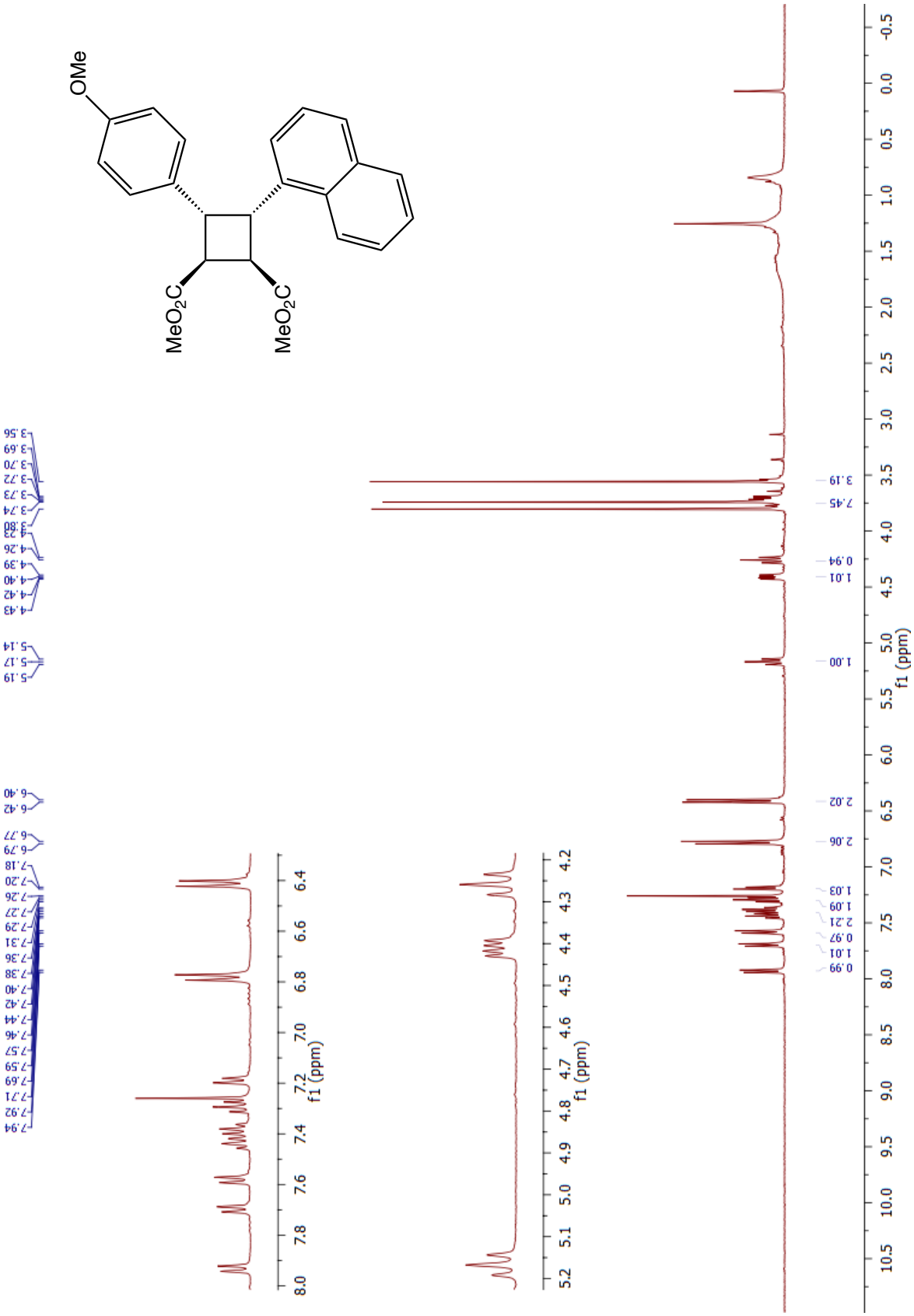

Figure 47. ^{1}H NMR spectrum of compound **18** in $CDCl_3$

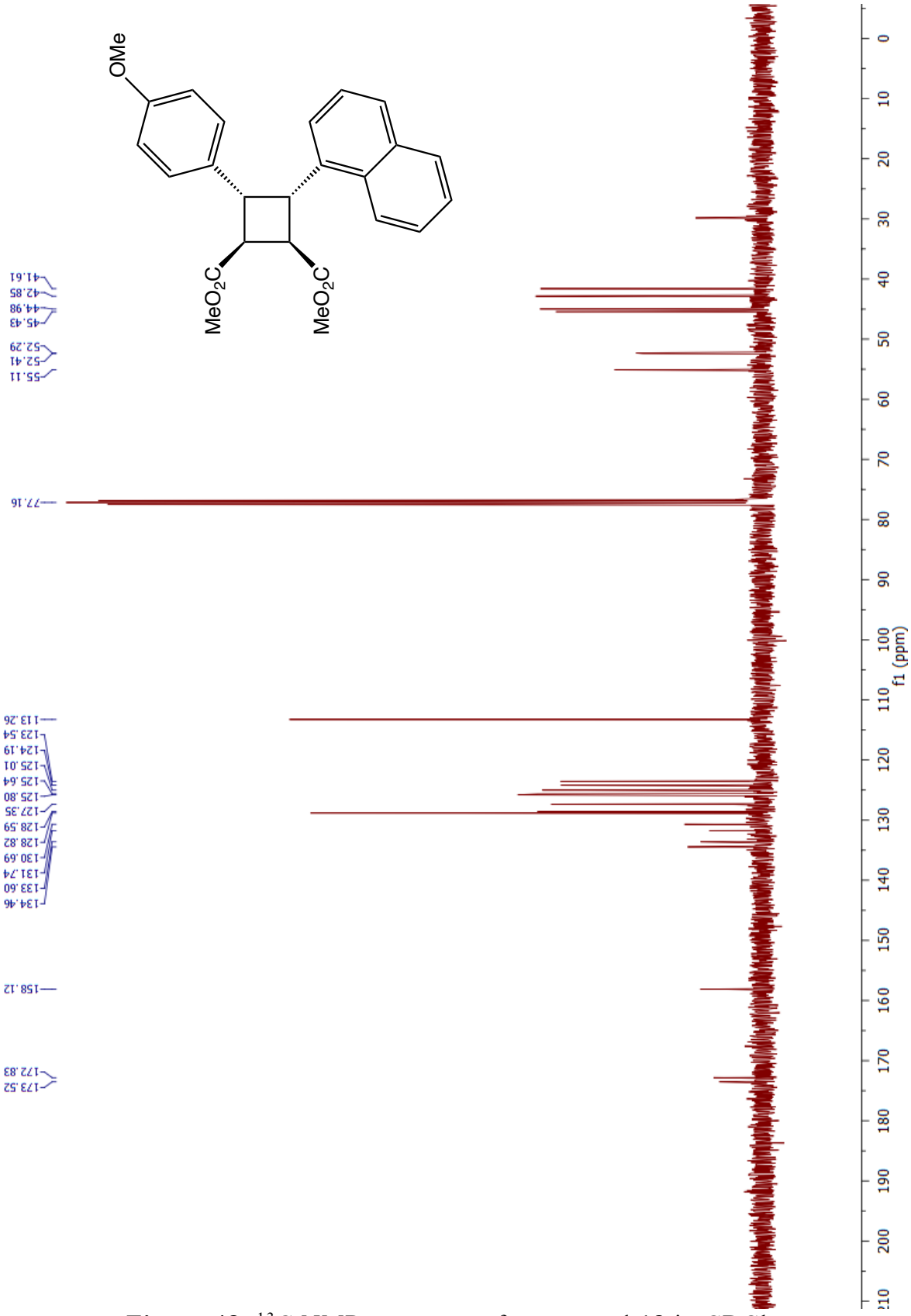

Figure 48. ^{13}C NMR spectrum of compound **18** in $CDCl_3$

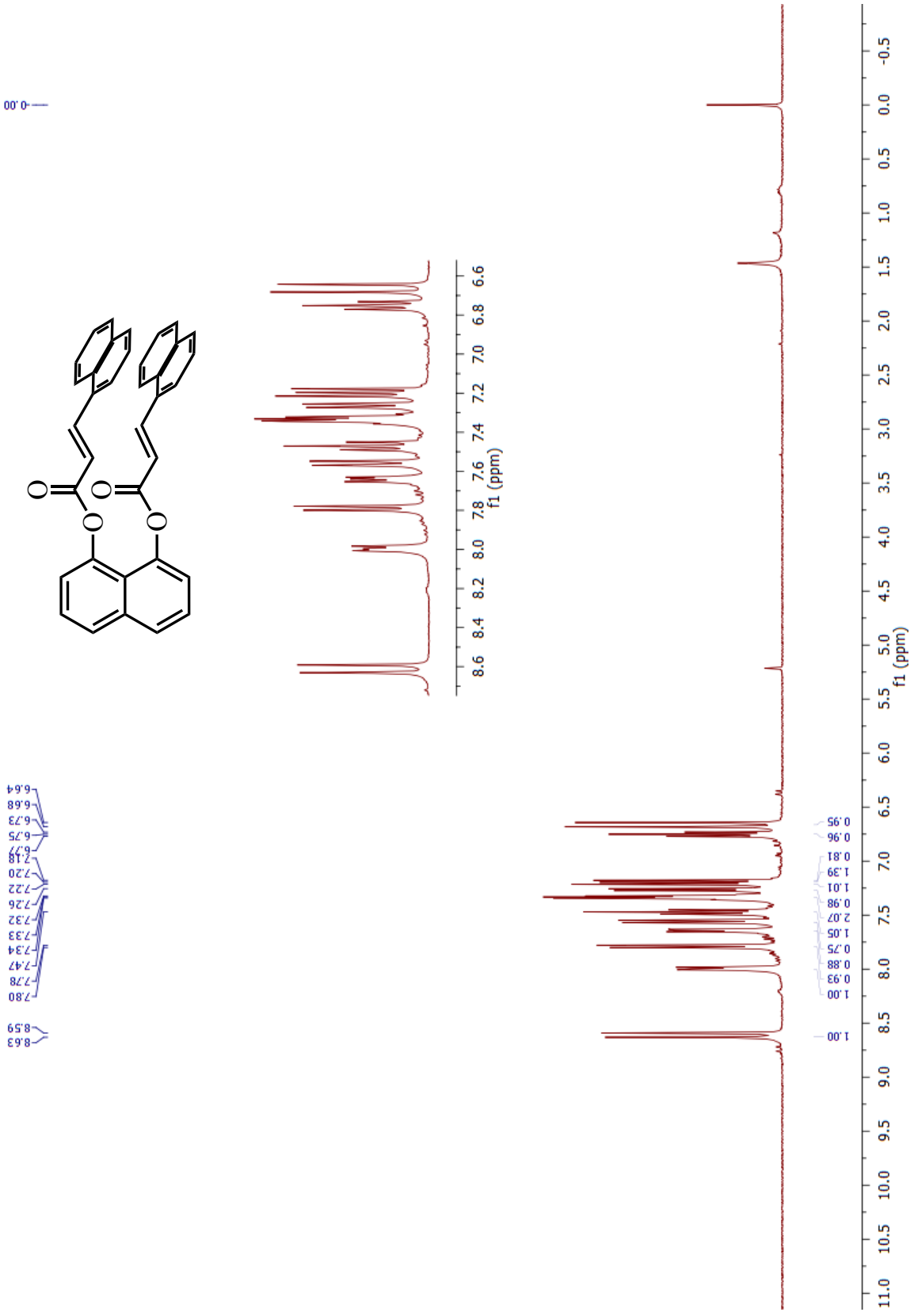

Figure 49. ^{1}H NMR spectrum of compound **26** in $CDCl_3$

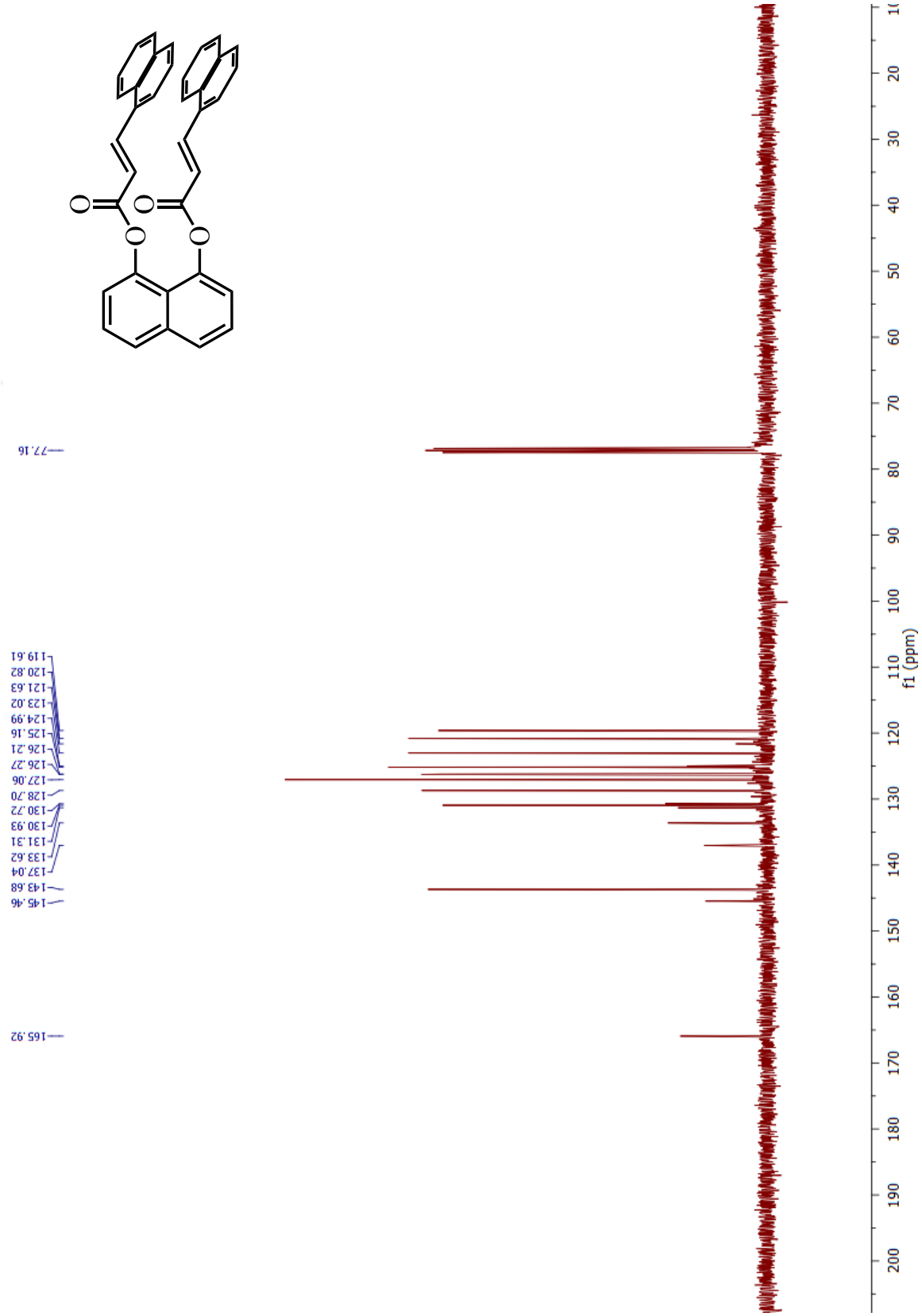

Figure 50. ^{13}C NMR spectrum of compound **26** in $CDCl_3$

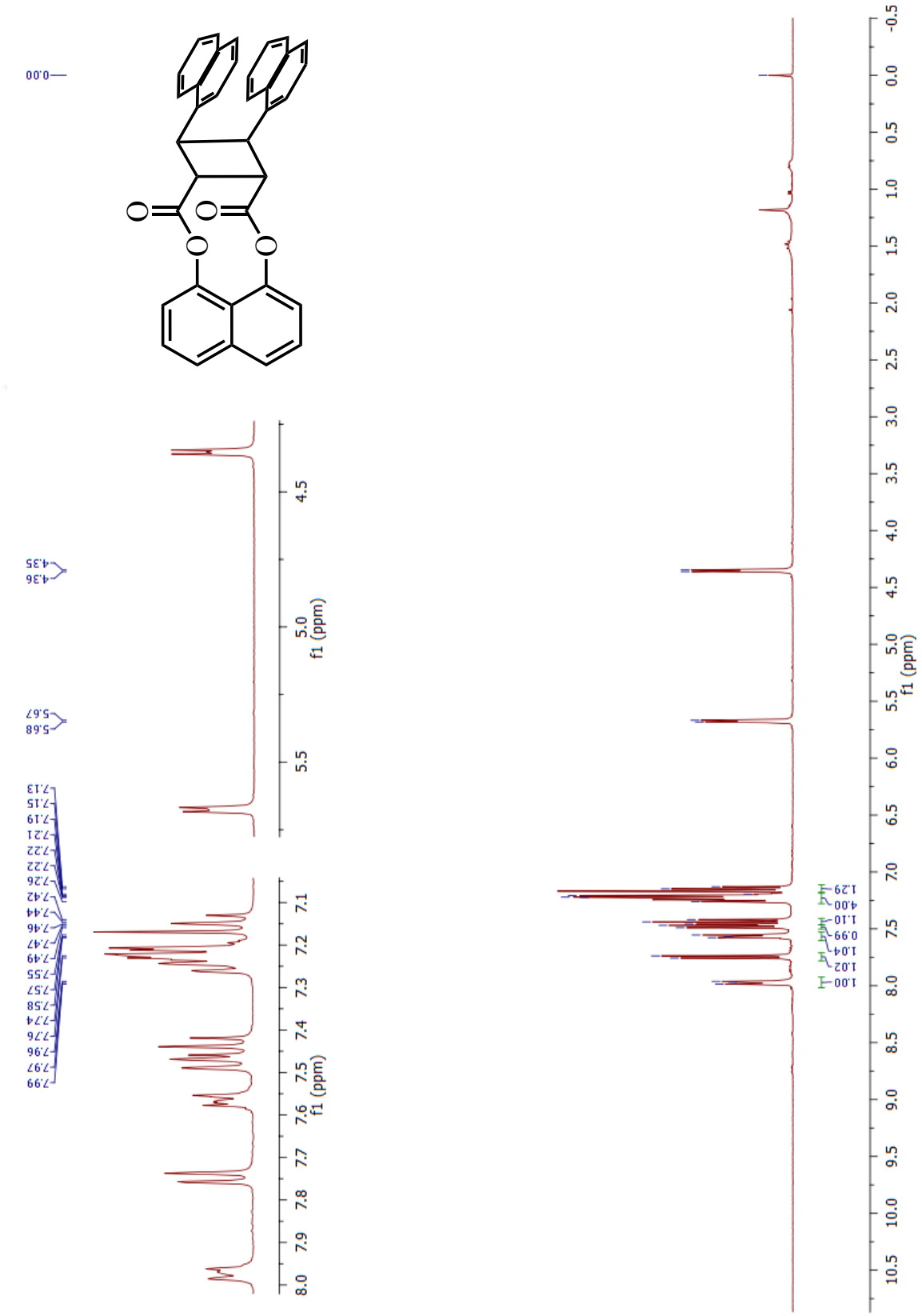

Figure 51. ^{1}H NMR spectrum of compound **27** in $CDCl_3$

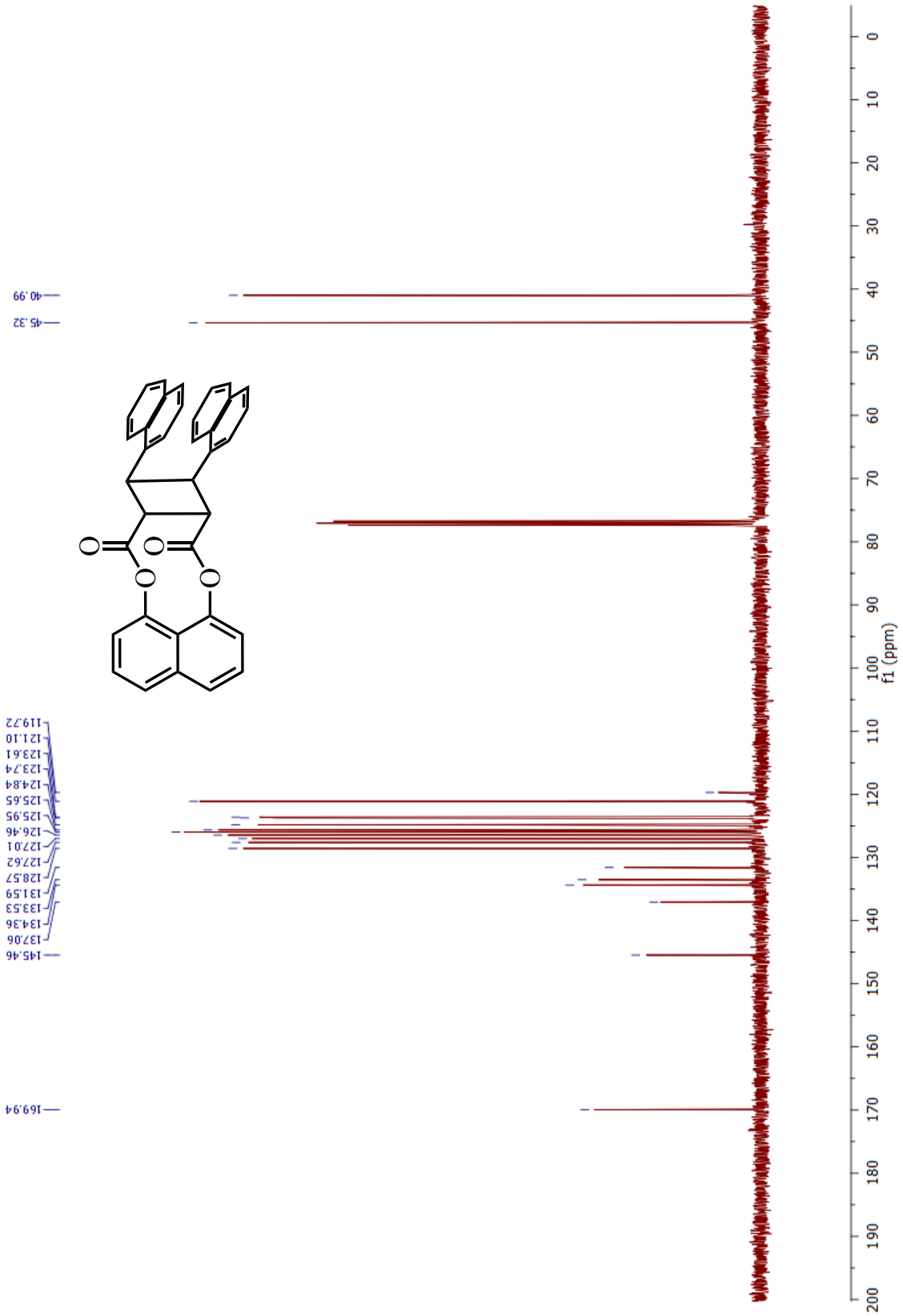

Figure 52. ^{13}C NMR spectrum of compound **27** in $CDCl_3$

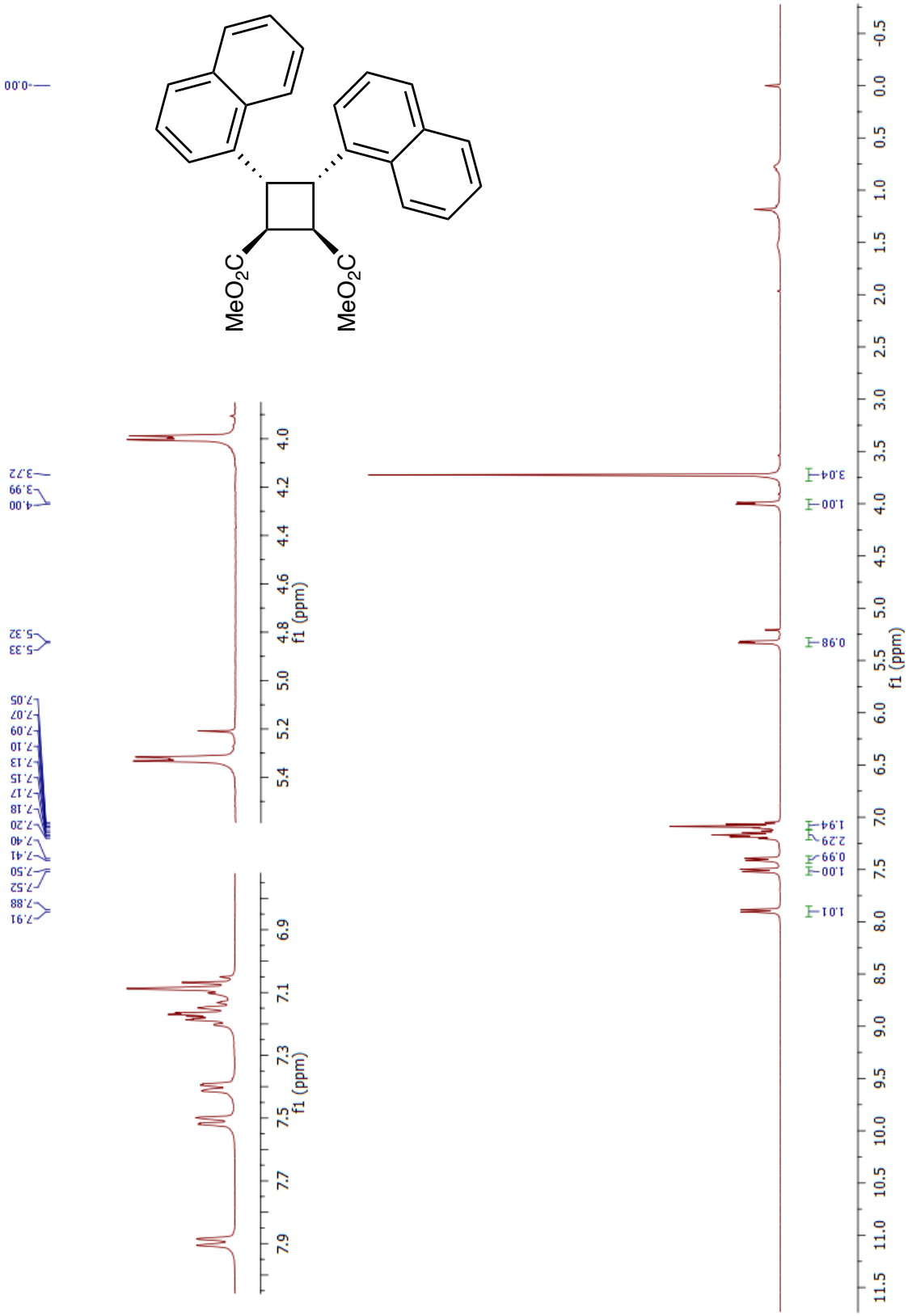

Figure 53. ^{1}H NMR spectrum of compound **35** in $CDCl_3$

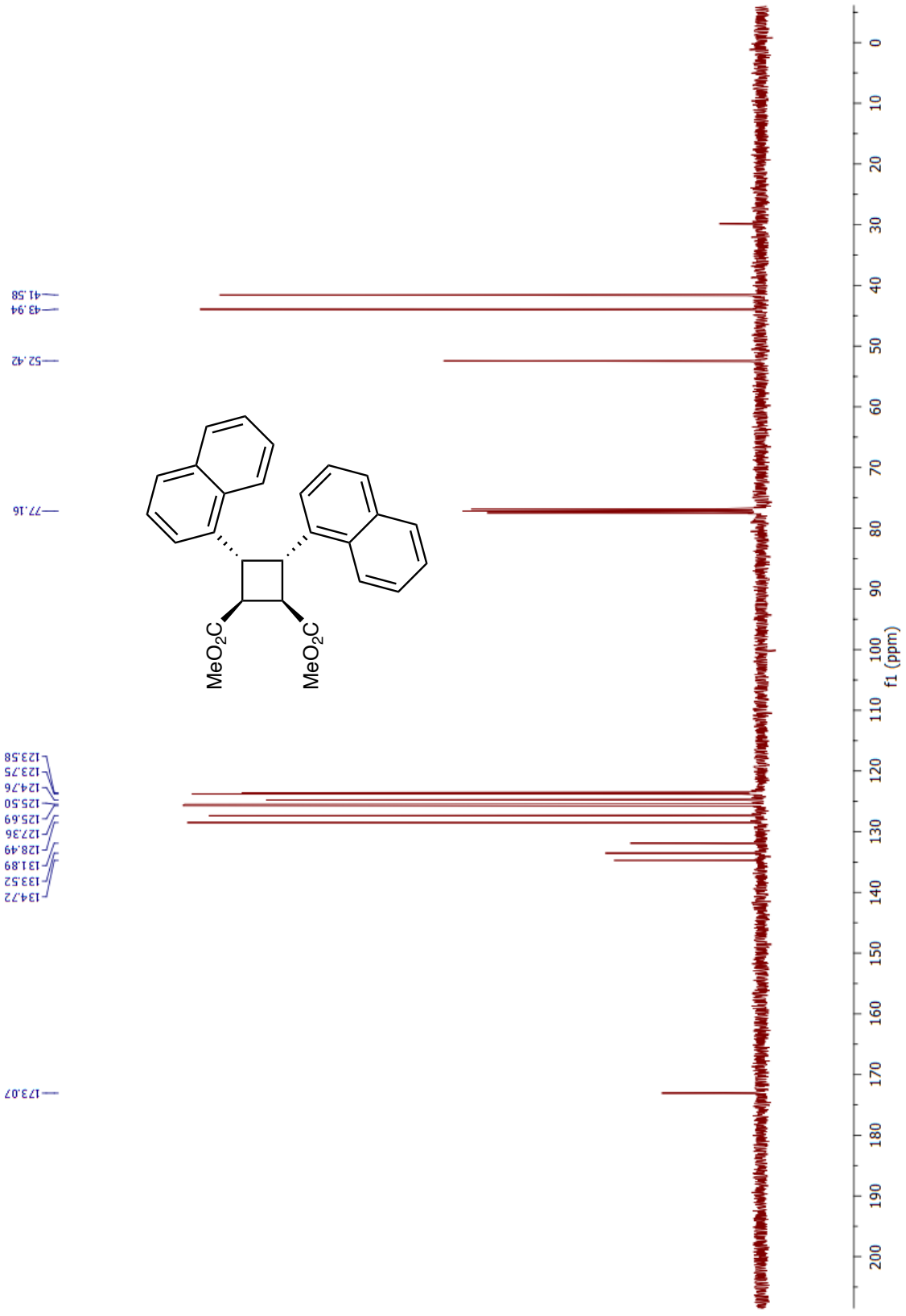

Figure 54. ^{13}C NMR spectrum of compound **35** in $CDCl_3$

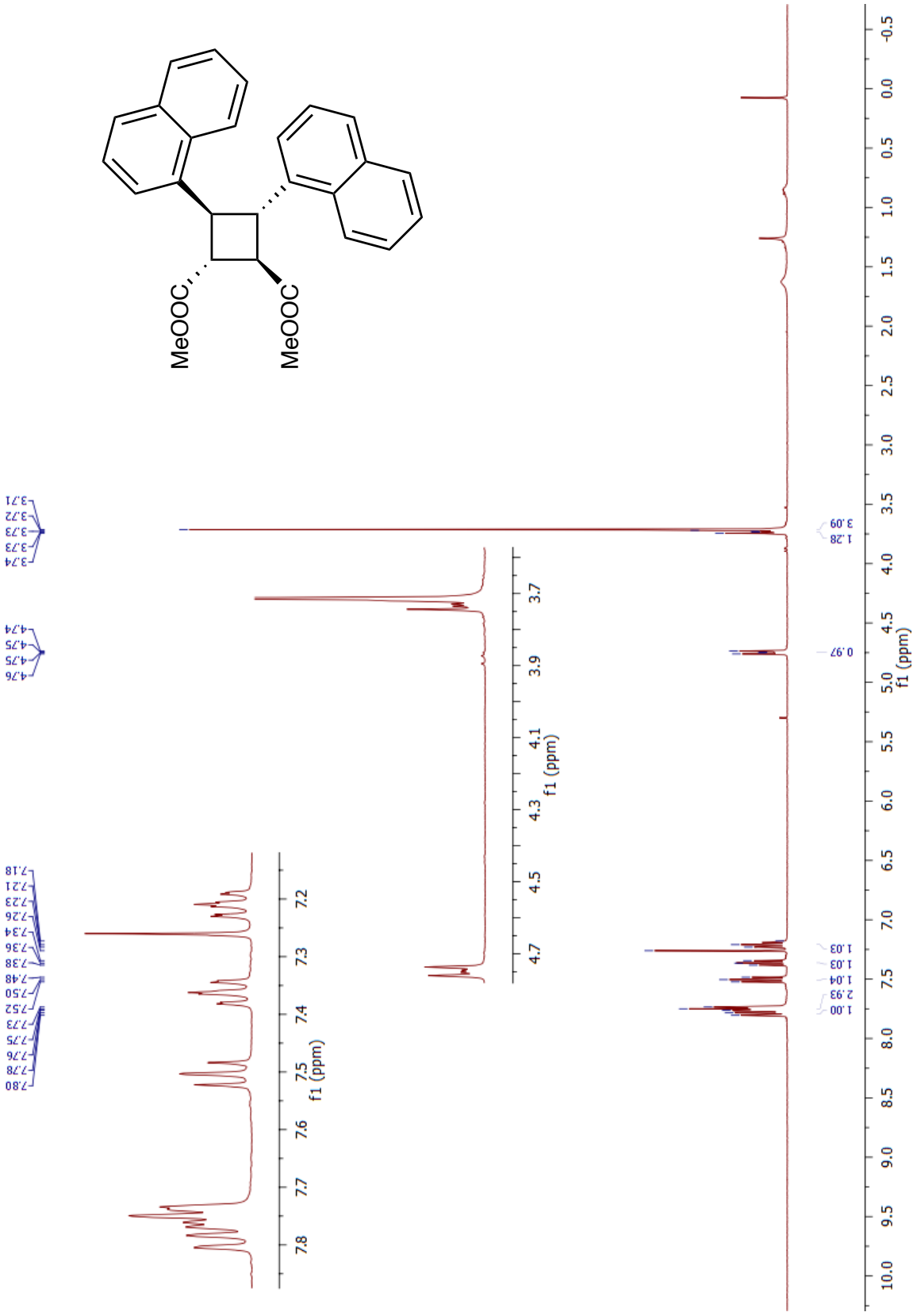

Figure 55. ^{1}H NMR spectrum of compound **36** in $CDCl_3$

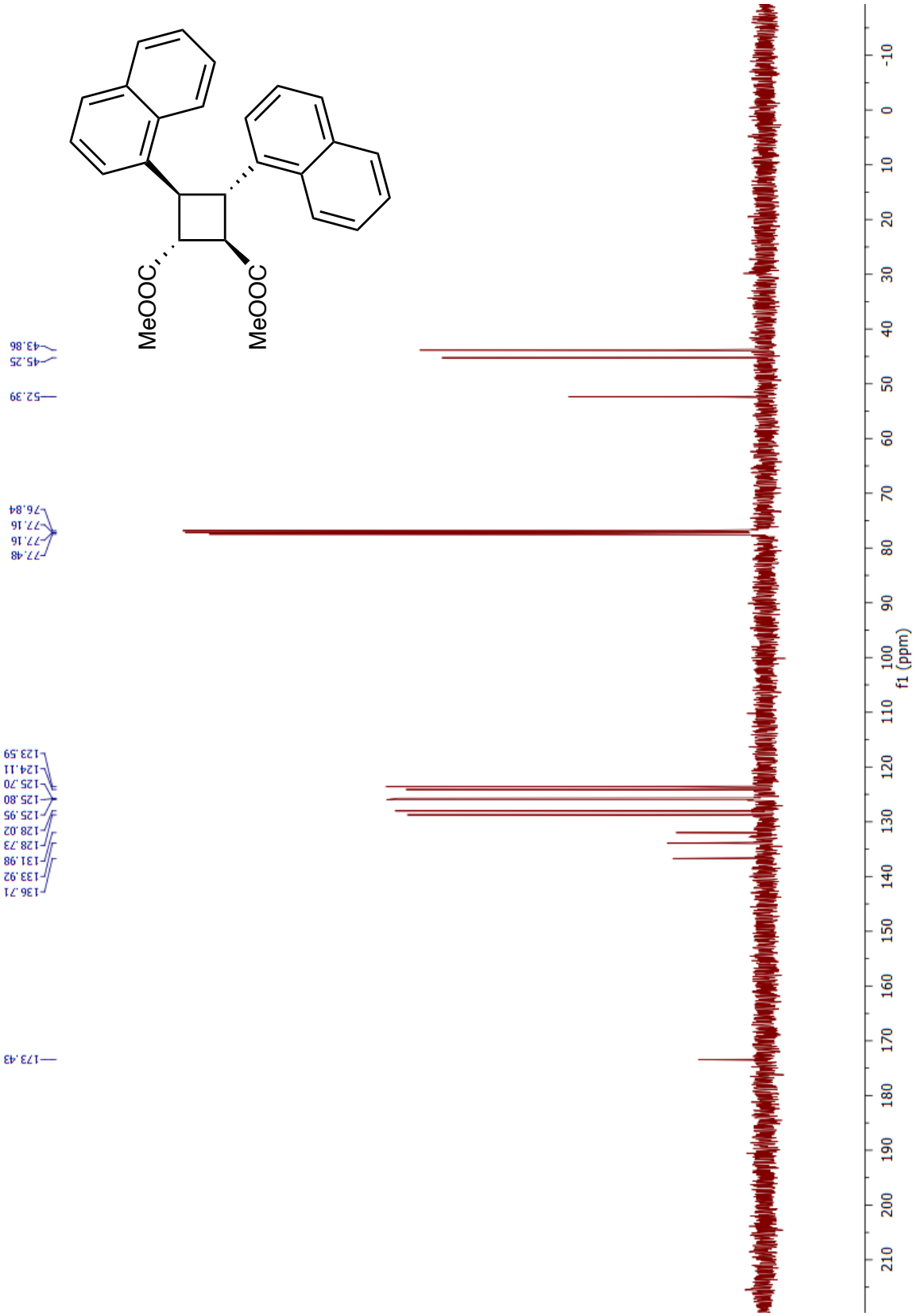

Figure 56. ^{13}C NMR spectrum of compound **36** in $CDCl_3$

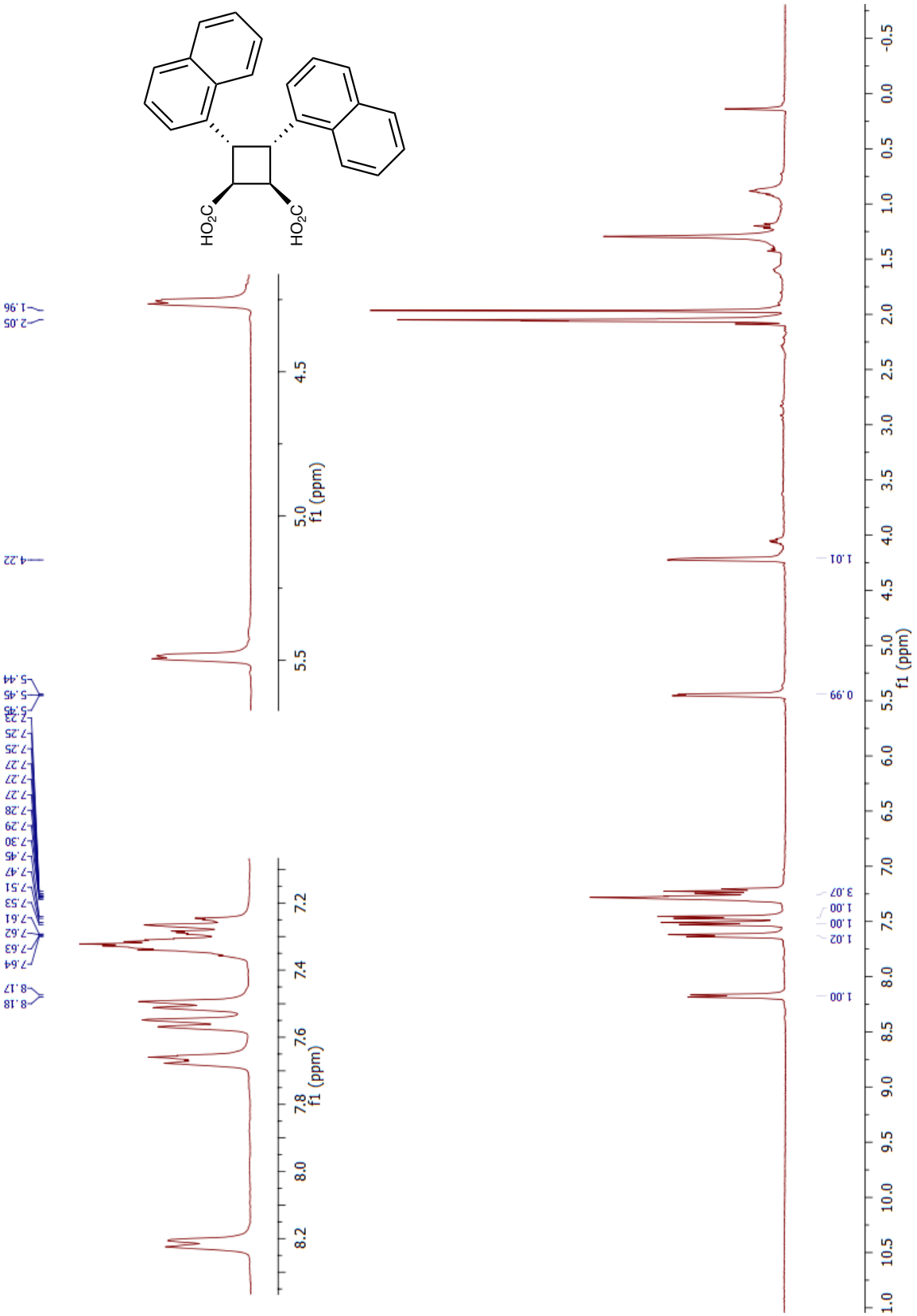

Figure 57. ^{1}H NMR spectrum of compound **37** in acetone-d_6

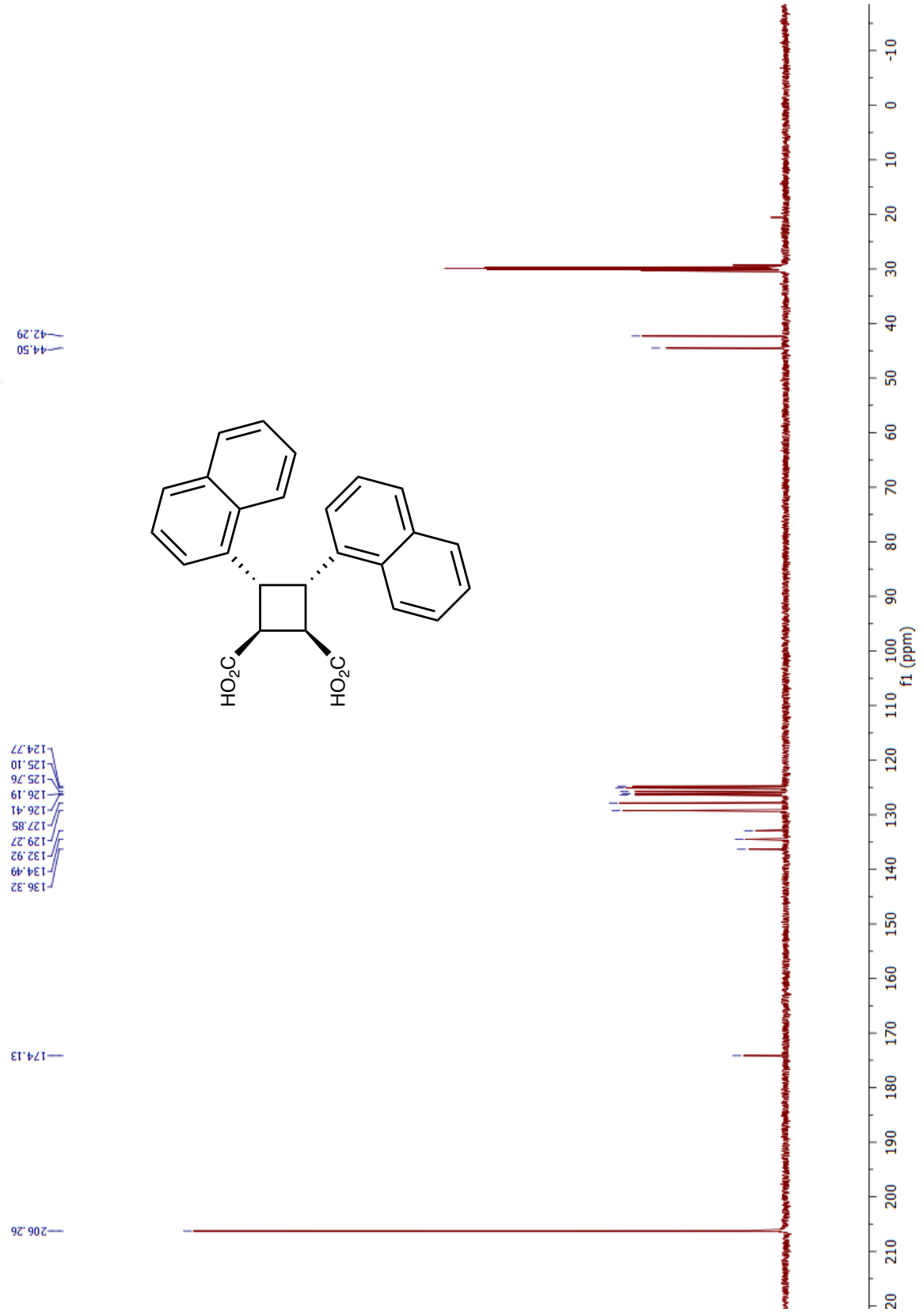

Figure 58. ^{13}C NMR spectrum of compound **37** in acetone-d_6

Bibliography:

(1) Yang, P.; Jia, Q.; Song, S.; Huang, X. [2 + 2]-Cycloaddition-Derived Cyclobutane Natural Products: Structural Diversity, Sources, Bioactivities, and Biomimetic Syntheses. *Nat. Prod. Rep.* **2023**, *40* (6), 1094–1129. https://doi.org/10.1039/D2NP00034B.

(2) Atanasov, A. G.; Zotchev, S. B.; Dirsch, V. M.; Supuran, C. T. Natural Products in Drug Discovery: Advances and Opportunities. *Nat. Rev. Drug Discov.* **2021**, *20* (3), 200–216. https://doi.org/10.1038/s41573-020-00114-z.

(3) Barker, D. Lignans. *Molecules* **2019**, *24* (7), 1424. https://doi.org/10.3390/molecules24071424.

(4) Boufadi, M. Y.; Keddari, S.; Moulaihacene, F.; Chaa, S. Chemical Composition, Antioxidant and Anti-Inflammatory Properties of Salvia Officinalis Extract from Algeria. *Pharmacogn. J.* **2020**, *13* (2), 506–515. https://doi.org/10.5530/pj.2021.13.64.

(5) Hui, C.; Wang, Z.; Xie, Y.; Liu, J. Contemporary Synthesis of Bioactive Cyclobutane Natural Products. *Green Synth. Catal.* **2023**, *4* (1), 1–6. https://doi.org/10.1016/j.gresc.2022.04.006.

(6) Allen, A. D.; Tidwell, T. T. Ketenes and Other Cumulenes as Reactive Intermediates. *Chem. Rev.* **2013**, *113* (9), 7287–7342. https://doi.org/10.1021/cr3005263.

(7) Cossío, F. P.; Arrieta, A.; Sierra, M. A. The Mechanism of the Ketene−Imine (Staudinger) Reaction in Its Centennial: Still an Unsolved Problem? *Acc. Chem. Res.* **2008**, *41* (8), 925–936. https://doi.org/10.1021/ar800033j.

(8) Sarkar, D.; Bera, N.; Ghosh, S. [2+2] Photochemical Cycloaddition in Organic Synthesis. *Eur. J. Org. Chem.* **2020**, *2020* (10), 1310–1326. https://doi.org/10.1002/ejoc.201901143.

(9) Fleming, I. *Pericyclic Reactions*; Oxford Univ. Press: Oxford, 1998.

(10) Rennie, R. *A Dictionary of Chemistry*; Oxford University Press, 2016. https://doi.org/10.1093/acref/9780198722823.001.0001.

(11) Scaiano, J. C. A Beginners Guide to Understanding the Mechanisms of Photochemical Reactions: Things You Should Know If Light Is One of Your Reagents. *Chem. Soc. Rev.* **2023**, *52* (18), 6330–6343. https://doi.org/10.1039/D3CS00453H.

(12) Medishetty, R.; Bai, Z.; Yang, H.; Wong, M. W.; Vittal, J. J. Influence of Fluorine Substitution on the Unusual Solid-State [2 + 2] Photo-Cycloaddition Reaction between an Olefin and an Aromatic Ring. *Cryst. Growth Des.* **2015**, *15* (8), 4055–4061. https://doi.org/10.1021/acs.cgd.5b00664.

(13) Fleming, S. A.; Parent, A. A.; Parent, E. E.; Pincock, J. A.; Renault, L. Mechanistic Analysis of the Photocycloaddition of Silyl-Tethered Alkenes. *J. Org. Chem.* **2007**, *72* (25), 9464–9470. https://doi.org/10.1021/jo7014664.

(14) König, B.; Leue, S.; Horn, C.; Caudan, A.; Desvergne, J.; Bouas-Laurent, H. Synthesis of Medium-Size Macrocycles by Cinnamate [2 + 2] Photoaddition. *Liebigs Ann.* **1996**, *1996* (8), 1231–1233. https://doi.org/10.1002/jlac.199619960802.

(15) Schmidt, G. M. J. Photodimerization in the Solid State. *Pure Appl. Chem.* **1971**, *27* (4), 647–678. https://doi.org/10.1351/pac197127040647.

(16) Gan, M.-M.; Yu, J.-G.; Wang, Y.-Y.; Han, Y.-F. Template-Directed Photochemical [2 + 2] Cycloaddition in Crystalline Materials: A Useful Tool to Access Cyclobutane

Derivatives. *Cryst. Growth Des.* **2018**, *18* (2), 553–565. https://doi.org/10.1021/acs.cgd.7b01308.

(17) MacGillivray, L. R.; Reid, J. L.; Ripmeester, J. A. Supramolecular Control of Reactivity in the Solid State Using Linear Molecular Templates. *J. Am. Chem. Soc.* **2000**, *122* (32), 7817–7818. https://doi.org/10.1021/ja001239i.

(18) Ghosn, M. W.; Wolf, C. Stereocontrolled Photodimerization with Congested 1,8-Bis(4′-Anilino)Naphthalene Templates. *J. Org. Chem.* **2010**, *75* (19), 6653–6659. https://doi.org/10.1021/jo101547w.

(19) Zitt, H.; Dix, I.; Hopf, H.; Jones, P. G. 4,15-Diamino[2.2]Paracyclophane, a Reusable Template for Topochemical Reaction Control in Solution. *Eur. J. Org. Chem.* **2002**, *2002* (14), 2298. https://doi.org/10.1002/1099-0690(200207)2002:14<2298::AID-EJOC2298>3.0.CO;2-E.

(20) Yagci, B. B.; Zorlu, Y.; Türkmen, Y. E. Template-Directed Photochemical Homodimerization and Heterodimerization Reactions of Cinnamic Acids. *J. Org. Chem.* **2021**, *86* (18), 13118–13128. https://doi.org/10.1021/acs.joc.1c01534.

(21) Yagci, B. B.; Munir, B.; Zorlu, Y.; Türkmen, Y. E. Access to Symmetrical and Unsymmetrical Cyclobutanes via Template-Directed [2+2]-Photodimerization Reactions of Cinnamic Acids. *Synthesis* **2023**, *55* (22), 3777–3792. https://doi.org/10.1055/a-2126-3774.

(22) Munir, B.; Yagci, B. B.; Zorlu, Y.; Türkmen, Y. E. Template-Directed Selective Photodimerization Reactions of 5-Arylpenta-2,4-Dienoic Acids. *J. Org. Chem.* **2024**, *89* (14), 10409–10418. https://doi.org/10.1021/acs.joc.4c01374.

(23) Türkmen, Y. E. Investigation of the Hydrogen Bond Donating Ability of 1,8-Naphthalenediol by NMR Spectroscopy and Its Use as a Hydrogen Bonding Catalyst. *Turk. J. Chem.* **2018**, *42* (5), 1398–1407. https://doi.org/10.3906/kim-1806-68.

(24) Musso, H.; Matthies, H. Über Wasserstoffbrücken, IV: Acidität Und Wasserstoffbrücken Bei Hydroxy-biphenylen Und Hydroxy-biphenylchinonen. *Chem. Ber.* **1961**, *94* (2), 356–368. https://doi.org/10.1002/cber.19610940211.

(25) Mammadova, F.; Hamarat, B.; Ahmadli, D.; Şahin, O.; Bozkaya, U.; Türkmen, Y. E. Polarization-Enhanced Hydrogen Bonding in 1,8-Dihydroxynaphthalene: Conformational Analysis, Binding Studies and Hydrogen Bonding Catalysis. *ChemistrySelect* **2020**, *5* (42), 13387–13396. https://doi.org/10.1002/slct.202002960.

(26) Yagci, B. B.; Zorlu, Y.; Türkmen, Y. E. Template-Directed Photochemical Homodimerization and Heterodimerization Reactions of Cinnamic Acids. *J. Org. Chem.* **2021**, *86* (18), 13118–13128. https://doi.org/10.1021/acs.joc.1c01534.

(27) Lee, G. S.; Kim, D.; Hong, S. H. Pd-Catalyzed Formal Mizoroki–Heck Coupling of Unactivated Alkyl Chlorides. *Nat. Commun.* **2021**, *12* (1), 991. https://doi.org/10.1038/s41467-021-21270-9.

(28) Konishi, H.; Manabe, K. Recent Progress on Catalytic Heck Carbonylations Using Carbon Monoxide Surrogates. *Tetrahedron Lett.* **2019**, *60* (42), 151147. https://doi.org/10.1016/j.tetlet.2019.151147.

(29) Nakashima, Y.; Hirata, G.; Sheppard, T. D.; Nishikata, T. The Mizoroki-Heck Reaction with Internal Olefins: Reactivities and Stereoselectivities. *Asian J. Org. Chem.* **2020**, *9* (4), 480–491. https://doi.org/10.1002/ajoc.201900741.

(30) Neises, B.; Steglich, W. Simple Method for the Esterification of Carboxylic Acids. *Angew. Chem. Int. Ed. Engl.* **1978**, *17* (7), 522–524. https://doi.org/10.1002/anie.197805221.

(31) 3-(1-Naphthyl)Acrylic Acid | C13H10O2 | CID 98307 - PubChem.

(32) Karplus, M. Contact Electron-Spin Coupling of Nuclear Magnetic Moments. *J. Chem. Phys.* **1959**, *30* (1), 11–15. https://doi.org/10.1063/1.1729860.

(33) Balcı, M. *Basic 1 H- and 13 C-NMR Spectroscopy*, 1. ed., transferred to digital print.; Elsevier: Amsterdam Heidelberg, 2005.

(34) Meier, H.; Stalmach, U.; Kolshorn, H. Effective Conjugation Length and UV/Vis Spectra of Oligomers. *Acta Polym.* **1997**, *48* (9), 379–384. https://doi.org/10.1002/actp.1997.010480905.

(35) De Luca, M.; Ioele, G.; Grande, F.; Ragno, G. Efficacy of Red Glass in Protecting 1,4-Dihydropyridine Antihypertensive Drugs in Liquid Formulations. *Appl. Sci.* **2021**, *11* (8), 3442. https://doi.org/10.3390/app11083442.

(36) Kumar, A.; Dutta, S.; Kim, S.; Kwon, T.; Patil, S. S.; Kumari, N.; Jeevanandham, S.; Lee, I. S. Solid-State Reaction Synthesis of Nanoscale Materials: Strategies and Applications. *Chem. Rev.* **2022**, *122* (15), 12748–12863. https://doi.org/10.1021/acs.chemrev.1c00637.

(37) Varga, K.; Volarić, J.; Vančik, H. Crystal Disordering and Organic Solid-State Reactions. *CrystEngComm* **2015**, *17* (6), 1434–1438. https://doi.org/10.1039/C4CE01915F.

(38) Kaupp, G. Organic Solid-State Reactions. In *Encyclopedia of Physical Organic Chemistry, 5 Volume Set*; Wang, Z., Ed.; John Wiley & Sons, Inc.: Hoboken, NJ, USA, 2016; pp 1–79. https://doi.org/10.1002/9781118468586.epoc2005.

(39) Chaudhary, A.; Mohammad, A.; Mobin, S. M. Recent Advances in Single-Crystal-to-Single-Crystal Transformation at the Discrete Molecular Level. *Cryst. Growth Des.* **2017**, *17* (5), 2893–2910. https://doi.org/10.1021/acs.cgd.7b00154.

(40) Ito, H.; Muromoto, M.; Kurenuma, S.; Ishizaka, S.; Kitamura, N.; Sato, H.; Seki, T. Mechanical Stimulation and Solid Seeding Trigger Single-Crystal-to-Single-Crystal Molecular Domino Transformations. *Nat. Commun.* **2013**, *4* (1), 2009. https://doi.org/10.1038/ncomms3009.

(41) Hu, F.; Bi, X.; Chen, X.; Pan, Q.; Zhao, Y. Single-Crystal-to-Single-Crystal Transformations for the Preparation of Small Molecules, 1D and 2D Polymers Single Crystals. *Chem. Lett.* **2021**, *50* (5), 1015–1029. https://doi.org/10.1246/cl.200931.

(42) Buchholz, V.; Enkelmann, V. Photochemical Single-Crystal-to-Single-Crystal Transformations. *Mol. Cryst. Liq. Cryst. Sci. Technol. Sect. Mol. Cryst. Liq. Cryst.* **1998**, *313* (1), 309–314. https://doi.org/10.1080/10587259808044292.

(43) Gao, X.-Y.; Li, Y.-L.; Liu, T.-F.; Huang, X.-S.; Cao, R. Single-Crystal-to-Single-Crystal Transformation of Tetrathiafulvalene-Based Hydrogen-Bonded Organic Frameworks. *CrystEngComm* **2021**, *23* (27), 4743–4747. https://doi.org/10.1039/D1CE00519G.

(44) Munawar, S.; Zahoor, A. F.; Hussain, S. M.; Ahmad, S.; Mansha, A.; Parveen, B.; Ali, K. G.; Irfan, A. Steglich Esterification: A Versatile Synthetic Approach toward the

Synthesis of Natural Products, Their Analogues/Derivatives. *Heliyon* **2024**, *10* (1), e23416. https://doi.org/10.1016/j.heliyon.2023.e23416.

(45) Maqbool, T.; Younas, H.; Bilal, M.; Rasool, N.; Bajaber, M. A.; Mubarik, A.; Parveen, B.; Ahmad, G.; Ali Shah, S. A. Synthesis of 1-(4-Bromobenzoyl)-1,3-Dicyclohexylurea and Its Arylation via Readily Available Palladium Catalyst─Their Electronic, Spectroscopic, and Nonlinear Optical Studies via a Computational Approach. *ACS Omega* **2023**, *8* (33), 30306–30314. https://doi.org/10.1021/acsomega.3c03183.

(46) Sherma, J.; Fried, B. *Handbook of Thin-Layer Chromatography*, 3rd ed., rev.expanded.; Marcel Dekker: New York, 2003.

(47) Commins, P.; Desta, I. T.; Karothu, D. P.; Panda, M. K.; Naumov, P. Crystals on the Move: Mechanical Effects in Dynamic Solids. *Chem. Commun.* **2016**, *52* (97), 13941–13954. https://doi.org/10.1039/C6CC06235K.

(48) Saragi, R. T.; Calabrese, C.; Juanes, M.; Pinacho, R.; Rubio, J. E.; Pérez, C.; Lesarri, A. π-Stacking Isomerism in Polycyclic Aromatic Hydrocarbons: The 2-Naphthalenethiol Dimer. *J. Phys. Chem. Lett.* **2023**, *14* (1), 207–213. https://doi.org/10.1021/acs.jpclett.2c03299.

(49) Deng, J.-H.; Luo, J.; Mao, Y.-L.; Lai, S.; Gong, Y.-N.; Zhong, D.-C.; Lu, T.-B. π-π Stacking Interactions: Non-Negligible Forces for Stabilizing Porous Supramolecular Frameworks. *Sci. Adv.* **2020**, *6* (2), eaax9976. https://doi.org/10.1126/sciadv.aax9976.

(50) Ajito, K.; Nakamura, M.; Tajima, T.; Ueno, Y. Terahertz Spectroscopy Methods and Instrumentation. In *Encyclopedia of Spectroscopy and Spectrometry*; Elsevier, 2017; pp 432–438. https://doi.org/10.1016/B978-0-12-409547-2.12092-X.

(51) Lewis, L.; Troost, P.; Lavery, D.; Nishikida, K. Pharmaceutical Polymorphism Studies by Infrared Spectroscopic Imaging. *Microsc. Microanal.* **2001**, *7* (S2), 158–159. https://doi.org/10.1017/S1431927600026866.

(52) Lei, T.; Zhou, C.; Huang, M.; Zhao, L.; Yang, B.; Ye, C.; Xiao, H.; Meng, Q.; Ramamurthy, V.; Tung, C.; Wu, L. General and Efficient Intermolecular [2+2] Photodimerization of Chalcones and Cinnamic Acid Derivatives in Solution through Visible-Light Catalysis. *Angew. Chem. Int. Ed.* **2017**, *56* (48), 15407–15410. https://doi.org/10.1002/anie.201708559.

(53) Dogga, B.; Kumar, C. S. A.; Joseph, J. T. Palladium-Catalyzed Reductive Carbonylation of (Hetero) Aryl Halides and Triflates Using Cobalt Carbonyl as CO Source. *Eur. J. Org. Chem.* **2021**, *2021* (2), 309–313. https://doi.org/10.1002/ejoc.202001328.

(54) Jia, X.; Wen, Y.; He, C.; Huang, X. Palladium Complexes with N, O-BIDENTATE Ligands Based on *N*-OXIDE Units from Cyclic Secondary Amines: Synthesis and Catalytic Application in MIZOROKI-HECK Reaction. *Chin. J. Chem.* **2024**, *42* (3), 294–300. https://doi.org/10.1002/cjoc.202300375.

(55) Atmaram Upare, A.; Gadekar, P. K.; Sivaramakrishnan, H.; Naik, N.; Khedkar, V. M.; Sarkar, D.; Choudhari, A.; Mohana Roopan, S. Design, Synthesis and Biological Evaluation of (E)-5-Styryl-1,2,4-Oxadiazoles as Anti-Tubercular Agents. *Bioorganic Chem.* **2019**, *86*, 507–512. https://doi.org/10.1016/j.bioorg.2019.01.054.